ASPECTS OF HOLOGRAPHY

by

DIRK MICHAEL FINDEIS

Submitted to the University of Cape Town in partial fulfilment of the requirements for the degree of Master of Science in Mechanical Engineering.

SEPTEMBER 1989

to Mandy

ABSTRACT

This study was aimed at broadening the knowledge of aspects of holography by examining three areas of importance, namely: i) qualitative holographic nondestructive testing, as applicable to flaw detection, ii) quantitative holographic interferometry and iii) white-light transfer reflection holography, with particular emphasis on the multiplexing principle.

The objects used to evaluate the viability of qualitative holographic nondestructive testing were various carbon fibre airframe sections, a ceramic tube and a ceramic mould.

The real-time and double-exposure holographic techniques were used to investigate the objects. Hot air was employed as the stress application medium.

The results obtained clearly show the viability of holography as a nondestructive testing technique for the detection of debonds, delaminations, cracks, etcetera.

In the second part of the study, the zero-order and fringe-counting techniques were applied to a cantilever loading experiment as a means of quantitatively determining the cantilever's displacement.

It was determined that displacements with an accuracy of

circa 85 % could be obtained by using the abovementioned techniques.

In the final part of this study the transfer and multiplexing principles were rigorously examined. As a result, it was found that when reflection holograms were used as masters, excessively dim transfer holograms were produced. Transmission masters produced much brighter transfer holograms and displayed the capability of individually reproducing the images recorded. However, the angle of visibility of the individual images produced was found to be unsatisfactory and therefore warrants further investigation.

ACKNOWLEDGEMENTS

I would like to express my sincere thanks to:

Associate Professor J. GRYZAGORIDIS for initially suggesting this study and for his invaluable guidance, encouragement, supervision, corrections, advice and help throughout this project.

Professor R. PENNY for his encouragement, advice, guidance and enthusiasm.

Mr V. APPELTON for his time and photographic assistance.

Mr M. BATHO for his technical assistance.

Mr J. MEYER for his enthusiasm and electronic expertise.

My parents HEIDI & BRUNO for their support and for organizing the computer.

Last, but by no means least, my future wife MANDY-LEE MALSCHINGER for her endless support, encouragement and willingness to take time off from her own thesis to assist with the compiling and editing as well as the typing of this dissertation.

TABLE OF CONTENTS

LIST OF FIGURES

LIST OF TABLES

CHAPTER 1

1. INTRODUCTION

1.1. THE PHENOMENON OF HOLOGRAPHY

> "Holography is perhaps the most revolutionary visual recording medium since the prehistoric cave paintings at Lascaux. For the first time in the history of literate man, we can communicate through a medium which has the same dimensional properties and characteristics as the world we live in."
>
> Rosemary Jackson
>
> The Holographic Handbook (1982)

Unlike photography, where only two dimensional effects can be obtained, holography reconstructs three dimensional images. This unique characteristic is what gave holography its name. The term was coined by the Hungarian physicist, Gabor, in 1948 and is derived from the Greek words 'holos' meaning "the whole" or "entire" and 'gramma' which means "message" or "record".

In recording techniques such as photography, the picture obtained is merely an intensity distribution of the light

emitted by the recorded scene. All phase information of the scene is negelected.

Holography, on the other hand, records the information present in the light emitted by the object, in its entirety, that is, storing both the amplitude and phase distribution of the scattered light. It is this phase distribution which is responsible for the depth of focus and perspective of the object. The light information emitted by the object is recorded on a hologram as a diffraction grid, with the result that, unlike photography, the image is not visible on the holographic plate. However, when the processed hologram is illuminated, the light incident on the hologram is diffracted by the recorded diffraction grid, producing a three dimensional image of the recorded object.

Due to the three dimensional property of holography, the image, when viewed, is indistinguishable from the object.

1.2. THE AIMS AND SIGNIFICANCE OF THIS THESIS

Holography is presently utilised in various fields. For example: i. display holography - advertising, security, etcetera , ii. holographic interferometry - as applicable to the area of nondestructive testing, iii. computer generated holograms, iv. in the medical and dental profession and so on. The two main areas of interest in

this thesis are holographic nondestructive testing and display holography.

Nondestructive testing is the descriptive title given to the field of material or object testing, where the specimen tested is not physically destroyed whilst determining either the material properties or the compliance to a set standard. Holographic nondestructive testing utilizes coherent optical techniques and the wavelength of laserlight as a unit of measure when determining the above mentioned properties and compliances.

The aim of this thesis was to present selected feasability studies on holographic interferometry, applied to objects supplied by industry. The objects were all of such a nature that the investigation of alternative testing techniques became necessary. This was due to the fact that the non-destructive testing techniques currently commercially available either yield results which are unsatisfactory and inconclusive or are considered to be time consuming and laborious.

In addition, the display aspect of holography was investigated. The aim of this section of the thesis was to examine the storing of more than one holographic image onto a single hologram and then to achieve selected replay of the recorded holograms in the reconstruction process.

1.3. PLAN OF THESIS DEVELOPMENT

The dissertation begins by briefly summarising the history and development of holography. The detailed discussion of the relevant holographic recording techniques is then presented. A literature survey is then conducted in which information relevant to the dissertation is expounded. The author's opinions about the reported results are also included.

Following a general description of the equipment and chemicals used in the University of Cape Town's holographic laboratory, the projects conducted are presented individually. Each report contains the aim of the investigation, the experimental set-up, the results obtained, the problems encountered, the conclusions deduced, recommendations made and also highlights any other features particular to the project.

CHAPTER 2

2.1. HISTORICAL BACKGROUND

2.1.1. EARLY HISTORY

In 1948, Gabor [1] proposed the idea of the holographic imaging process in an attempt to improve the resolution in electron microscopy. The proposal entailed the capturing of a scattered light field, produced by illuminating an object with X-rays, onto a plate coated with a photographic emulsion. See Figure 2.1. According to Gabor, the scattered field would form a diffraction grid which, when illuminated with coherent light, would produce a three dimensional image of the recorded object.

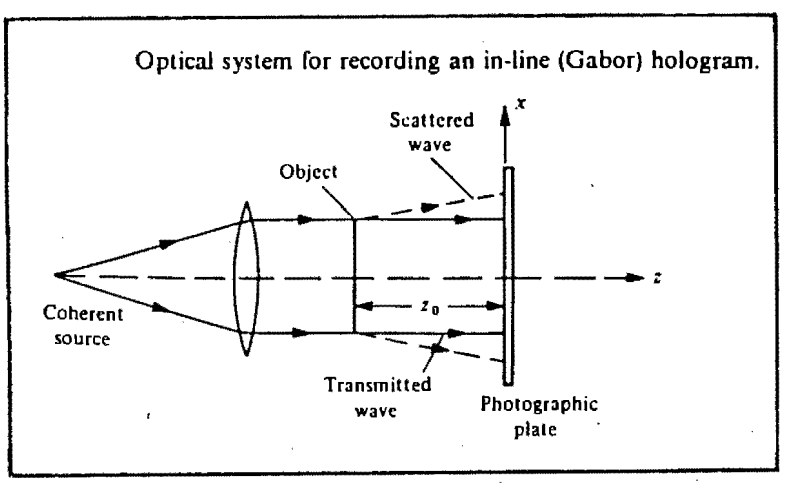

FIGURE 2.1 (HARIHARAN, 1984)

This hologram, when illuminated with coherent light, produced one image behind the hologram - the virtual image -

and one image in front of the hologram - the real image - superimposed. This was due to the production of two diffraction waves opposite to one another, producing two images.

Even though the validity of Gabor's work was recognised by himself as well as other scientists, the results obtained were far from satisfactory. Various techniques were proposed to eliminate the real image, all of which proved fruitless. In addition, the poor quality of the coherent light sources led to lack of progress in holography.

A number of years later, Emett Leith, an American research physicist, developed a technique currently known as side-looking radar. This technique was found to be similar to the holographic recording technique that was proposed by Gabor.

Based upon their earlier radar work, Leith and Upatnieks [2] developed the off-axis reference beam technique, which offset the real from the virtual image, thereby preventing them from overlapping.

This was achieved by using a separate reference wave incident to the photographic plate at an appreciable angle with respect to the object wave when recording. In the reconstruction process, using the original reference beam, the virtual image was visible, offset from the real image,

as is diagrammatically indicated in Figure 2.2.

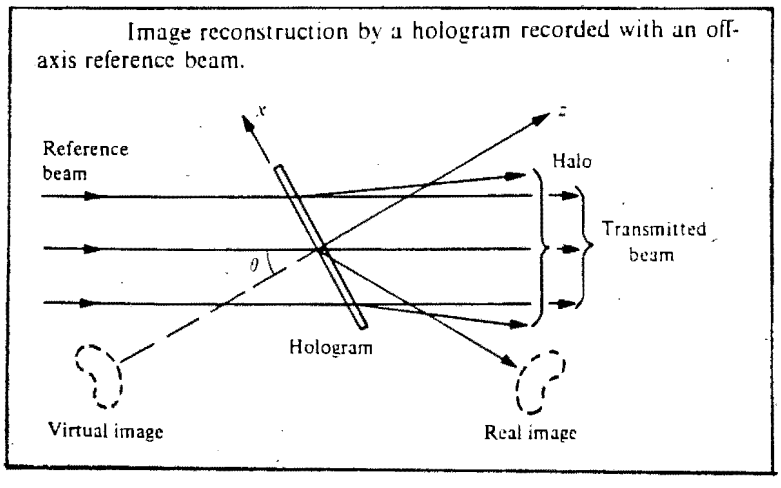

FIGURE 2.2 (HARIHARAN, 1984)

However, one problem still remained, namely, the lack of a sufficiently coherent light source.

In 1958, Townes and Schawlow [3] proposed the conditions which enabled the achievement of Light Amplification by Stimulated Emission of Radiation, namely, the laser. In July 1960, Mainan [3] announced the first successful operation of a pulsed laser which produced a highly coherent light source. In 1961 [3], the first continuous wave laser, namely, the He-Ne, was successfully operated, which incidentally still is the most commonly used continuous wave laser.

2.1.2. FURTHER DEVELOPMENTS

Just when it seemed that laser light had no practical

application, Leith and Upatnieks began experimenting with laser light in relation to the holographic process.

In 1963 [4], they made the first true hologram using their off-axis reference beam method and a laser beam as the coherent light source. In 1964 [5], they presented the first publication showing reconstructions of diffusely reflecting objects - the now famous little model train engine. The holographic reconstructions were so accurate that it was optically impossible to differentiate between the true and the reconstructed image.

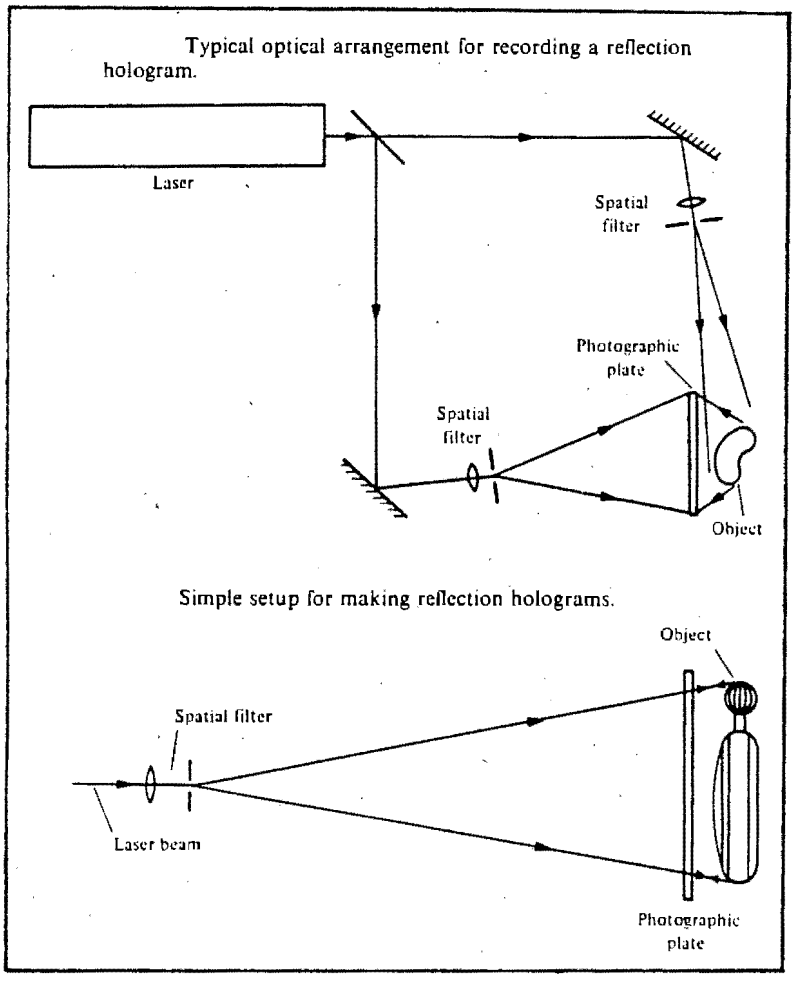

FIGURE 2.3 (HARIHARAN, 1984)

At about the same time, another major development in holography was reported by Denisyuk [6] of the Soviet Union. In his technique, the object and reference waves were incident on the photographic emulsion from opposite sides. See Figure 2.3.

Using the abovementioned process, plain incoherent white light can be used in the reconstruction process. The diffraction grid of the hologram selectively reflects only a narrow wavelength band and thus reconstructs a monochromatic image.

With the basic holographic methods having been established, optical holography developed at a rapid rate and soon found a large number of scientific applications.

At the University of Michigan in 1965, Stetson and Powell [7] discovered the interferometric process whilst investigating faults in holograms. In the National Physics Laboratory in England, Burch [8] also discovered holographic inteferometry at roughly the same time.

Brooks and colleagues, at T.R.W. Systems [9], accidentally came across holographic inteferometry when the pulsed laser with which they were working pre-fired, resulting in a double pulse. When the processed hologram which was a recording of a bullet in motion, was illuminated, the air surrounding the bullet was reconstructed as an

interferometric pattern. This recording technique is currently known as double-exposure holography.

Thus, with the discovery and development of the holographic interferometric technique, a powerful tool became available which is now widely used in the field of non destructive testing.

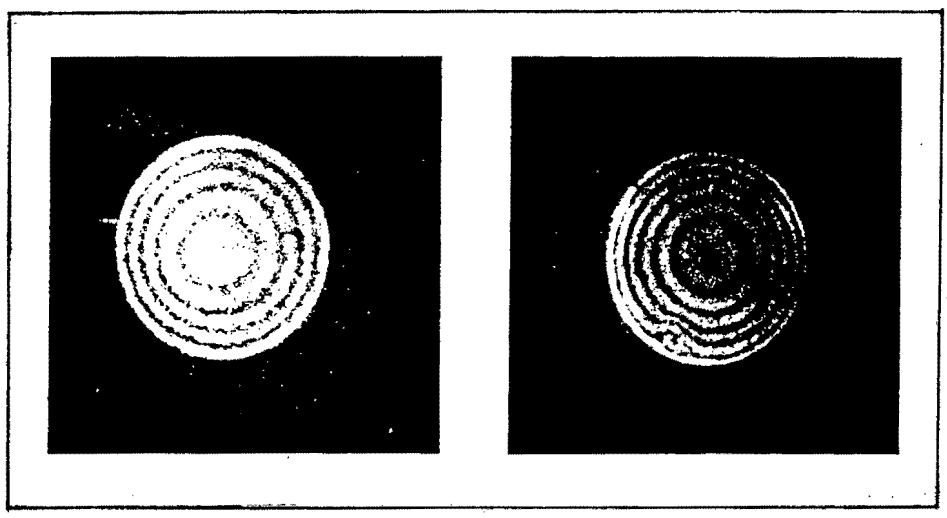

Typical interferometric fringe pattern

FIGURE 2.4 (BUTTERS, 1968)

2.2. THE VARIOUS HOLOGRAPHIC TECHNIQUES

2.2.1. LEITH-UPATNIEKS OFF-AXIS METHOD

This was the first successful technique used to produce a hologram - known as a transmission hologram - which overcame all the problems encountered by Gabor.

The method, as the description indicates, employs an off-axis reference beam, that is, not normal to the holographic plate, which is directed onto the recording medium, and a second beam which is directed onto the object and reflected onto the recording medium. See Figure 2.5.

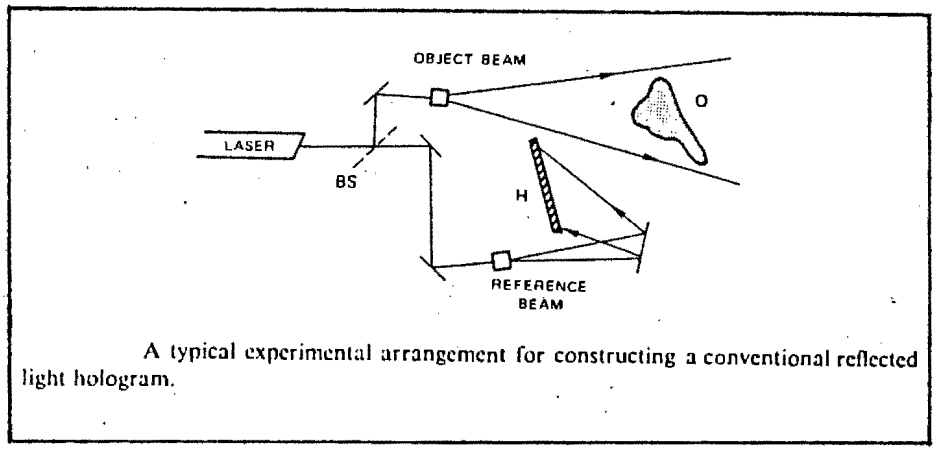

A typical experimental arrangement for constructing a conventional reflected light hologram.

FIGURE 2.5 (ERF, 1974)

It is essential that the light source used is coherent and that all light falling onto the holographic plate emanates from one common light source, namely, the laser. In addition, it is essential that when the light originating from the source is split, the difference in length of the split beams is neither greater than nor less than the coherent length of the laser light used. This is illustrated in Figure 2.6 below.

The longitudinal coherent length is the path difference between two beams that can be tolerated whilst still producing good holograms. The coherent length is characteristic of the laser type used and originates from

the round trip transit time of a photon in the laser cavity.

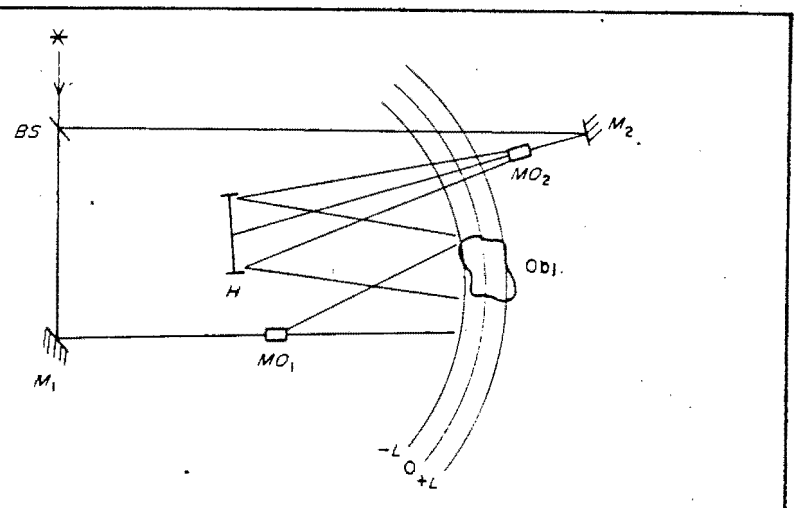

A general configuration of mirrors and beam splitters comprising a holocamera. The asterisk is any coherent light source, generally a laser. In this case, it has coherence length L. BS is the beam splitter, M_1 (M_2) is a mirror in the object (reference) beam. MO_1 (MO_2) is a microscope objective in the object (reference) beam, and H is the photographic plate that will become the hologram.

FIGURE 2.6 (SOLLID IN SHARPE ED., 1973)

The irradiance, which essentially is an intensity distribution and is recorded onto the holographic plate, is obtained by squaring the complex wavefront produced by the reference beam and object reflection. Mathematically, the irradiance is expressed as:

$$I = A_o^2 + A_r^2 + 2A_oA_r * \cos(\varphi_o(_r) - k(r \sin 1 + r^2/22)) \qquad (2.1)$$

Essentially this formula consists of three spatially dependant terms. The first two quadratics represent the intensities of the object and reference beam respectively. Into the third quadratic term is encoded the spatially dependant phase of the object and reference beams in terms

of intensities as expressed in the argument.

For the full derivation of the formula, please refer to Erf (1974).

In order to reconstruct the image, the processed hologram is illuminated with the original reference beam. Two expressions can be mathematically obtained to describe the wavefronts produced:

$$A_o A_r^2 * \text{expi}\ (\varphi_o(r) + wt) \qquad (2.2)$$

$$A_o A_r^2 * \text{expi}\ (-\varphi_o(r) + wt + k(2r \sin 1 + r^2/22) \qquad (2.3)$$

Equation (2.2) produces a wavefront which is proportional to the original wavefront. When observing this wavefront a virtual image is produced which is indistinguishable from the original object and contains all the effects of normal three dimensional viewing.

Equation (2.3) describes the formation of the real image. The result is a spatially inverted (pseudoscopic) image of the object. The location of the real image is generally in front of the hologram, for it is a conjugate wave emanating from the hologram, as indicated by the minus sign in the argument. Refer to Erf (1974) for the detailed mathematical approach.

Another aspect worth considering is the use of the conjugate of the reference beam in the reconstruction process, namely, a wavefront propagating in the opposite direction, with respect to the original wavefront. This conjugate reference wave, when multiplied with equation (2.1), results in the disappearance of the argument of equation (2.3). This reduces equation (2.3) to the conjugate of equation (2.2) as is indicated by the minus sign in equation (2.4).

$$A_o A_r^2 * \text{expi}\ (-\varphi_o(r) + wt) \qquad (2.4)$$

See Erf (1974) for mathematical detail.

Equation (2.4) represents a pseudoscopic real image which is located in the same position as the position of the virtual image. Figure 2.7 graphically depicts this phenomena.

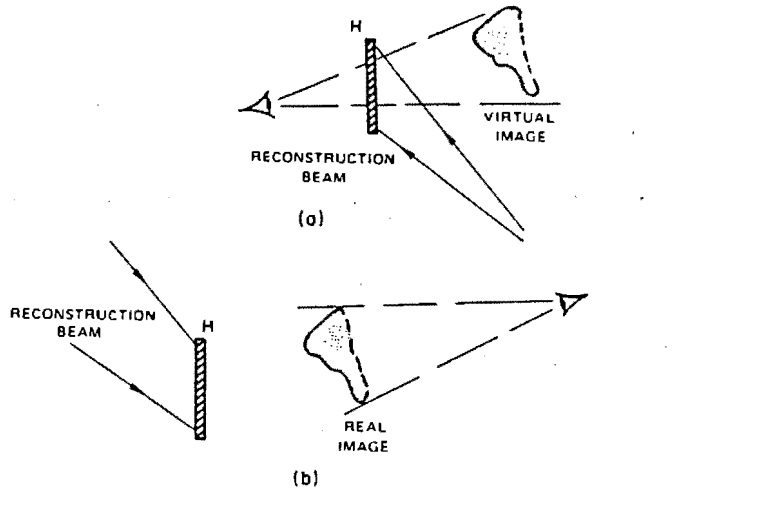

Schematic diagrams illustrating holographic reconstruction of (a) the virtual image and (b) the real image.

FIGURE 2.7 (ERF, 1974)

The off-axis system presented above, is only one of numerous configurations. However, the underlying concept of using an off-axis reference beam always remains the same.

2.2.2. (DENISYUK) WHITE-LIGHT HOLOGRAMS

In 1962, Y.N. Denisyuk [6] of the U.S.S.R, developed the white-light holographic technique. This technique was further developed by American scientists. The white-light hologram is similar to the off-axis hologram in that a seperate reference beam is used. However, the technique, which in addition utilizes the Bragg diffraction effect and the properties of a thick photographic emulsion, produces a hologram which can be viewed in ordinary daylight.

The following must be taken into account when discussing the Bragg diffraction effect:

When two coherent plane waves impinge onto a photographic emulsion, an interference plane is created at the bisector of the two planes. This bisecting plane is known as a Bragg plane and propagates through the emulsion. See Figure 2.8.

Considering the triangle ABC in Figure 2.8 the relationship

$$2 \Lambda \sin (\phi/2) = \lambda \qquad (2.5)$$

is obtained.

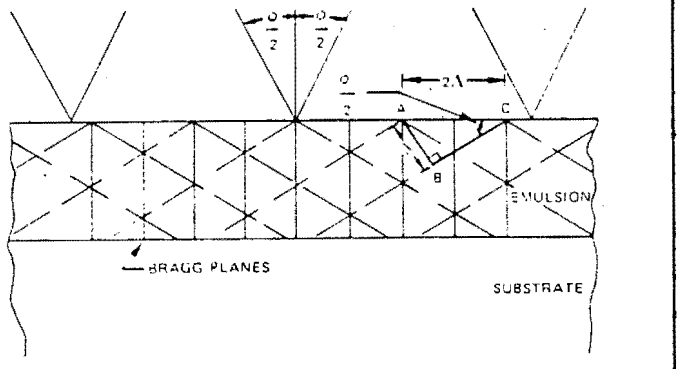

Creation of Bragg planes in a thick photographic emulsion.

FIGURE 2.8 (ERF, 1974)

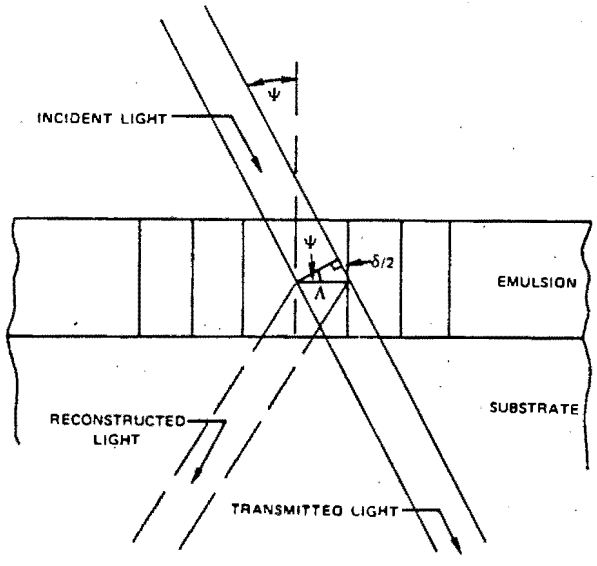

Partial reflection of light from the Bragg planes as in the reconstruction of a white light hologram.

FIGURE 2.9 (ERF, 1974)

Upon reconstruction, Figure 2.9 can be used to calculate

$$\delta = 2\Lambda \sin \psi \qquad (2.6)$$

where δ is equal to the path difference between two reflected rays from two successive Bragg planes. For

reconstruction to occur δ must equal λ, i.e. equation (2.5) and (2.6) are equated and reduce to sin (ψ) = sin (ϕ/2). This means that the optimum angle used in the reconstruction process is equal to the angle used in the construction process.

The Bragg effect can be utilised to absorb all but one wavelength of white light, which results in the reconstruction of a clear image. In order to achieve this, white-light, whilst traversing through the emulsion, has to pass many Bragg planes, each plane contributing to absorbing all but the required wavelength.

If the object wave and reference wave are separated by one hundred and eighty degrees and lie approximately normal to the emulsion in the recording process, Bragg planes will be formed parallel to the emulsion. This is characteristic of white light holograms. If the emulsion is ten to twenty nanometres thick, as many as thirty to sixty Bragg planes can be recorded within the thickness of the emulsion.

To produce a reflection hologram, the following technique is employed:
Coherent light is used to illuminate the object, scattering a light wave onto the emulsion from one side. From the other side, a reference beam is directed onto the emulsion, resulting in the formation of Bragg planes roughly parallel to the emulsion.

During reconstruction, the virtual image is formed by the light reflected from the Bragg planes. If the angle of incidence is changed when viewing, another wavelength within the visible spectrum will satisfy the Bragg condition and form the virtual image. The hologram is thus viewable at a whole range of angles.

The experimental set-up is depicted in Figure 2.10, showing; (a) the construction and (b) the reconstruction processes.

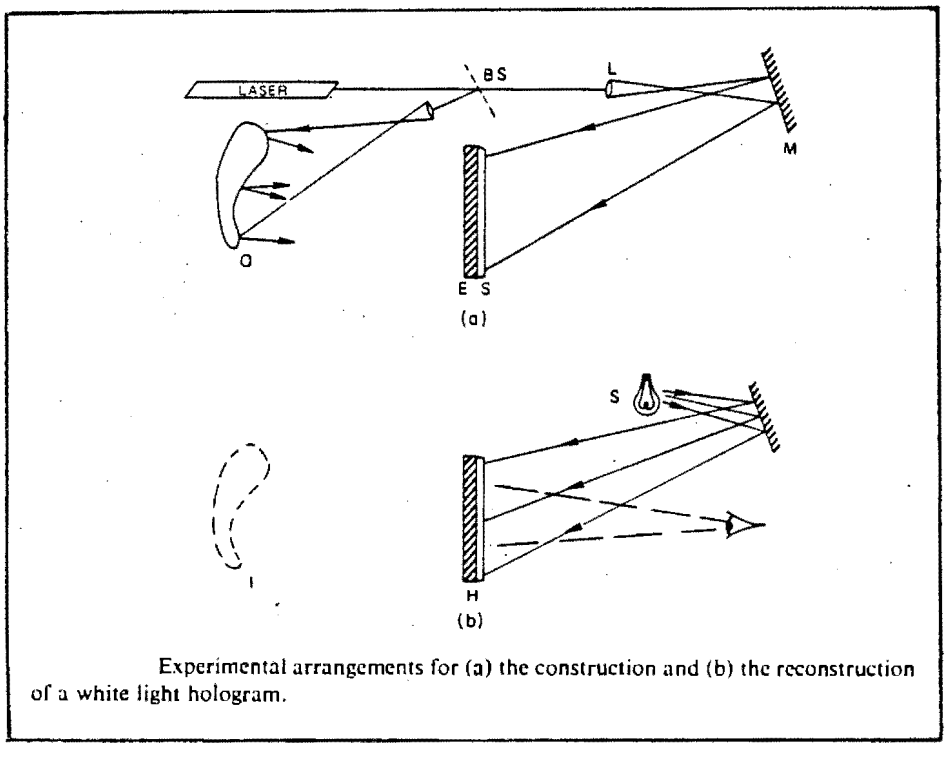

Experimental arrangements for (a) the construction and (b) the reconstruction of a white light hologram.

FIGURE 2.10 A & B (ERF, 1974)

Many types of set-ups can be used for white-light reflection holography. One of them, which is of interest to this thesis, is the technique describing the transfer process.

2.2.2.1. TRANSFER HOLOGRAPHY

The transfer process first utilises the off-axis method and then the white-light holographic process.

First a high quality off-axis hologram is produced and processed. This transmission hologram is referred to as a master hologram. From it, a so called transfer hologram is created which essentially is a white-light hologram. This is done as follows:

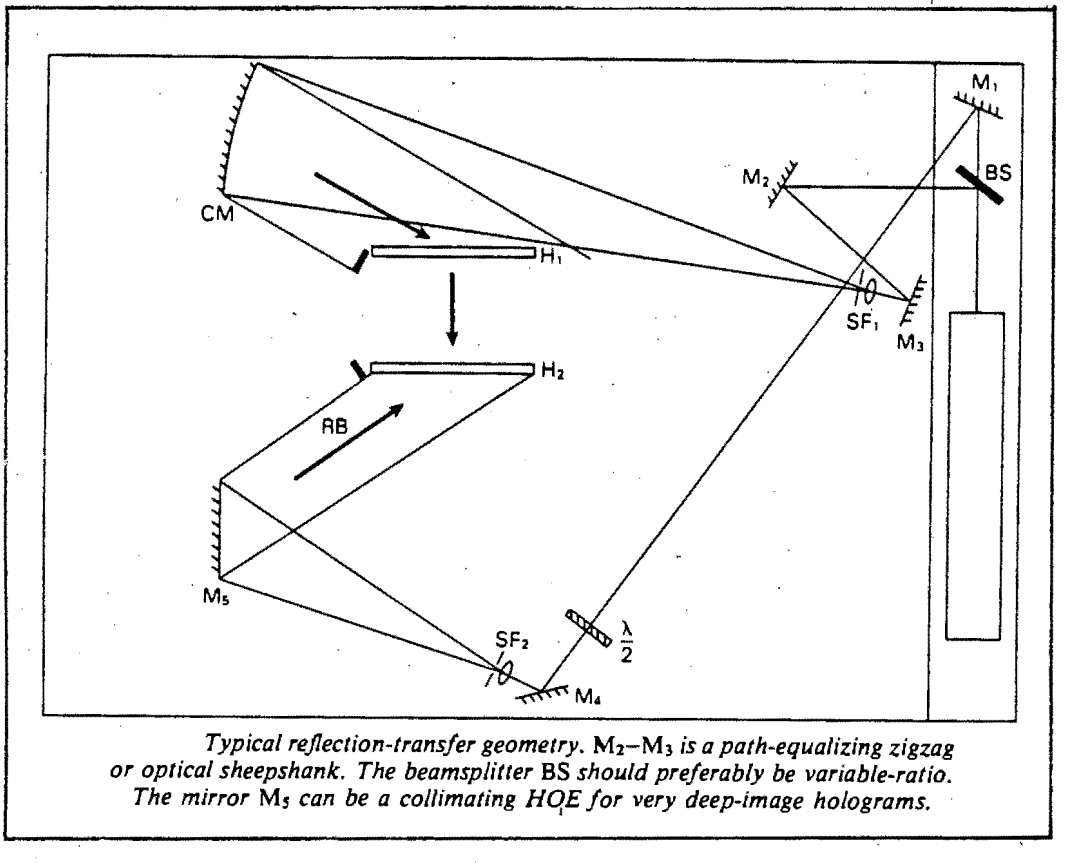

Typical reflection-transfer geometry. M_2–M_3 is a path-equalizing zigzag or optical sheepshank. The beamsplitter BS should preferably be variable-ratio. The mirror M_5 can be a collimating HOE for very deep-image holograms.

FIGURE 2.11 (SAXBY, 1988)

The master hologram is set up so that, during the

reconstruction process, a conjugate reference beam is used to project the real image. In the plane of focus a holographic plate is placed with a reference beam incident at the desired angle of illumination. See Figure 2.11.

The hologram is then recorded and processed in the conventional way.

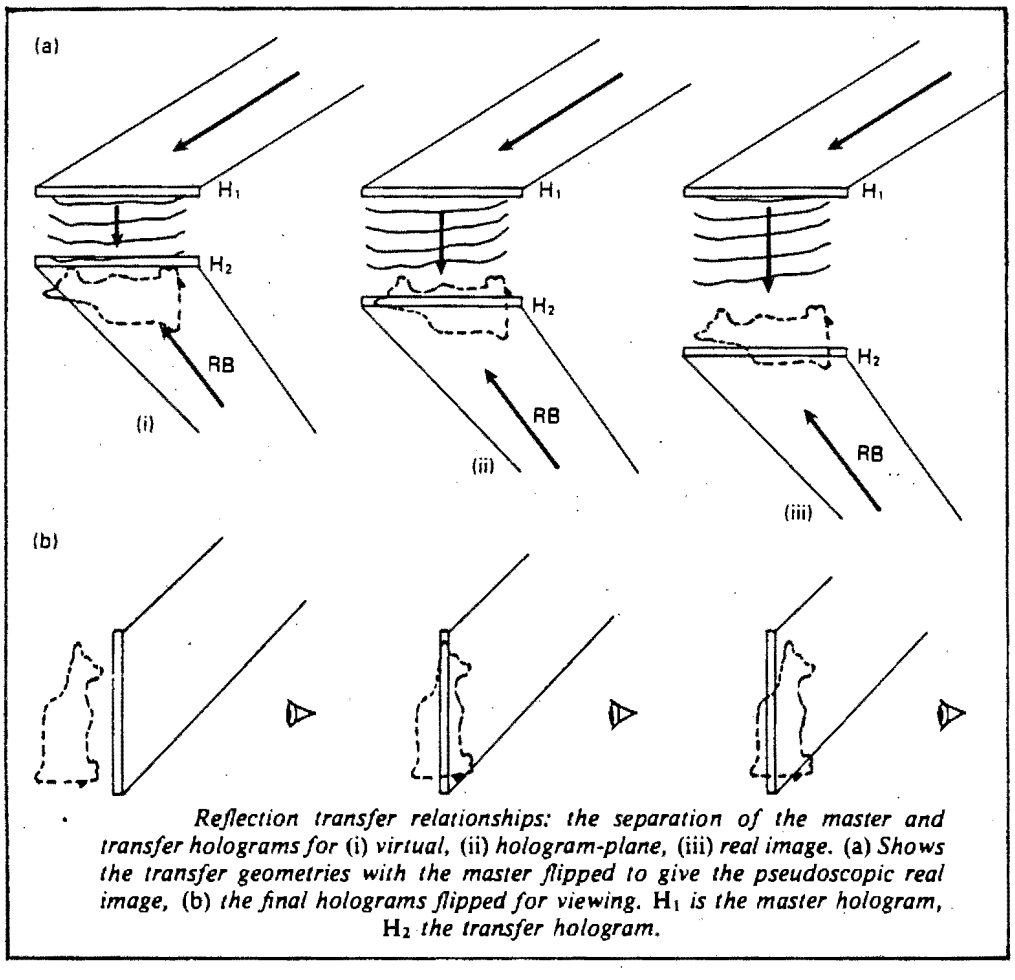

Reflection transfer relationships: the separation of the master and transfer holograms for (i) *virtual,* (ii) *hologram-plane,* (iii) *real image.* (a) *Shows the transfer geometries with the master flipped to give the pseudoscopic real image,* (b) *the final holograms flipped for viewing.* H_1 *is the master hologram,* H_2 *the transfer hologram.*

FIGURE 2.12 A & B (SAXBY, 1988)

The reconstruction process which employs plain white light to illuminate the hologram, reveals the object focused at

approximately the plane of the hologram. This is dependant upon the position of location of the hologram during recording. This is illustrated in Figure 2.12 A & B.

All three dimensional characteristics are replayed according to the original object. However, the object is only visible if the angle of viewing is incident with the angle of projection of the real image from the master hologram.

This transfer process has been utilised to a great extent in the display field of holography. The transfer process forms part of the thesis and its application in an experimental set-up is discussed in chapter three.

2.2.3. HOLOGRAPHIC INTERFEROMETRY

Holographic interferometry, an extension of the interferometric measurement technique, finds many applications in the nondestructive testing industry. It permits the detection of minute changes in the surfaces of objects by providing a process for the comparison of each point on the surface, before and after a change takes place. Because of this sensitivity to surface deformation, the technique can be used to gain information with regard to the structural characteristics of a component.

In the application of holographic interferometry, at least

one of the light waves interfering and therefore creating the interference pattern is produced from the reconstruction process of a hologram. The interference pattern obtained typically consists of a series of alternating bright and dark bands which are superimposed on the image of the object. There is no mechanical contact between the hologram and the object and therefore holographic interferometry can even be carried out in hostile environments.

Two basic types of holographic interferometry are widely used, namely, real-time and double-exposure. Both processes generally utilise the off-axis recording technique. Real-time holography, as the name implies, enables the immediate observation of various interference patterns produced by the distortions of the object, whereas double-exposure holography entails a 'freezing' of the interference pattern onto the hologram. Once recorded, this 'frozen' pattern cannot be altered.

2.2.3.1. REAL-TIME HOLOGRAPHIC INTERFEROMETRY

In this technique a transmission hologram is made of the object under examination. After processing of the recorded hologram, it is placed back into the position in which it was situated during recording. When this hologram is illuminated with the original reference beam, the hologram

produces the virtual image where the object was. However, the object is still positioned in exactly the same place and is illuminated with the object beam. As a result, the object and the virtual image coincide.

If the object is then distorted slightly, interference fringes are observed. The fringes are created due to the interference of the wavefront which is produced by the hologram and the new wavefront which is produced by the illuminated object in its displaced position. The interference fringes are a measure of the displacement of the object. Further displacement of the object will result in the creation of a new interference pattern between the object and the image.

To succeed with the interferometric process, a very stable working environment in required. This is because the image produced by the hologram has to coincide exactly with the object. To ensure this, the movement of the set-up as a whole has to be kept below a wavelength of the laser light. If the motion is greater, spurious fringes will be observed before stressing of the object has occurred. These spurious fringes affect the interference patterns obtained when stressing the object and thus affect the results.

For the mathematical detail of the interference obtained between the object and image, refer to Hariharan (1984).

2.2.3.2. DOUBLE-EXPOSURE HOLOGRAPHIC INTERFEROMETRY

In double-exposure holographic interferometry, interference occurs due to the interaction of two wavefronts produced by two holograms stored on one holographic plate. Generally, the first hologram is a hologram of an object in an unstressed condition and the second hologram, a recording of the object, still in the same place, but in a different state of stress. When illuminated, the interaction of the two holographically produced wavefronts form an interference pattern which reveals the change in shape of the object between the two exposures.

Double-exposure holography is simpler than real-time holography because the two wavefronts interfering with each other are always reconstructed with an identical reference beam. Distortion of the emulsion affects both wavefront producing interference grids equally, thus eliminating distortion of one wavefront with respect to the other.

2.3. LITERATURE SURVEY

The material presented prior to this chapter was intended to provide a general background in the theory and basic application of holography. In all aspects however, the emphasis has been on the basic principles and laboratory methods only.

In this chapter of the thesis, some of the work previously conducted, will be surveyed. Most of the holographic non destructive testing literature is found in scientific journals and is therefore very seldom reported in "open" literature.

Specialised procedures which have been developed were investigated with the intention of obtaining relevant information. It is however impossible to review all the excellent work previously undertaken in the field of optical holography.

2.3.1. OBJECT SIZE

Holographic interferometry can be used to test objects of varying sizes. The laser system employed is dependent upon the surface area of the object to be inspected, and a wide range of lasers with varying outputs have therefore been utilised.

As an example, IBM [10] experienced component failure problems in a certain cardreader range. Scientists at IBM General Systems Division used double exposure holographic interferometry to investigate the stresses present when the part was in operation. See Figure 2.13. A continuous wave laser beam was used in the recording process.

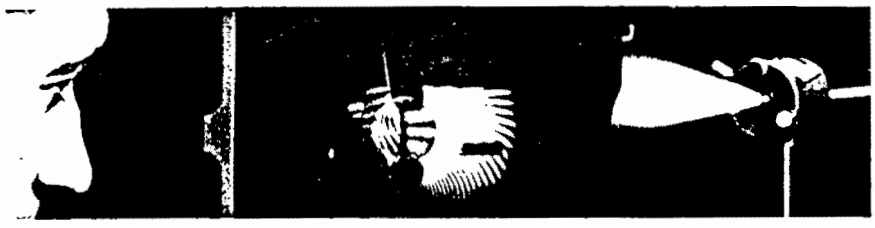

Study of the holographic reconstruction of a new card reader part, recorded under load, reveals areas of stress the part will experience in operation. [Courtesy IBM.]

FIGURE 2.13 (ERF, 1974)

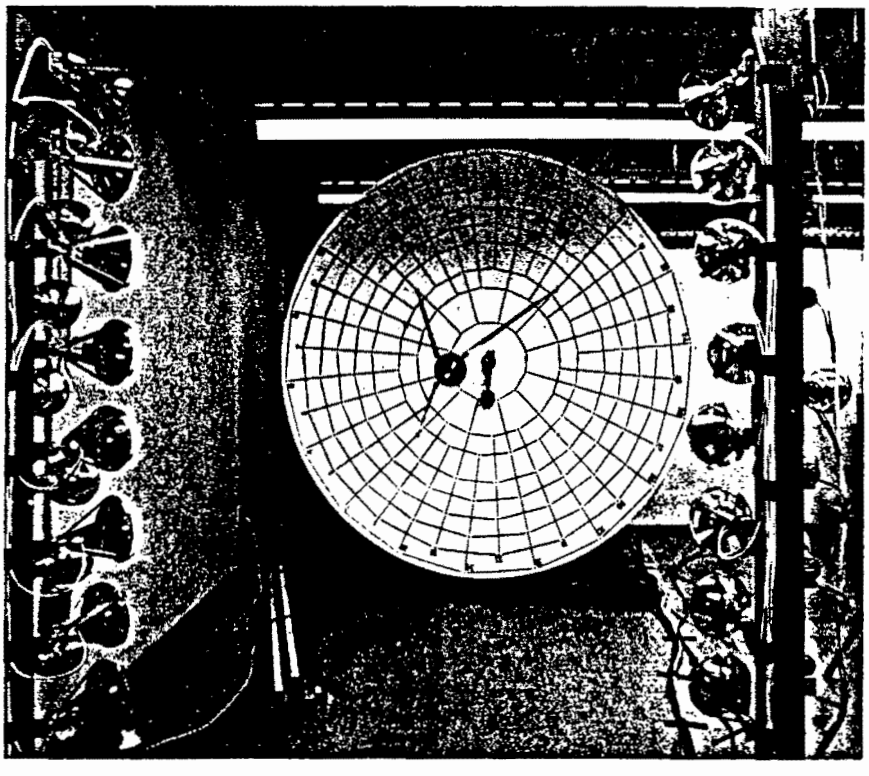

End-on view of a 9-ft-diam spacecraft microwave antenna as it was set up for interferometric holographic study of the effects of thermal loading. [Courtesy R. F. Wuerker, TRW Systems.]

FIGURE 2.14 (ERF, 1974)

Wuerker and Heflinger at TRW Systems [10] have, on the other

hand, conducted work on more spectacular components. These were generally of a larger nature, precluding the use of continuous wave techniques, in favour of pulsed laser techniques. As an example, figure 2.14 depicts the holographic interferometric set-up used to test a nine foot diameter spacecraft antenna exposed to thermal heating. Figure 2.15 illustrates the reconstruction of a double exposure hologram where the mechanical deformation of the antenna is produced by finger pressure.

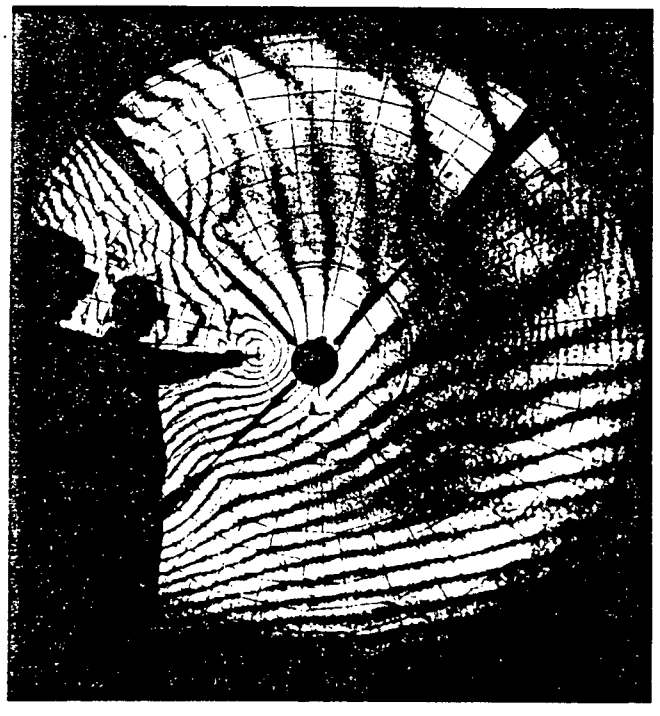

Reconstruction of an interferometric hologram depicting the mechanical surface deformation induced in the antenna of Fig. 8.1.3 as a result of finger pressure being applied between the two exposures. L. O. Heflinger is seen in silhouette and with his shadow. [Courtesy R. F. Wuerker, TRW Systems.]

FIGURE 2.15 (ERF, 1974)

Another of Wuerker and Heflingers'[10] applications of

pulsed holographic interferometry was performed on Donatella's painted wood carving statue of San Giovani Battista. Figure 2.16 presents the reconstruction of a double exposed hologram where the right side of the head was warmed up between exposures, revealing cracks in the wood in the area of the cheek.

Photographic reconstruction which illustrates the use of interferometric holography to study the thermally induced distortions in ancient statuary. The hologram was of the head of San Giovanni Battista with the right side slightly warmed between the two exposures. [Courtesy R. F. Wuerker, TRW Systems.]

FIGURE 2.16 (ERF, 1974)

2.3.2. STRESS APPLICATION TECHNIQUES

In conjunction with an experiment conducted by Leonard A. Kersch [11] on laminate structures, a closer look was taken at three object stressing techniques, namely; thermal stressing, pressure stressing and vibration stressing.

2.3.2.1. THERMAL STRESSING

Thermal stressing relies on a variation in a surface deformation caused by differences in thermal expansion which are a direct result of the material parameters. Examples of differences in thermal expansion are:

- Interface insulation in composite materials due to dissimilar laminates, or dissimilar bonding mediums in similar laminates.
- Objects consisting of different materials.

During thermal stressing, a certain amount of elastic stressing will occur as a result of the dissimilar expansion coefficients of the laminates. A disbonded area that is present in the structure, will not be constrained. Therefore, the thermally stressed object should deform to to a greater extent in the area of debonding and thereby reveal its position.

According to Kersch [11], thermal stressing is the easiest

and most rapidly applied technique available, and is employed as follows: A real-time hologram of the object at ambient temperature is required. The object is then heated by a few degrees using infrared or hot air as the heating medium. It was established that due to cooling, the interference pattern is not static.

The debonded areas are visible as fringe distortions. However, due to the high spatial frequency of the fringe pattern, small flaws are generally masked. Experimental results showed that detection problems arose if the debonded area was smaller than half an inch in diameter and one twenty fifth of an inch in depth. In addition, viscoelastic materials were found to be incompatible due to a loss in correlation.

It is felt that the minimal detection dimensions are subject to the material under examination and are therefore to be considered as guidelines only. In addition, it should be noted that the application of heat should be carefully monitored in terms of uniformity, so as to ensure even heating of the surface, or else irregular temperature gradients could affect results obtained.

It is also felt that the success of thermal stressing, is not necessarily dependent upon laminate structures, for a defect within any suitable material should change the expansion characteristics and reveal the flaw when tested.

2.3.2.2. VACUUM OR THERMAL STRESSING

Vacuum or pressure stressing of an area of the object can be applied by placing an optically transparent vacuum vessel on the surface of the object. The vacuum within the vessel can then be varied, allowing the debonded area to elastically bulge. This detection technique, however, is generally restricted to honeycomb-type laminate defects and is not suited for adhesive to face sheet interface debonds. In addition, using vacuum, the maximum pressure difference applicable is one atmosphere.

For successful debond detection, Kersch [11] again lists minimum pressure stressing values. These values are as follows: minimum diameter of three eights of an inch and a maximum depth of one twentieth of an inch. One listed problem encountered when using pressure vessels was the deformation of the pressure vessel which occurred during a pressure change and which had an effect on the interference pattern obtained. Another general observation was that this technique is slower than the thermal stressing technique.

An obvious influence on the success of pressure stressing, is the shape of the object under inspection with respect to affixing the pressure vessel to the object surface. The minimal detection dimensions stated for pressure stressing, should again only be seen as guidelines.

2.3.2.3. VIBRATION STRESSING

Vibration stressing requires elaborate electronic equipment such as a wideband signal oscillator, a high power linear amplifier and a transducer. Upon inspection, using real-time holography, the oscillator is scanned and the interference pattern observed for loss in real-time fringes which generally outline the flawed area. As the frequency is increased, an interference pattern of a detectable flawed area will continue to break up as further sets of normal vibration modes are encountered. Minimal flaw detection parameters are listed as a quarter of an inch in diameter and one twentieth of an inch in depth.

In general, this technique has been found to be inferior to the thermal and pressure stressing techniques. In addition, the whole object can oscillate in mode sets, thereby masking the debonded area, and as such, a great amount of experience is required to interpret the interference pattern obtained. If the frequency required to oscillate the debonded area is high, strong amplifiers are required and the elastic limits of the material may ultimately be exceeded by the required force.

Another aspect worth considering, is the clamping required to prevent the object from translating as well as the effect that this clamping may have upon the vibration characteristics of the object.

2.3.3. CRACK DETECTION

Charles M. Vest [12] conducted an experiment to investigate the magnitude of perturbations induced by various sized cracks. As criteria for deflection, he mentions that the displacement deviation should be in a direction normal to the object surface and secondly, that the effect of cracking should either be localised in the neighbourhood of the crack, or else should yield abrupt changes of fringe curvature at the location of the crack.

The object used in the investigation was a channel section - three inches wide and thirty inches long - with six five-sixteenth inch holes drilled through each side of the ribs. Using a stress-etch technique, radial cracks of controlled length were produced, ranging from one hundredth to forty four hundredths of an inch.

The off-axis holographic set-up was used and the double-exposure technique was employed.

Stress was applied by drawing a tapered bolt through the hole, incrementing the applied torque between exposures. Figure 2.17 A,B,C & D illustrate the results obtained. Figure A is considered to be an interference pattern of a defect free hole and is used as a reference pattern. Interference patterns 'B,C, & D' are of holes with radial crack lengths of forty four hundredths of an inch, seventeen

hundredths of an inch and one tenth of an inch respectively. In all instances, clear interference pattern deviations from the reference pattern are visible, the areas of discontinuity depict the crack location.

Crack lengths below the order of one tenth of an inch were not considered to be conclusively detectable as it was not possible to detect their locations.

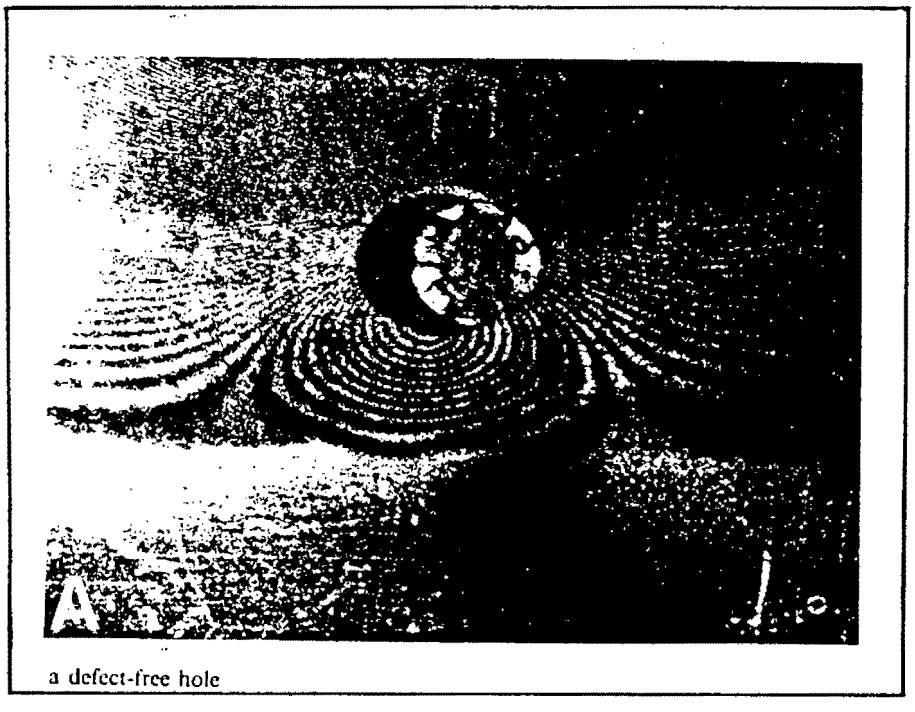

FIGURE 2.17 A (VEST ET AL, 1971)

In conclusion, it can be seen that detection of small cracks is possible using holographic interferometry. However, there is no evidence indicating the first criterion is valid, for upon drawing the bolt through the hole, expansion occurs parallel and not normal to the object surface.

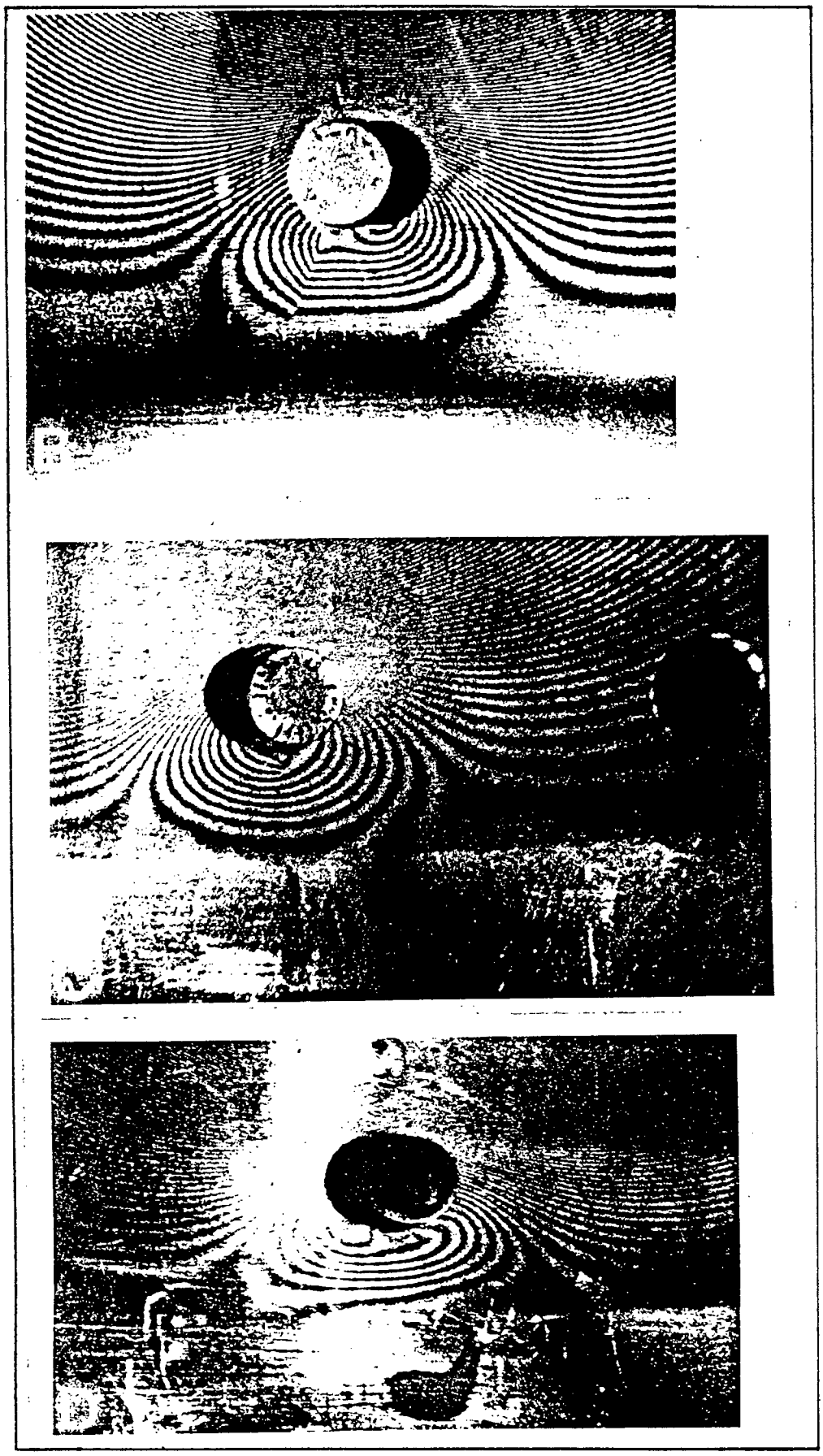

FIGURE 2.17 B C & D (VEST ET AL, 1971)

2.3.4. LAMINATE STRUCTURE INSPECTION

Leonard A. Kersch [11] conducted an experiment in which he attempted to observe the differential displacement between bonded and disbonded areas in laminate structures, by means of holographic interferometry.

Kersch presented the interference patterns from the various objects chosen and these are depicted in Figure 2.18.1 through 5.

The aluminium laminate, automotive clutchplate and simulated uranium fuel element are amongst the objects thermally stressed, whereas vibrational and thermal stressing mechanisms were compared on the graphite epoxy jet-engine fan blade. The final set of illustrations presents the effectiveness of pressure stressing on three further examples.

No final conclusions are drawn from the experiments undertaken, nor is there any mention of problems encountered. It was most probably assumed that the figures were self-explanatory, which of course they are in terms of results obtained. However, this unfortunately does not help establish the feasibility of the testing technique.

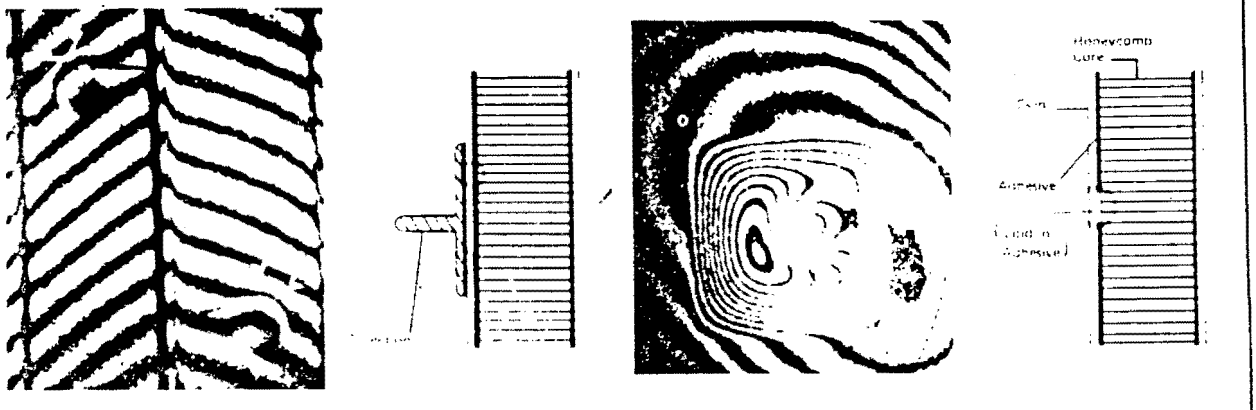

Examples of thermal stressing in (A) two different aluminum laminates with phenolic resin bonding with 5 F temperature change

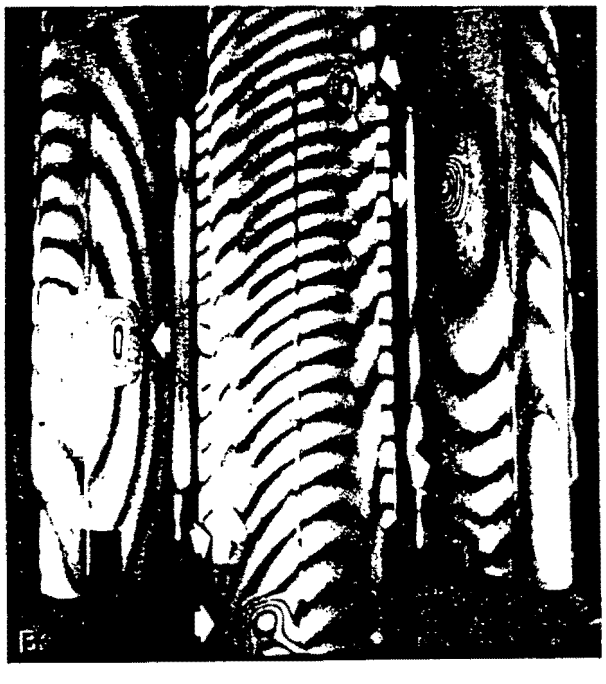

a simulated cylindrical uranium fuel element

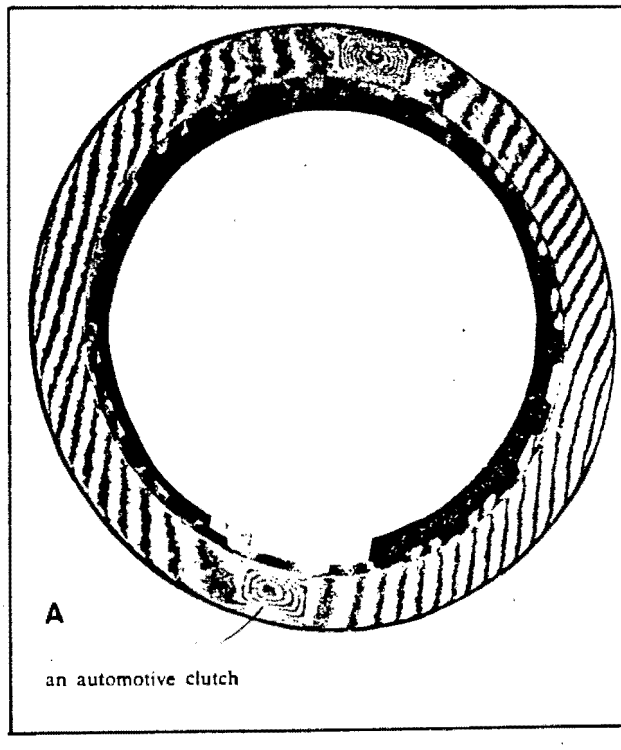

an automotive clutch

FIGURE 2.18. 1 2 & 3 (ERF, 1974)

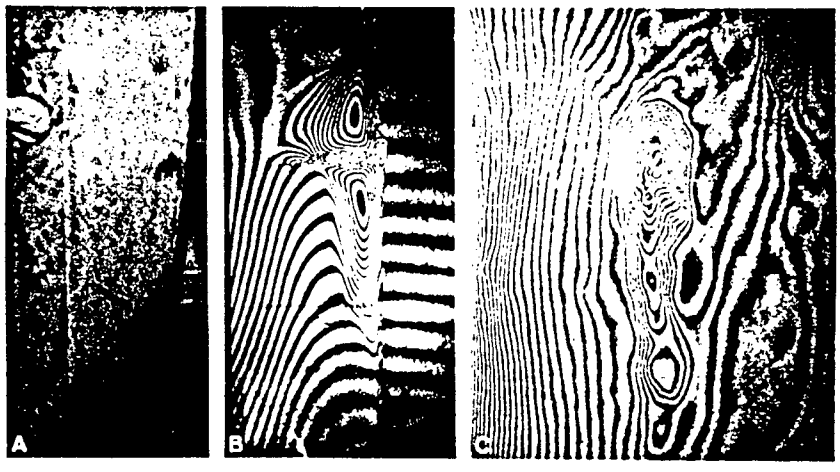

Inspection of graphite epoxy jet-engine fan blades with metal leading-edge strips using (A) vibration stressing (65 kHz); and (B, C) thermal stressing. In C a large disbond about 6 layers deep (0.018 in.) is illustrated with the blade being heated from the opposite side.

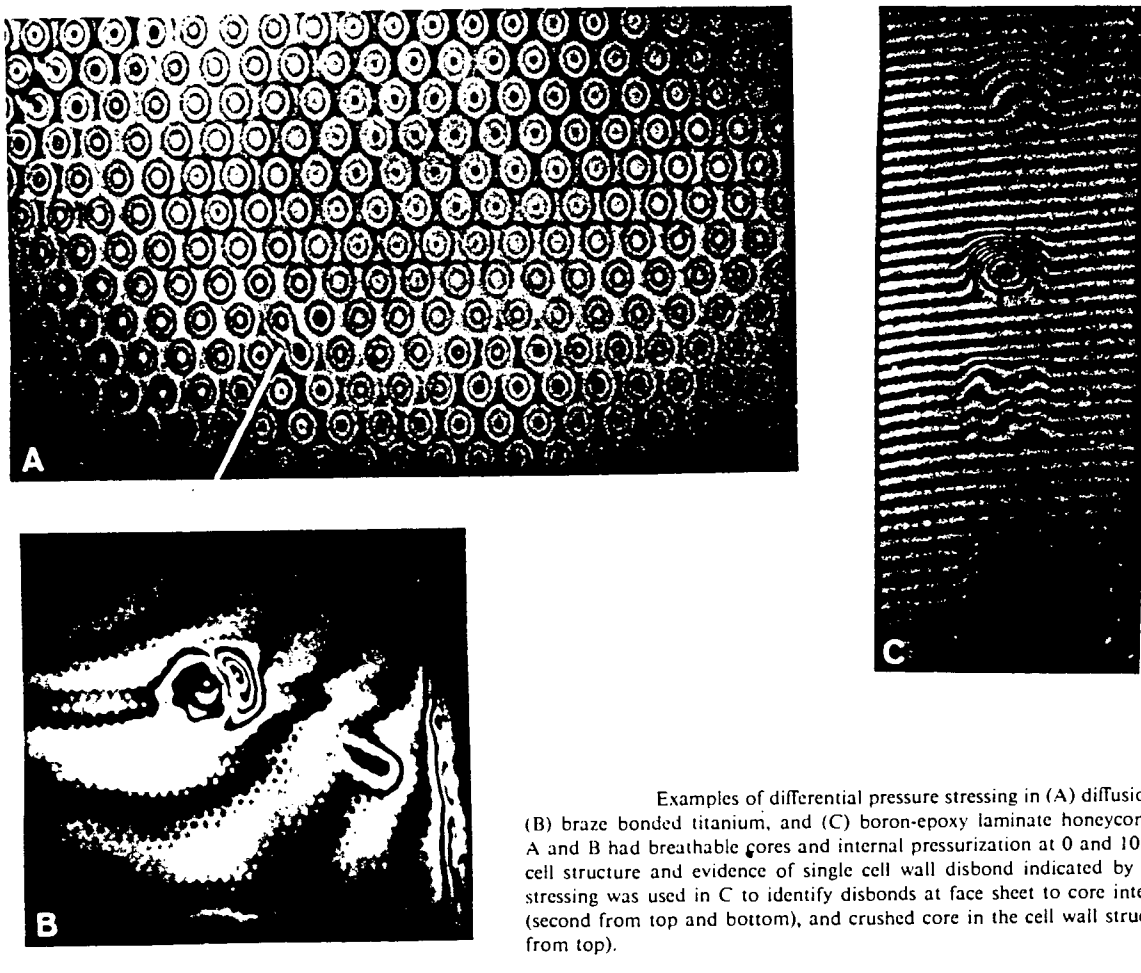

Examples of differential pressure stressing in (A) diffusion bonded titanium, (B) braze bonded titanium, and (C) boron-epoxy laminate honeycomb structures. Both A and B had breathable cores and internal pressurization at 0 and 10 psi was used. Note cell structure and evidence of single cell wall disbond indicated by line in A. Vacuum stressing was used in C to identify disbonds at face sheet to core interface 0.025 in. deep (second from top and bottom), and crushed core in the cell wall structure (top and third from top).

FIGURE 2.18. 4 & 5 (ERF, 1974)

All the figures show clear irregularities present in the interference patterns due to the differential displacement in the region of the debond. Vibration stressing proves to be the least effective of the techniques, with thermal and pressure stressing producing clear identification of defective areas.

It is assumed that each set-up would have to be a customisation of the off-axis technique which is believed to have been employed in this instance. This is emphasised in Figure 2.18.3.

2.3.5. ACOUSTIC STRESSING OF COMPOSITE MATERIALS

As has been previously mentioned, acoustic stressing techniques can be employed to detect flaws using holographic interferometry. Robert K. Erf [13] employed this technique to test composite blades constructed from both fibre reinforced resins and metal bonded fibres.

Using piezo electric transducers, coupled via an exponential horn to the object, a wide excitation range can be obtained. The transducer is driven at object resonance frequency and the horn thus couples a high level of acoustic energy into the sample. This is depicted in Figure 2.19.

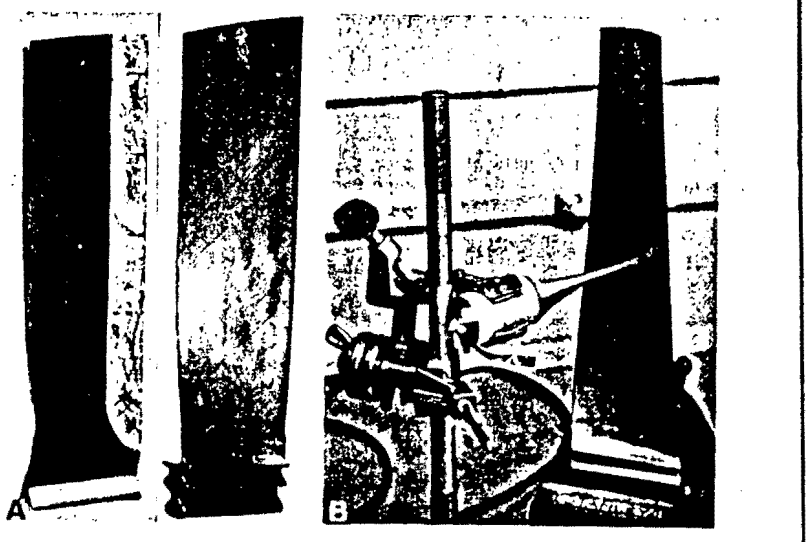

Typical composite structures (A) which have been studied include a boron–polyimide airfoil (left) and a Borsic–aluminum fan blade (right), with the latter shown set up (B) for holographic inspection using an exponential horn transducer drive assembly to introduce stress.

FIGURE 2.19 (ERF, 1974)

Figure 2.20 shows a prepared sample as well as the test results. The interference pattern reveals the fringes produced by the various sized defects in the various layers of the composite.

When inspecting the object at resonant frequency, it is necessary to devise a technique to seperate debond related resonance patterns from object related resonance patterns in the produced interference pattern.

The technique that Erf [13] employed to achieve this separation, was the dual holographic system. This is a modification of the off-axis system consisting of two object and two reference beams. Two holograms are thus simultaneously recorded, one of the front of the object and

one of the rear of the object. See Figure 2.21.

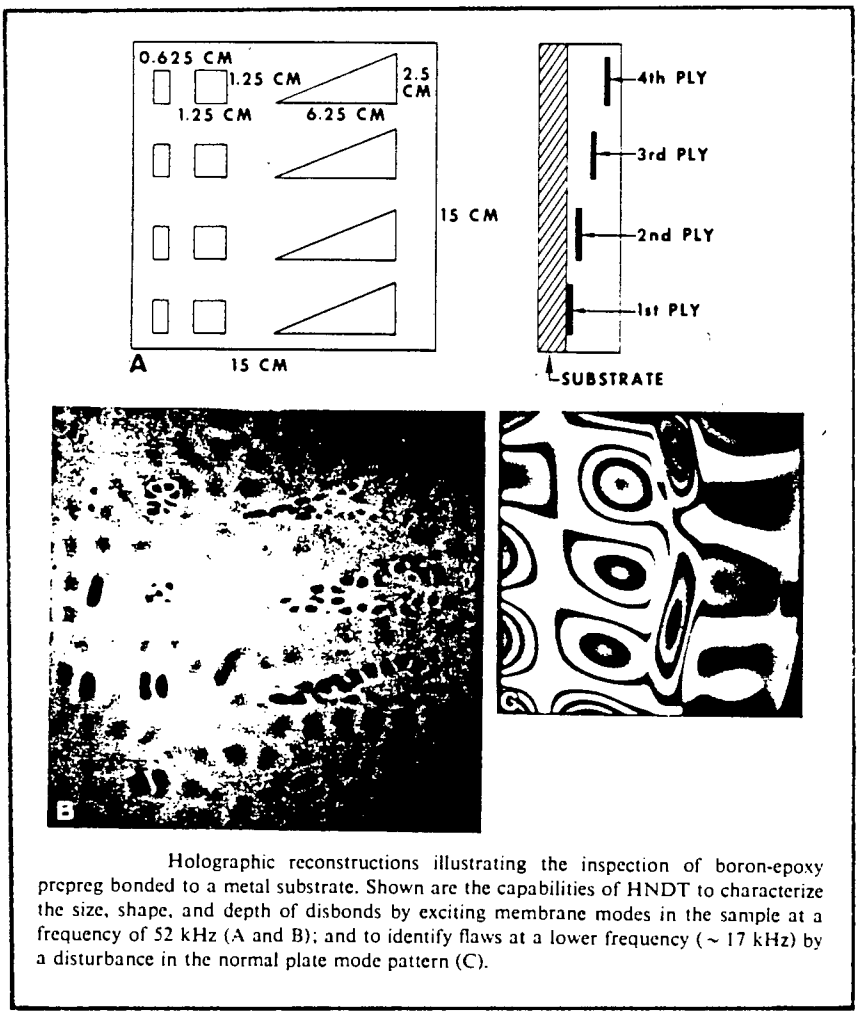

Holographic reconstructions illustrating the inspection of boron-epoxy prepreg bonded to a metal substrate. Shown are the capabilities of HNDT to characterize the size, shape, and depth of disbonds by exciting membrane modes in the sample at a frequency of 52 kHz (A and B); and to identify flaws at a lower frequency (~ 17 kHz) by a disturbance in the normal plate mode pattern (C).

FIGURE 2.20 (ERF, 1974)

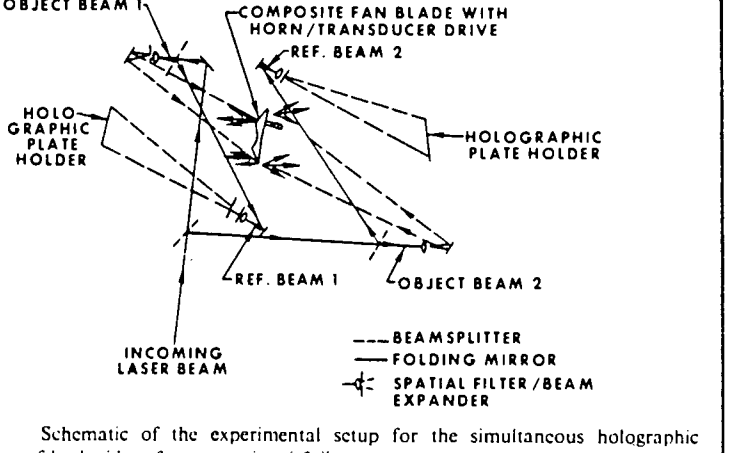

Schematic of the experimental setup for the simultaneous holographic examination of both sides of a composite airfoil.

FIGURE 2.21 (ERF, 1974)

When comparing the recorded holograms, a one to one relationship between interference patterns indicates object resonation and the areas of irregularity indicate debond resonation. Figure 2.22 and 2.23 indicate the interference patterns obtained from a good and faulty turbine blade, respectively. In addition, ultrasonic probe tests are also depicted for comparison.

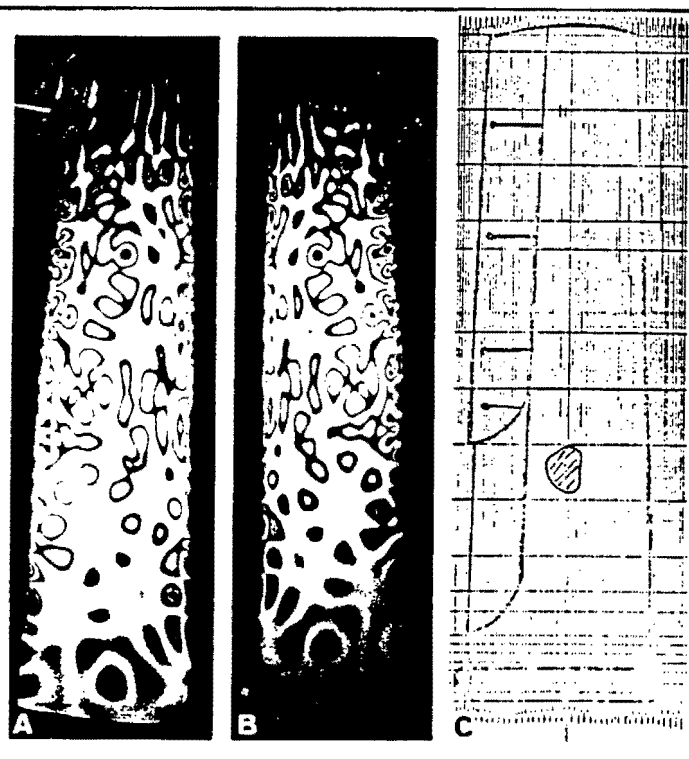

(A and B) Holographic reconstructions of an airfoil with no significant defects illustrating the one-to-one correspondence in the mode patterns between the (A) pressure and (B) suction sides, and (C) a schematic diagram depicting the ultrasonic probing results for the same airfoil.

FIGURE 2.22 (ERF, 1974)

The main advantage listed by Erf [13] is the superiority of accoustic stressing holographic non destructive testing over conventional ultrasonic testing. In addition, the technique is capable of determining the size and shape of the flaw as

well as the possiblity of determining the depth of its location.

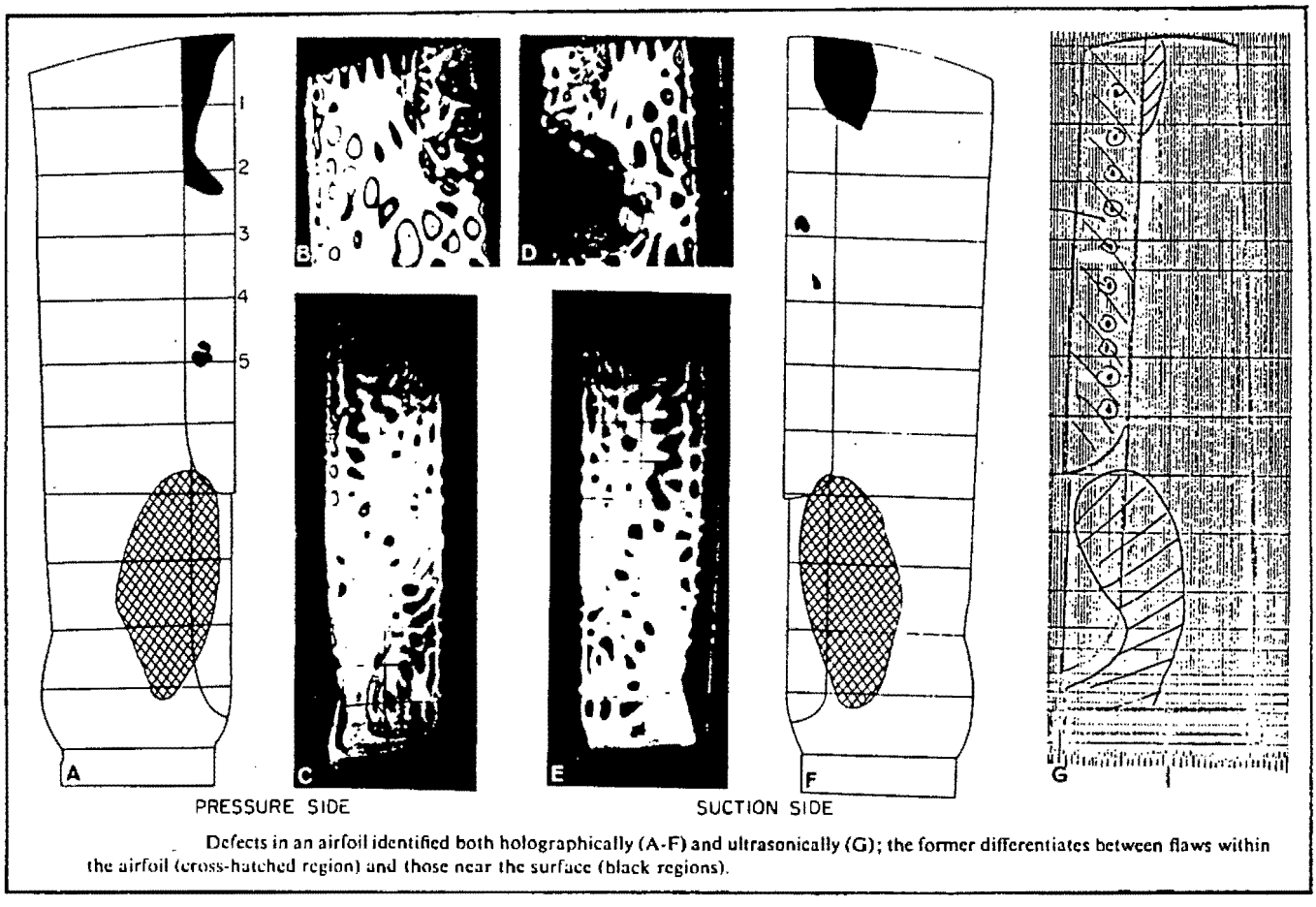

Defects in an airfoil identified both holographically (A-F) and ultrasonically (G); the former differentiates between flaws within the airfoil (cross-hatched region) and those near the surface (black regions).

FIGURE 2.23 (ERF. 1974)

The disadvantages listed include the need for careful and extensive study of the component, the expected defects and the interference patterns obtainable, in other words, much effort is required to develop the object testing proceedure and to evaluate the results obtained.

However, as shown in Figure 2.22, holographic interferometry, did not reveal flaws which were revealed by the ultrasonic testing technique - as marked by the shading.

This leads to speculation about the detectability merits of both systems. In addition, in Figure 2.23, the interference patterns do not clearly indicate the exact regions of debonding - as marked on the diagram. The ultrasonically obtained defect regions compare with the holographically obtained results, further creating doubt as to the superiority of the acoustic stressing technique.

Finally, the complexity of the procedure and the need for two holograms, limits the application and makes the thermal or pressure stressing technique more favourable.

2.3.6. EXAMINATION OF PRE-BUCKLING OF AXIALLY LOADED CYLINDERS

I. Leadbetter and T. Allen [14] performed an investigation into the buckling behaviour of axially loaded cylinders. The experiments performed were of a qualitative nature and the double-exposure holographic interferometric recording technique was employed.

The apparatus used to conduct the experiment basically consisted of a top and bottom platform in between which, the cylinders were placed. Stress was applied by rotating a threaded central shaft which lowered the top platform.

Double exposure holograms were recorded at set worm

rotations with incremental worm rotations applied between exposures.

The initial set of results was obtained with a cork washer between test cylinder and testing rig. It is reported that the shell buckled at a total of fifty one rotations. The results obtained are presented in Figure 2.24.

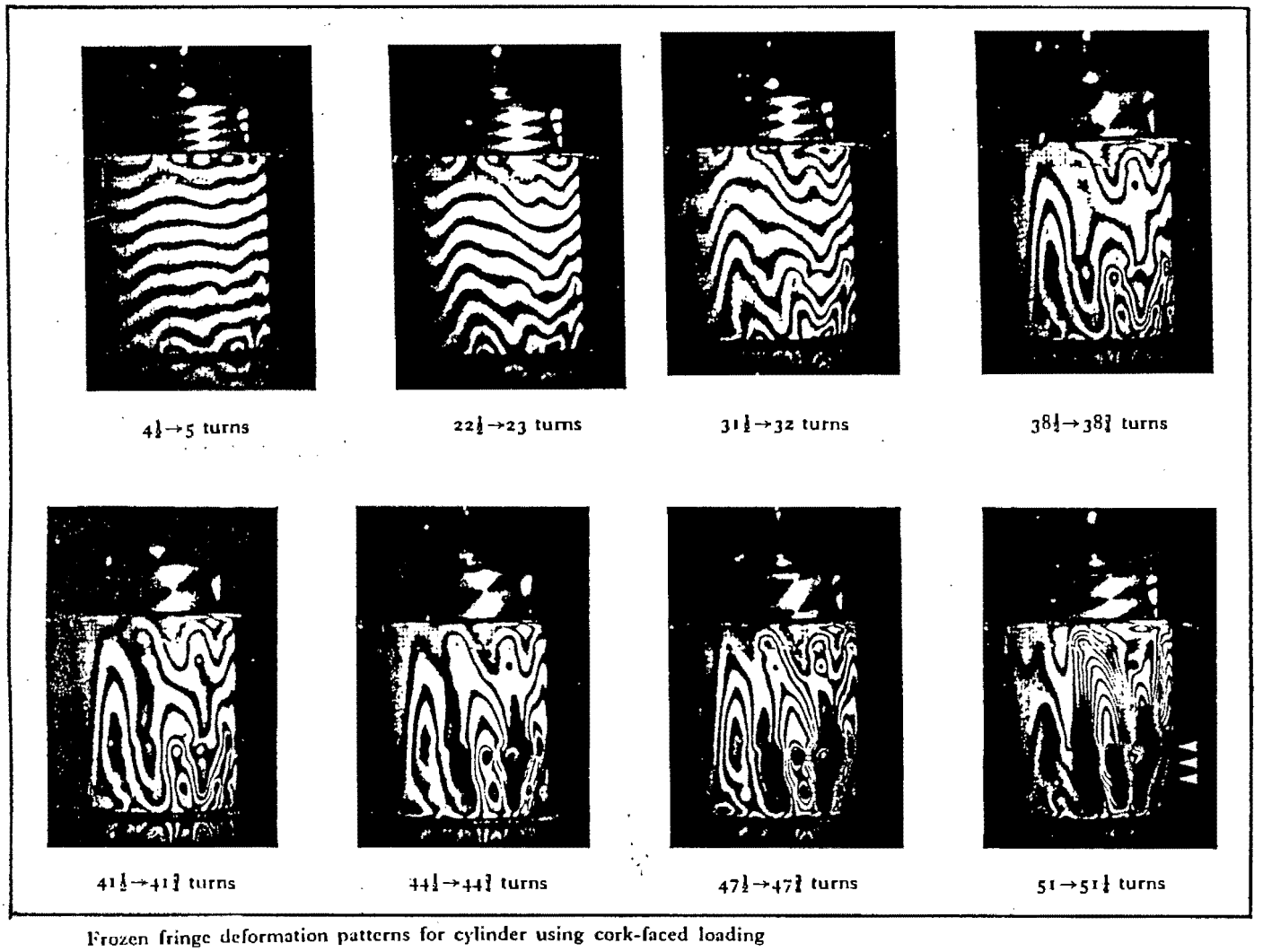

Frozen fringe deformation patterns for cylinder using cork-faced loading

FIGURE 2.24 (LEADBETTER & ALLEN IN ROBERTSON ED., 1970)

From the interference pattern, it was interpreted that barrel-type distortion had initially ocured. Edge effects

were to be ignored due to the effects of the cork washers. Maximum activity was noted to take place at roughly thirty five turns and was centered in the lower right quadrant. Evidence of vibration was also visible. Buckling finally took place in the area of maximum activity.

The second experiment was conducted by eliminating the cork washer and then recording two holograms, one of the left and one of the right side of the cylinder. The results are depicted in Figure 2.25.

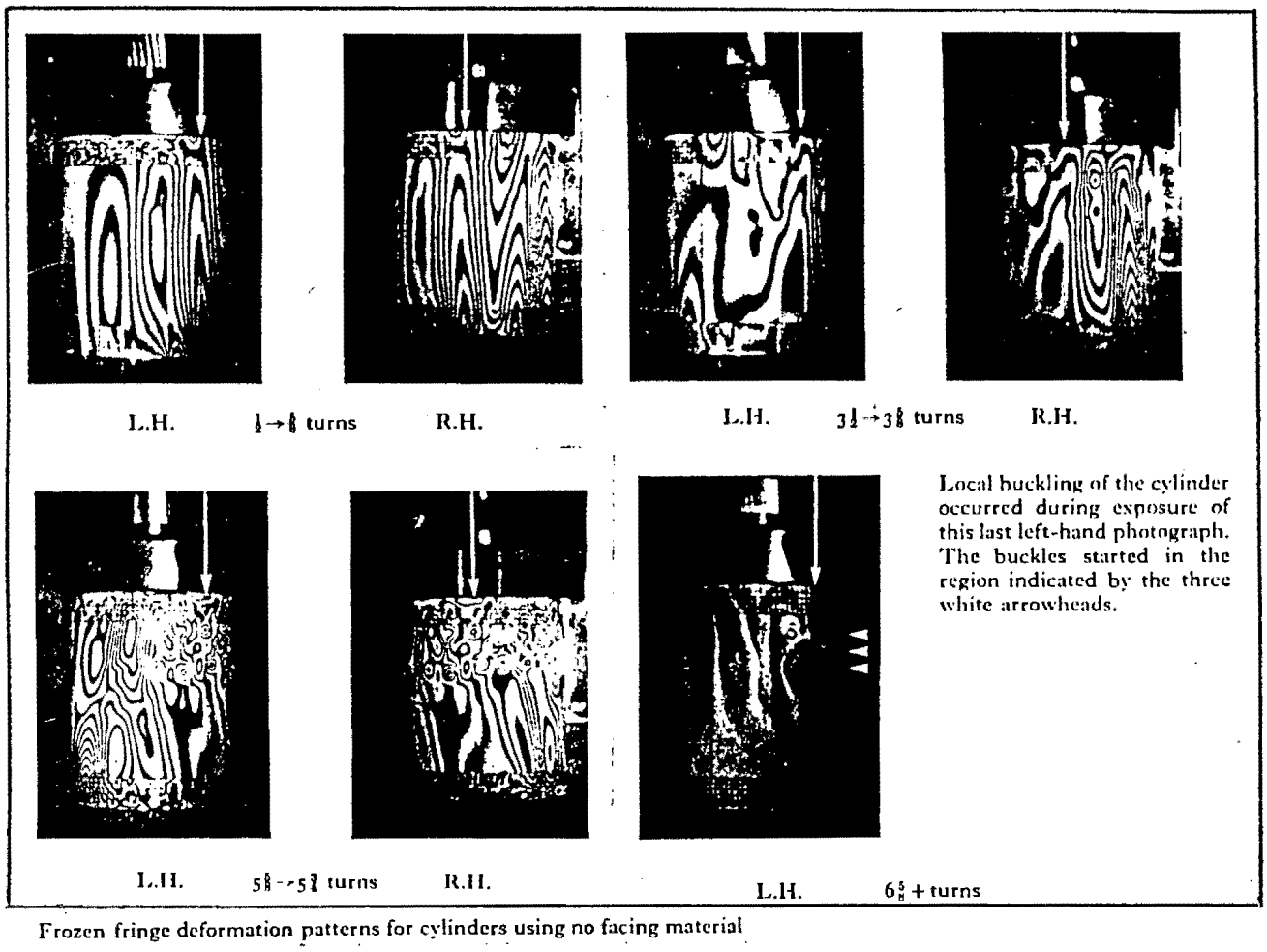

Frozen fringe deformation patterns for cylinders using no facing material

FIGURE 2.25 (LEADBETTER & ALLEN IN ROBERTSON ED., 1970)

The results indicate that no barrel-type distortion was present. The maximum area of disturbance was found to be in the top right-hand quadrant of the left-hand view where eventual buckling occurred. Vibration was also apparent when the cylinder buckled.

It became obvious that the cork caused a cushioning effect and was therefore responsible for the barrel-type distortion present in the first experiment. This explains the difference in fringes obtained between the two experiments, as well as the differences in worm rotation required to initiate buckling. It is therefore felt that the boundary conditions applied are extremely important and that their effect must be known in order to prevent misinterpretation. In addition, the experiment deduces that properties such as manufacturing conditions, material imperfections, etc., will affect the final results obtained.

Finally, the large discrepancy that exists between the theoretically predicted uniform expansion and the highly irregular interference pattern obtained should be noted.

2.3.7. SURFACE DISPLACEMENT ANALYSIS

J. Vienot et al. [15] have performed some work in the area

of determining the fringes obtainable from selected motions. The double-exposure off-axis technique was used to record interference holograms.

The object holder which was kinematically mounted, produced the required displacements. The mount was mobile in the three principle directions and was rotational about two axis.

The reconstruction process employed either the original reference beam which allowed the viewing of the virtual image - or the conjugate reference beam - which facilitated viewing of the real image. Viénot's report on the results obtained when analysing translations is as follows:

Translation perpendicular to the direction of observation yielded rectilinear interference fringes which were perpendicular to the direction of displacement, located in a plane which was not dependent on the importance of the displacement. Visibility was high, irrespective of the size of the reconstruction beam. Figure 2.26 illustrates the displacement direction and the fringes obtained.

The loss in clarity and density of the fringes was due to the fact that the fringe location was behind the object and was therefore out of focus in the photograph.

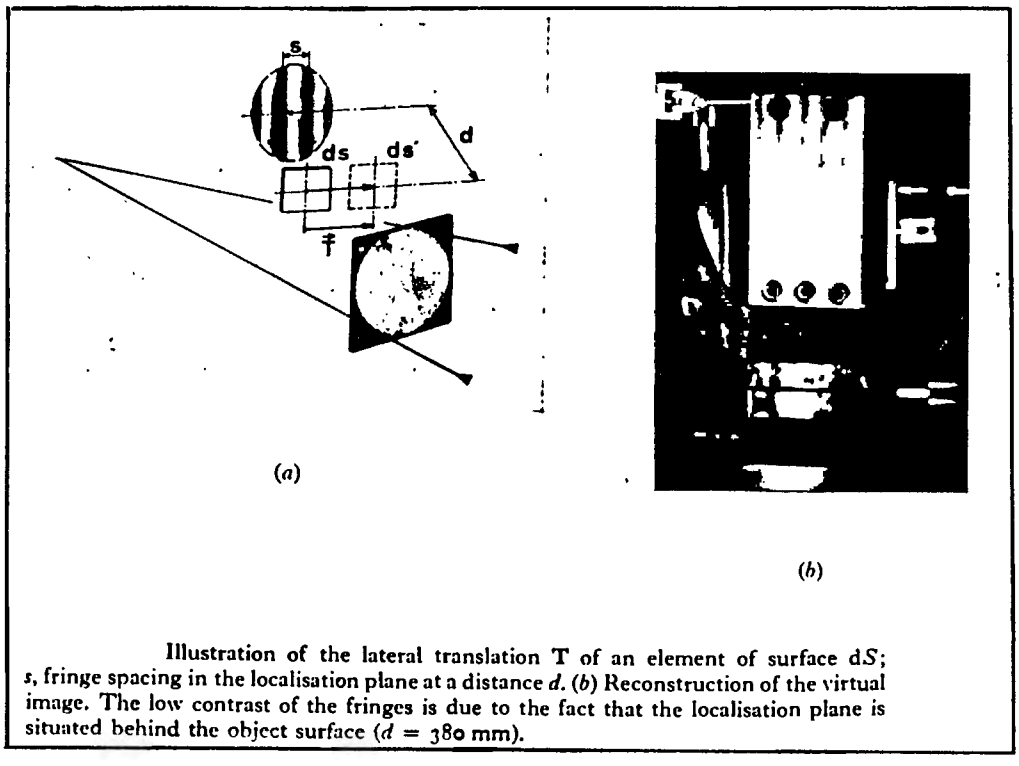

Illustration of the lateral translation T of an element of surface dS; s, fringe spacing in the localisation plane at a distance d. (*b*) Reconstruction of the virtual image. The low contrast of the fringes is due to the fact that the localisation plane is situated behind the object surface (d = 380 mm).

FIGURE 2.26 (VIÉNOT IN ROBERTSON ED., 1970)

If the working area of the hologram was kept large, translation parallel to the direction of observation yielded an interference pattern with no visible fringes. If the area was reduced, that is, using a restricted aperture, rings either semi-complete or complete, appeared in a poorly defined location plane. On the other hand, it was reported [15] that if a plane wave was used on the object in the recording process, then in the reconstruction process, rings which were localised at infinity and were highly contrasted were visible. This phenomenon is illustrated in Figure 2.27.

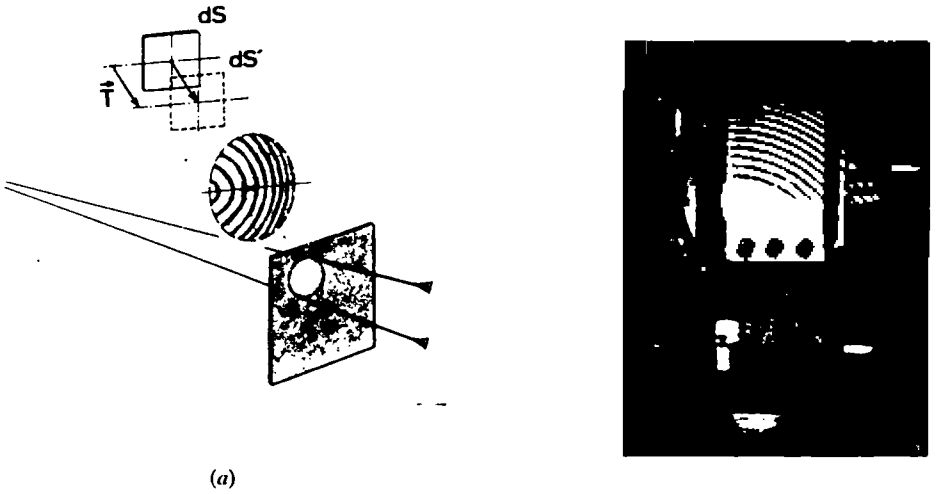

(a)

(b)

Translation parallel to the direction of observation: (a) principle, (b) reconstructed image.

FIGURE 2.27 (VIÉNOT IN ROBERTSON ED., 1970)

Rotation about an axis perpendicular to the direction of observation resulted in interference fringes which were well contrasted and localised on the plane of the object, and were located parallel to the axis of rotation. This is depicted in Figure 2.28.

Rotation about an axis parallel to the direction of observation resulted in the formation of parallel fringes in the interference pattern. Their contrast decreased as the working area of the hologram increased. In addition, the orientation of the fringes were dependent on the area of illumination of the hologram as is seen in Figure 2.29.

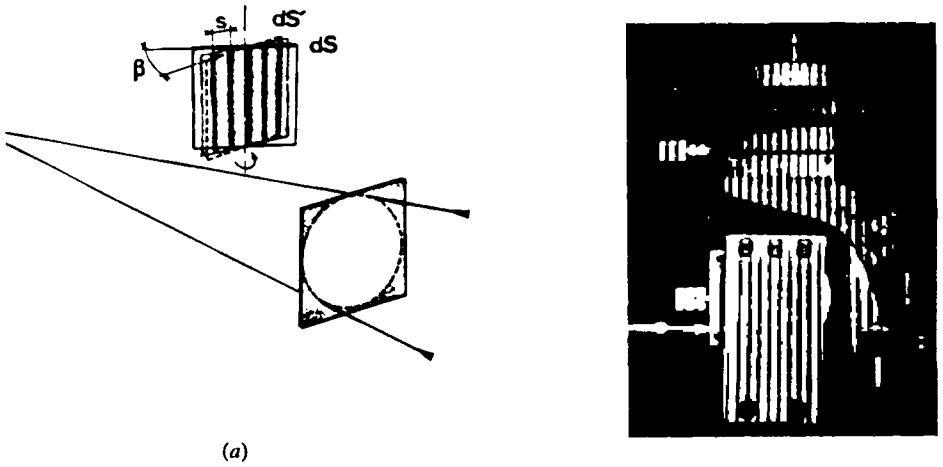

(*a*)

(*b*)

Pure rotation of the element of surface dS through an angle β about an axis perpendicular to the direction of observation: (*a*) principle. (*b*) reconstructed image, its average plane is the same as that of fringe localisation.

FIGURE 2.28 (VIÉNOT IN ROBERTSON ED., 1970)

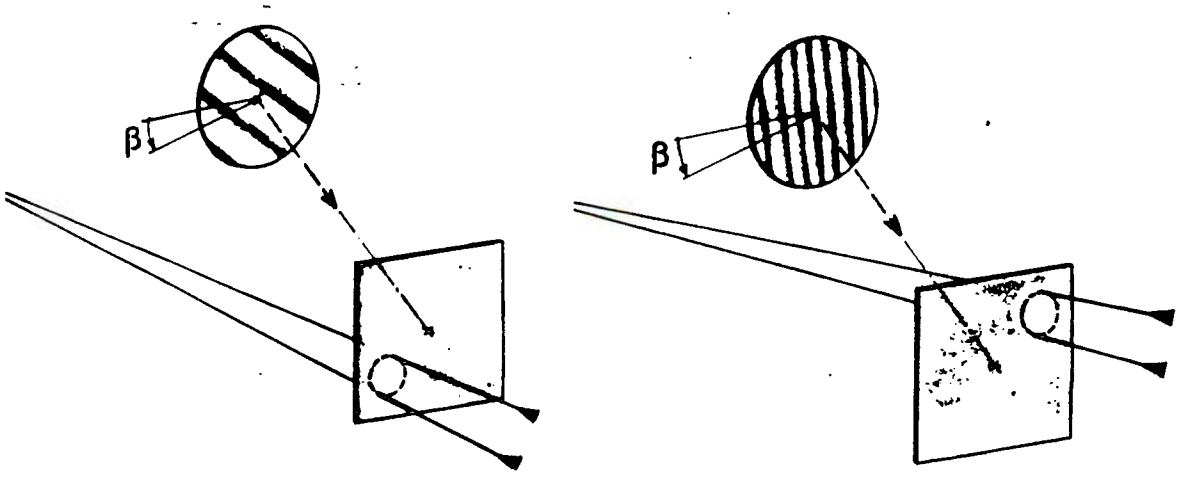

(*a* and *b*). Rotation about an axis parallel with the direction of observation: the interference pattern depends on the working region on the hologram.

FIGURE 2.29 (VIÉNOT IN ROBERTSON ED., 1970)

In summary, the authors mention that by establishing characteristic fringe structures related to known types of motion, within an interference pattern, the object displacement can be determined.

Ennos [16] has also written a paper on fringe interpretation and he suggests methods such as a point by point examination of the hologram using a restricted reconstruction aperture. A type of spatial filtering on the recorded film is also suggested. Here again, it is necessary to associate the visible fringe pattern with its known displacement in order to obtain the type of translation recorded by holography.

In his report, Jon E. Sollid [17] emphasises that special care must be taken when analysing fringe patterns, as radically different displacements can essentially produce identical fringe patterns.

Erf [18] reports significant differences in interference patterns obtained when using either continuous wave lasers or pulsed lasers for the holographic interferometric process. In addition, he states that when attempting to analyse motion in defect regions of an object, it is essential to have a record of the fringe pattern obtained from an identical, defect free, object. These two interference patterns are essential for comparison when determining object motion due to defects within the object.

In theory, the technique is applicable and is certainly successful in elementary cases. It is however dubious as to whether all the components of a compound translation can be resolved and whether its principle direction can be derived. In addition, it should be noted that all the displacements derived from the fringe patterns observed up to now are of a qualitative nature only.

2.3.8. INTERPRETATION OF HOLOGRAPHIC INTERFERENCE

J.D. Briers [19] presented a paper in which various quantification methods applicable to holographic interferometry were compared. The quantification of holographic interferometry is a technique with which the interference pattern obtained, caused by stressing an object, is evaluated in terms of the displacement of the object due to the stress applied.

Various methods have been proposed during the course of history. Of the four techniques presented, the two that receive the best merits are the zero-fringe technique, developed by Ennos [20], and the fringe counting technique, developed by Aleksandrov and Bonch-Bruevich [21].

The basic method employed by Ennos's zero-fringe technique is the calculation of the optical path differences between the images that form the interference pattern. The

technique is best applied when the fringes are localised on the object, that is, when the deformation is of a rotational nature or if the deformation is out of plane.

Once the interference pattern is obtained, the zero-order fringe must be located. It is reported that a piece of rubber linked between the object and a secure base is normally used. The base will have no fringes and will therefore be of zero-order nature. The fringe-order formed on the object can be related to the zero-order base via the rubber. Using the equation, path difference = $m\lambda$ (2.7) , where m designates the fringe order and λ designates the wavelength of the laser light used. Once m is determined, the optical path difference can be calculated. The problem then is one of pure geometry to relate the path difference to the displacement at the required point.

The fringe counting technique uses the fringe parallax method to determine the displacement of a point in an interference pattern. This is because, the fringes are generally located some distance from the object. Therefore, if one scans the reconstructed hologram from one side to another, the fringes are seen to pass through a noted point on the object. By counting the number of fringes, passing through this point, the equation $dx = N\lambda L/x$ (2.8)can be used to determine the translation dx, where N designates the number of fringes counted,λdesignates the wavelength of light, L designates the distance between hologram and reconstructed

image and x designates the length of hologram scanned. The displacement dx is the component of the in plane displacement relative to the bisector of the angle through which scanning of the hologram took place. The above is illustrated in Figure 2.30.

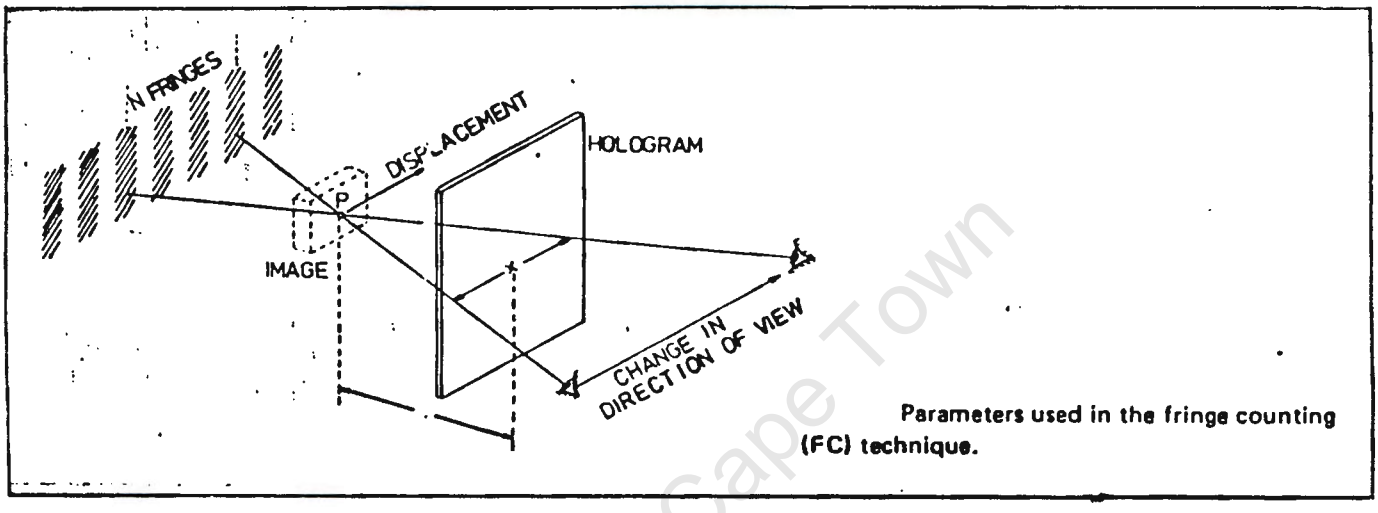

FIGURE 2.30 (J.D. BRIERS, 1976)

There seems to be discord amongst authors as to whether or not there is a plane of localisation of fringes and whether it should rather be called a plane of maximum visibility of fringes.

Haines and Hildebrandt [22] devised a quantification technique in which the establishment of the plane of fringe localisation was essential in determining the displacement. However, predicted accuracy of the results obtained from their tests was often as poor as around sixty percent.

It is felt that the quantitative theories presented do fundamentally represent a sound mathematical interpretation. However, relating the optical path difference to the actual three dimensional distortion of the object under inspection, is considered to be a far more complex task than is suggested above.

2.3.9. APPLICATIONS OF HOLOGRAPHIC INTERFEROMETRY

The various holographic applications have led to the development of customised commercially available testing rigs for specific objects.

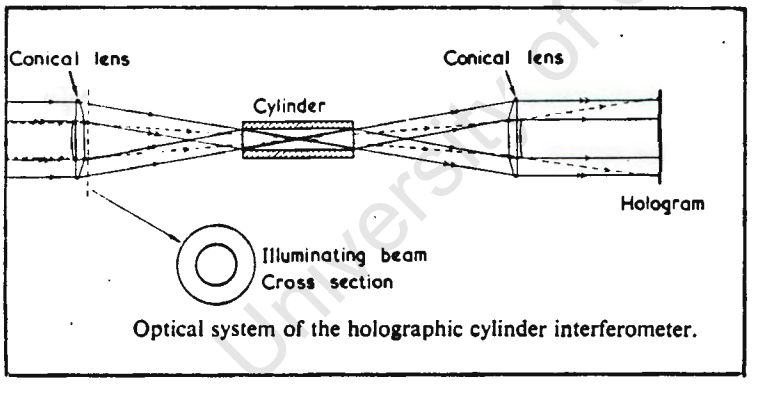

Optical system of the holographic cylinder interferometer.

FIGURE 2.31 (ENNOS ET AL, 1967)

One of these, designed and reported by Ennos [23], was the holographic cylinder interferometer. Real-time holography made it possible to compare a cylinder bore, produced in a workshop, with an image of a master cylinder bore which was

projected by a holographic recording of the object. For interference to take place between the object and the image, precise location was necessary. This was achieved by using ball bearing locators. In addition, smooth object surfaces were essential. Special annular conical lenses were used to illuminate both the object and the hologram with the same laser beam. See Figure 2.31.

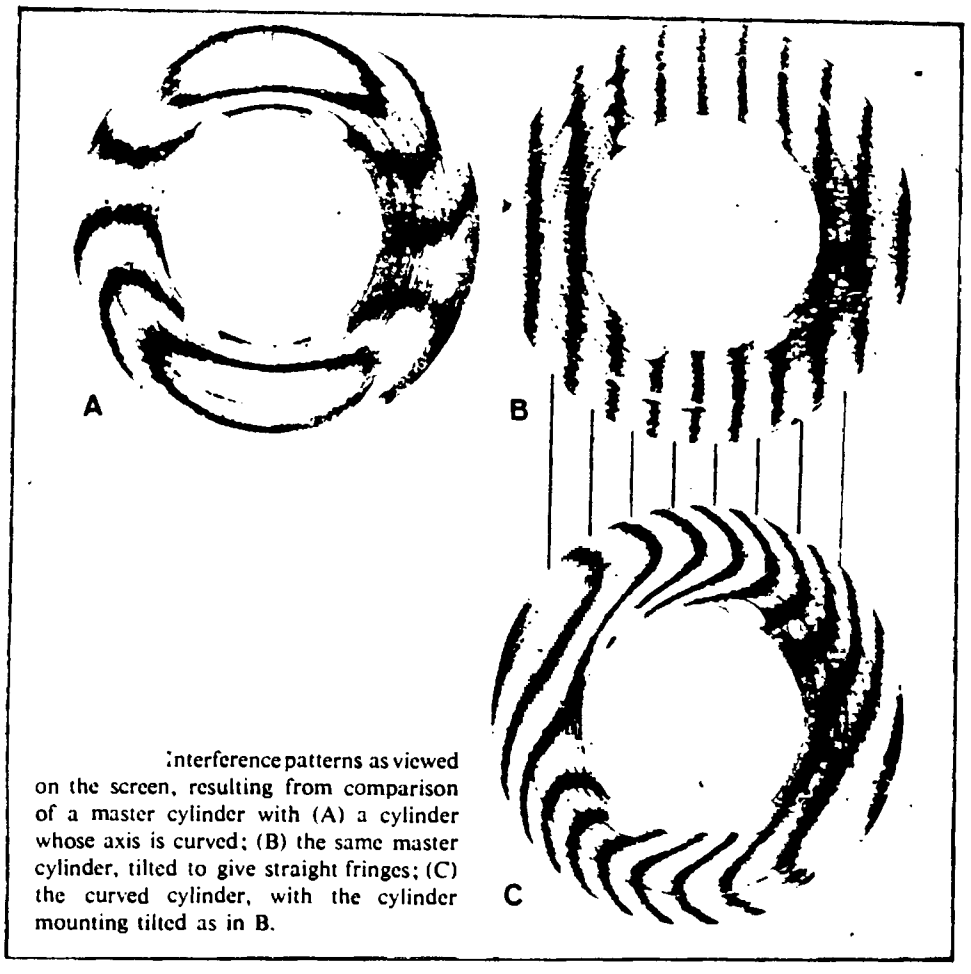

Interference patterns as viewed on the screen, resulting from comparison of a master cylinder with (A) a cylinder whose axis is curved; (B) the same master cylinder, tilted to give straight fringes; (C) the curved cylinder, with the cylinder mounting tilted as in B.

FIGURE 2.32 (ENNOS ET AL, 1967)

It is reported that with this system in operation, an interference pattern, which resulted from the interaction

between the lightwaves of the inner bore of the object and the image, were obtainable. These interference patterns were then indicative of the conformity between the master image and the object as shown in Figure 2.32.

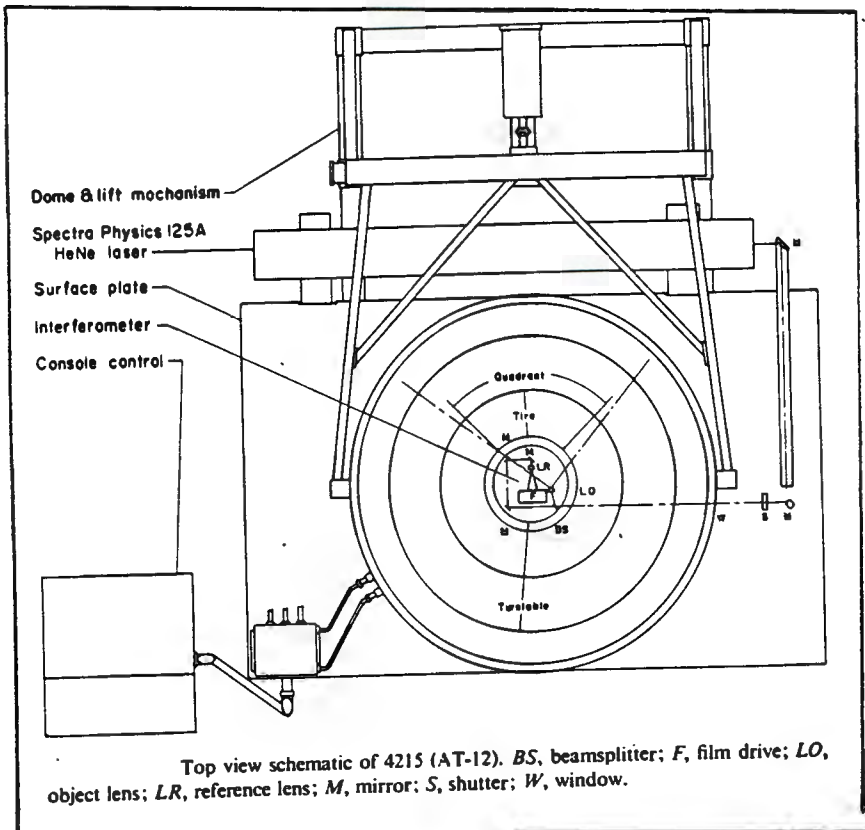

Top view schematic of 4215 (AT-12). *BS*, beamsplitter; *F*, film drive; *LO*, object lens; *LR*, reference lens; *M*, mirror; *S*, shutter; *W*, window.

Photograph of GCO Model 4215 (AT-12) tire separation tester with 60-in.-i.d. dome.

FIGURE 2.33 (BROWN, 1973)

Another interesting inspection system developed was the tyre separation tester which was designed by Gordon M. Brown [24] and colleagues at GCO Inc.

Brown reported that the system used the vacuum inside method which was described as follows:

Double-exposure holograms were recorded of the inside of the tyre, the first exposure being recorded at atmospheric pressure and the second, at one tenth to one third atmospheres below atmospheric pressure. The whole tyre and holographic set-up was encapsulated in a vacuum chamber. Figure 2.33 depicts the tester and the top schematic view.

It has been reported that the tester is capable of detecting tread, ply and liner separations, broken glass belts, cord to rubber unbonds, bead to rubber unbonds, voids and types of porosity. Figure 2.34 depicts some of the interference patterns obtained by the tester.

It is felt that designs such as these are of major importance as they offer a new and valuable inspection tool and emphasise the viability of holographic non destructive testing in industry. However, it should be noted that the design is customised to suit the objects tested.

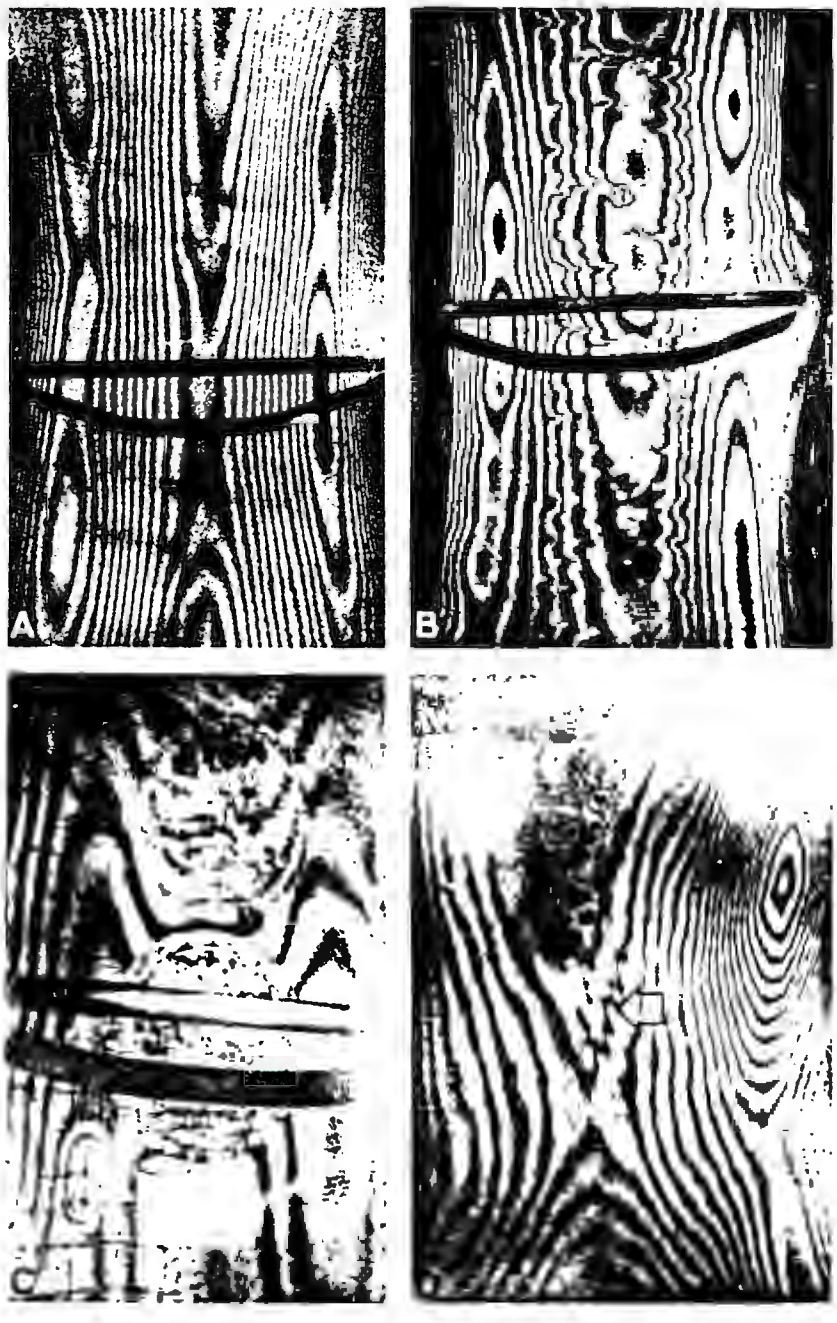

Holographic reconstructions showing: (A) typical fringe signature of gross motion on a normal automobile tire with no separations; (B) glass belted 16.5 · 380 radial automobile tire with belt separations resulting from road tests; (C) 900-20 16 P.R. nylon and steel radial truck tire with (1) a 1 · 2-in. belt edge separation 0.4 in. below the inner surface and (2) two poorly bonded balance patches [courtesy AST]; and (D) 1000-20 12 P.R. nylon truck tire showing irregular or jagged fringe signature in the tread region, indicating cord-to-rubber unbonding [courtesy AST].

FIGURE 2.34 (BROWN, 1973)

2.3.10. DISPLAY HOLOGRAPHY

One aspect of holography which is not related to the non destructive testing field, is display holography. The reconstruction process of the hologram could either be of a transmission or reflection nature. Almost every practically oriented book on holography elaborated on the making of various reflection holograms. However, if reflection holograms are to be made commercially available, they must be reproducible. These holograms are generally called transfer or copy holograms and can be viewed in white light.

According to Unterseher et al [25], a good transfer hologram can only be made from a good master hologram. Generally, they are of the off-axis transmission type (as discussed in chapter 2.2.1). They must be bright, have a low level of noise and must not be distorted.

They can also be of the reflection type (as described in chapter 2.2.2), but the set-up then generally becomes more complicated.

The transfer technique - discussed in chapter 2.2.2.1 - facilitates the production of very bright white-light holograms. It has been reported [26] that by restricting the aperture of the master hologram, the luminance can be severely increased.

A modification of this technique is multiplexing. Saxby [26] reports that in this technique, several individual objects are recorded either individually onto segments of the master hologram, or onto individual holograms which are placed next to each other.

In the recording process, all the images are stored on the transfer hologram. However, when the transfer hologram is viewed, the individual images of the object appear and disappear as the viewing position is changed. It is however essential that each section of the master hologram has a recording of only one of the objects. Figure 2.35 illustrates the multiplexing principle with the "Yalta" hologram.

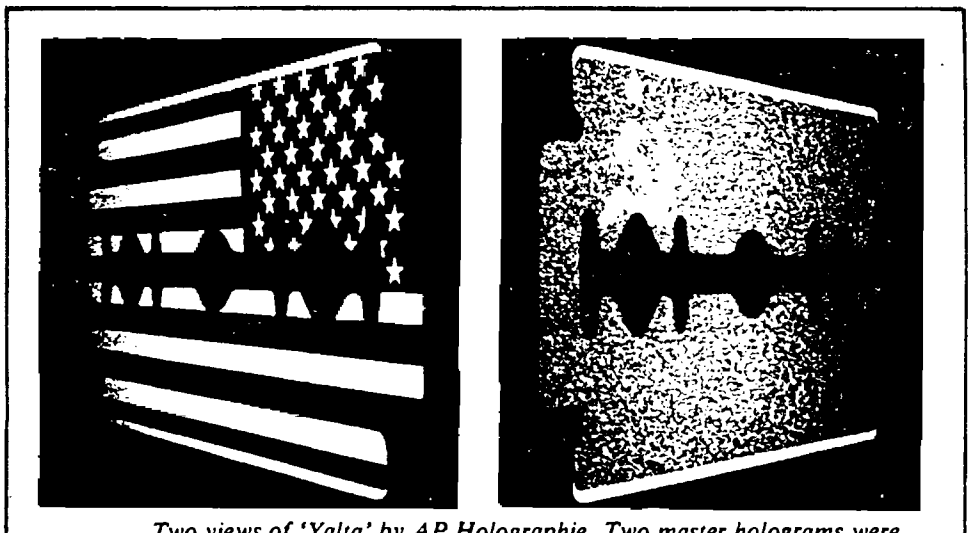

Two views of 'Yalta' by AP Holographie. Two master holograms were used in order to obtain a wide angle of view.

FIGURE 2.35 (SAXBY, 1988)

It has been reported that only two images can be stored if the change from one image to the other occurs whilst horizontally changing the observation position. However, if

this occurs vertically, up to nine images can be stored and reconstructed separately.

It is obvious that with this technique there is unlimited scope for further experimentation. It is also felt that in this field pure experience and 'feel' can obtain optimum results.

CHAPTER 3

Three areas of holography were investigated in the form of projects. These were qualitative holographic interferometry, quantitative holographic interferometry and white-light transfer holography.

3.1. OPTICAL EQUIPMENT AND CHEMICALS

The experiments were performed upon an air cushioned mild steel plate. The optical elements employed were secured to the metal plate by means of magnets fixed into their individual bases. The basic optical elements utilised are briefly described below, and except for the laser, are shown in Figure 3.1.

No. 1: LASER

The laser used was a Spectra Physics 35 mW Helium-Neon continuous wave laser with an output wavelength of 633 nm.

No. 2: BEAMSPLITTER

The beamsplitter used in the laboratory was a circular wedge variable beamsplitter. One side of the circular wedge was aluminium coated, the density of which varied with the angle of rotation.

FIGURE 3.1 Optical elements used.

No. 3: BEAM EXPANDER

The beam expander consisted of a 40x microscope objective, a precision made 5 micron pinhole and a fine focusing mechanism. The pinhole used, acted as a spatial filter to 'clean up' the beam.

No. 4: EMULSION PLATE HOLDER

The precision plate holder consisted of a base and a plate holding frame. The plate was located on the frame with spring clips and the frame, by using knife edges as locators, was placed onto the base mount. In addition, micrometers allowed the mount to be adjusted vertically or horizontally.

No. 5: ADJUSTABLE MIRROR

The adjustable mirrors were used to direct the laser beam. They were aluminized on the front surface and included a fine adjusting mechanism.

No. 6: COLLIMATING LENS & MIRROR

The collimating lens or mirrors were used to direct an expanding beam and at the same time influence the beam expansion.

All chemical processing of the exposed holograms projects conducted employed the pyrogallol and sodium carbonate based developers. During the course of this study, a new formula still based on the original chemicals, but now containing metol, was tested. This developer has the advantage of

enabling final colour control of the reflection holograms as well as enhancing fringe contrast in holographic interferometry. Both formulae are listed in Appendix A.

3.2. QUALITATIVE HOLOGRAPHIC INTERFEROMETRY

3.2.1. AIMS:

During the course of this study, various articles of interest to industry were presented to the holographic laboratory for analysis. The main aim of the projects investigated was the feasibility of holographic interferometry as a qualitative nondestructive testing technique. The field of imperfections studied, includes flaws such as debonds, delaminations cracks and so on.

An indirect result of the investigation, was the comparison of double-exposure and real-time holographic interferometry, in terms of valid results obtained and the applicability of the two recording techniques as a nondestructive testing tool.

3.2.2. OBJECTS TESTED

The objects that were examined are shown in Figure 3.2 , 3.3 and 3.4 below. Figure 3.2 depicts composite aircraft airframe sections and a fibreglass reinforced tube. Figure 3.3 depicts a ceramic tapered tube and Figure 3.4 depicts a ceramic cast wax mould.

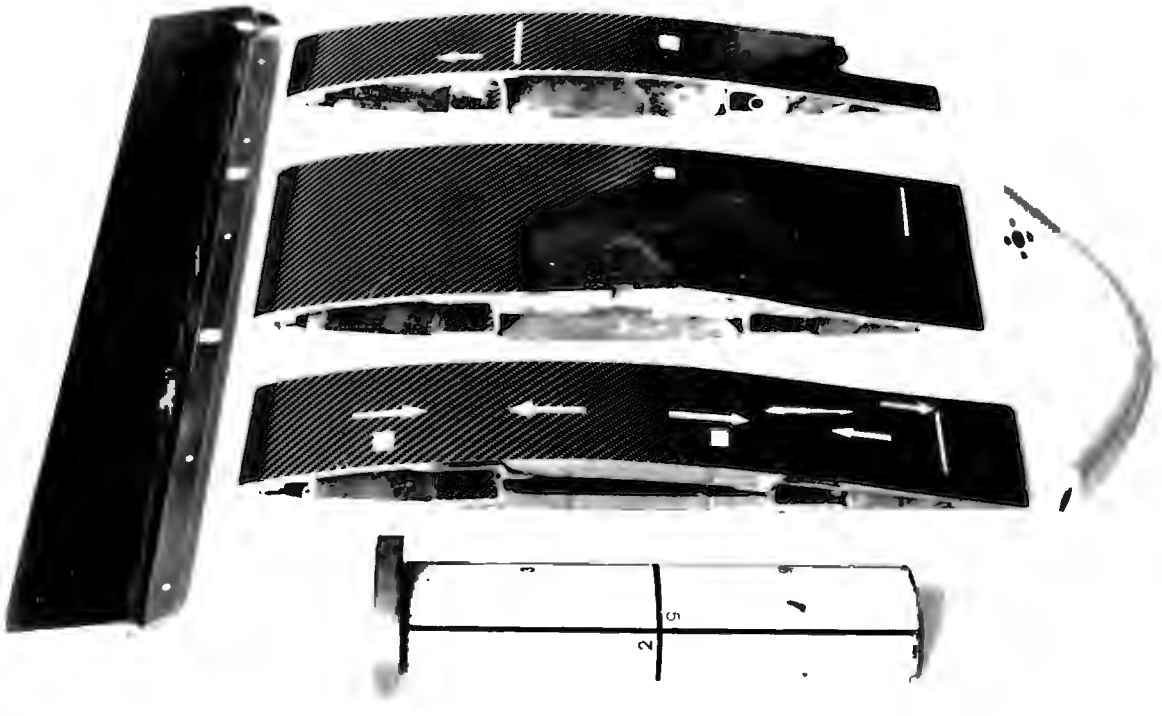

FIGURE 3.2 Composite airframe sections tested.

The airframe sections were constructed from carbon fibre reinforced preformed sheets which were then epoxied together to obtain the desired structure. The tube was a thin-walled filament-wound fiberglas reinforced polyester tube, seventy-five millimeters in diameter.

FIGURE 3.3 Ceramic tube examined.

The first of the ceramics, namely, the conical extruded tube, was produced with 'built-in' flaws. The second ceramic shown, is a mould obtained from the lost wax mould making technique. Into this mould, various molten metals can be poured, which when cooled, form tensile specimen samples.

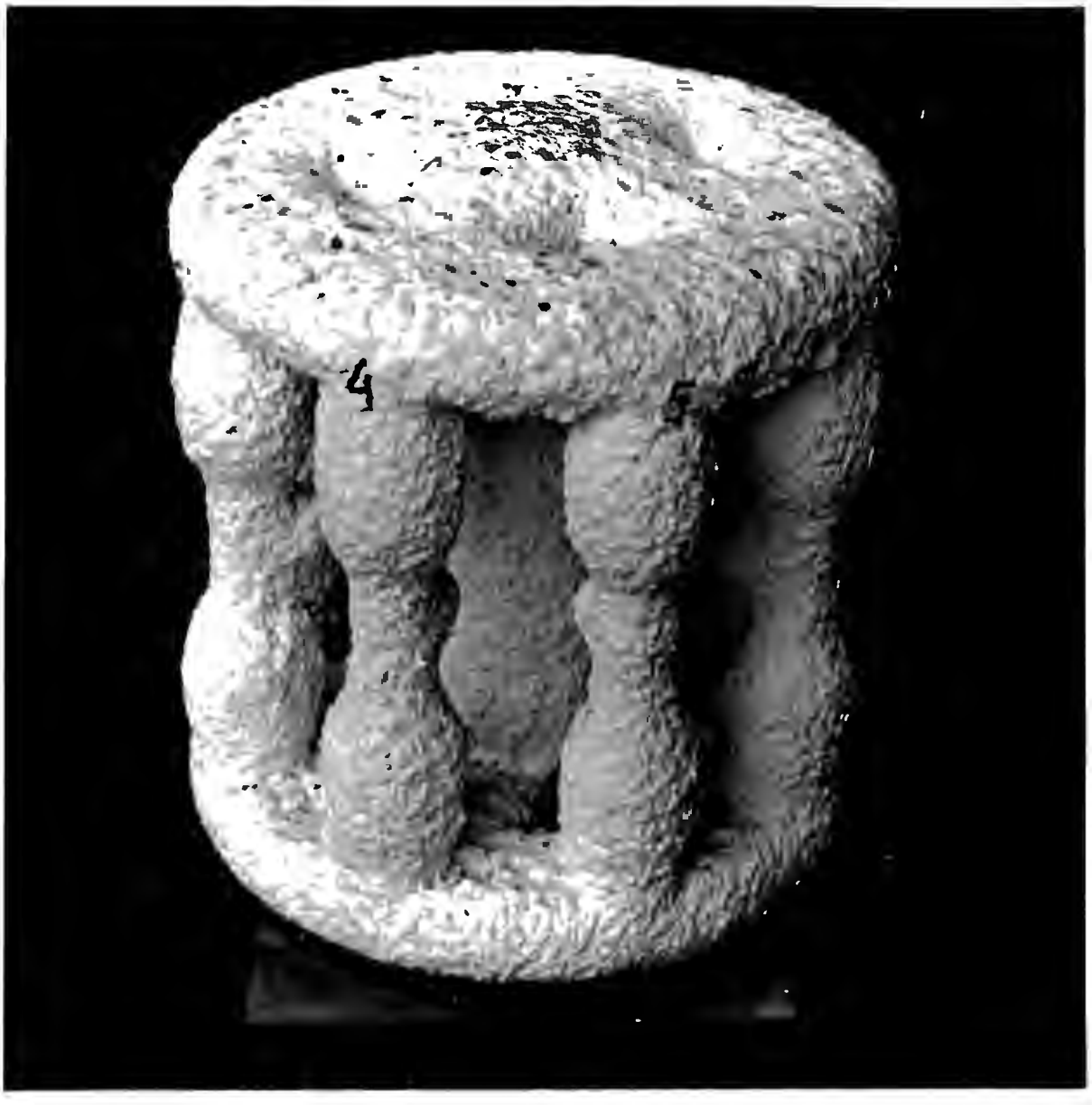

FIGURE 3.4 Ceramic cast wax mould

3.2.3. PRELIMINARY CONSIDERATIONS

Because of the testing technique employed, a stress application method had to be decided upon in order to produce the desired interference patterns.

According to Kersch [11], three types of stressing apply to laminate structures. It was felt that acoustic stressing would be too complicated and involved, adding to the problem of interpreting the fringes obtained. It was reported that pressure and thermal stressing techniques were successful and relatively uncomplicated. However, thermal stressing, because of its flexibility, was felt to be better suited than pressure stressing and was therefore employed whilst testing the composite material structures.

Due to the shape of the cast wax mould, only thermal stressing could be considered. However, the ceramic tube, because of its shape, was thought to be best suited to the pressure stressing technique. This was conducted by sealing off both ends of the tube and applying an internal pressure.

3.2.4. EXPERIMENTAL PROCEDURE

The experimental set-up as depicted in Figure 3.5 below is the classical transmission set-up and was employed for both the double-exposure and the real-time holographic interferometric techniques.

As shown in Figure 3.5, the reference beam, reflected by the beamsplitter, was directed through a beam expander and with the aid of the collimating mirror, fell onto the holographic plate at approximately forty degrees to the normal. The

FIGURE 3.5 Transmission inspection set-up.

1 - Laser 2 - beamsplitter 3 - adjusting mirror 4 - beam expander

5 - object 6 - plate holder 7 - collimating mirror

object beam, transmitted through the beamsplitter, was directed through a beam expander onto the object and its diffuse reflection was captured by the holographic plate.

The objects were located in front of the holographic plate. Depending on the object and its size, the two beam paths had to be adjusted slightly in order to maintain near equal beam lengths.

Referring back to Figure 3.2, object No. 1 - the fibreglass tube - had to be stabilised. This was achieved by affixing a metal disk onto the base which was then, in turn, clamped onto the table with a magnet. The circular shape of the fibreglass tube neccessitated that it be divided into six sections - two per third of a revolution. Each was numbered in order to facilitate identification of the holographic segments.

Object No. 2, due to its size, also had to be holographed in sections. It was mounted side-up on an elevated platform and was stabilised by means of a G-clamp which was securely fitted onto the table and the centre section of the object. Areas of interest, namely, the leading and trailing edge, were indicated by means of white arrows which showed the direction in which the inspection was undertaken.

Object No. 3 was of similar dimensions to object No. 2 and was therefore also examined in sections. The areas of

interest here, were the trailing edge and central section of the airframe where individual thickness variations were visible. This object was mounted in a similar fashion to the previous object.

Object No. 4 was narrow enough to be clamped in a vertically positioned vice - see Figure 3.5. Again, the leading and trailing edge were the prime areas of interest.

Object No. 5 was tapered in its cross-section and was also analysed in sections. It was clamped in position - in a vice - at the base where the No. 5 tags had been placed. The light weight of the object led to speculation that a foam was present under the skin, and that it was possibly stiffened by stringers. This speculation caused great interest as to whether holography could reveal the object structure.

Object No.6 which was curved and elliptic in cross-section was clamped in a vice magnetically fixed to the table. The object was gripped in such a manner that the free end curved upwards into the object beam. This clamping technique necessitated two holograms for the purpose of full analysis.

The ceramic tube - shown in Figure 3.3 - was fitted with two end plates with threaded holes in the centre and thread stock which allowed the tightening of the two plates against the ends of the tube. O rings were fitted into the end

plates to ensure a good seal. An inlet valve was fitted onto one of the end plates to enable pressurisation of the resultant chamber.

Preliminary results revealed that the ceramic was too porous and as a result absorbed too much of the liquid that was used to pressurize the tube. Consequently, it was decided to coat the inner tube surface with a lacquer and thereby seal it. With the modified set-up, good interference patterns were obtainable. However, it was quickly discovered that the edge effects induced by the end plates affected the overall interference patterns.

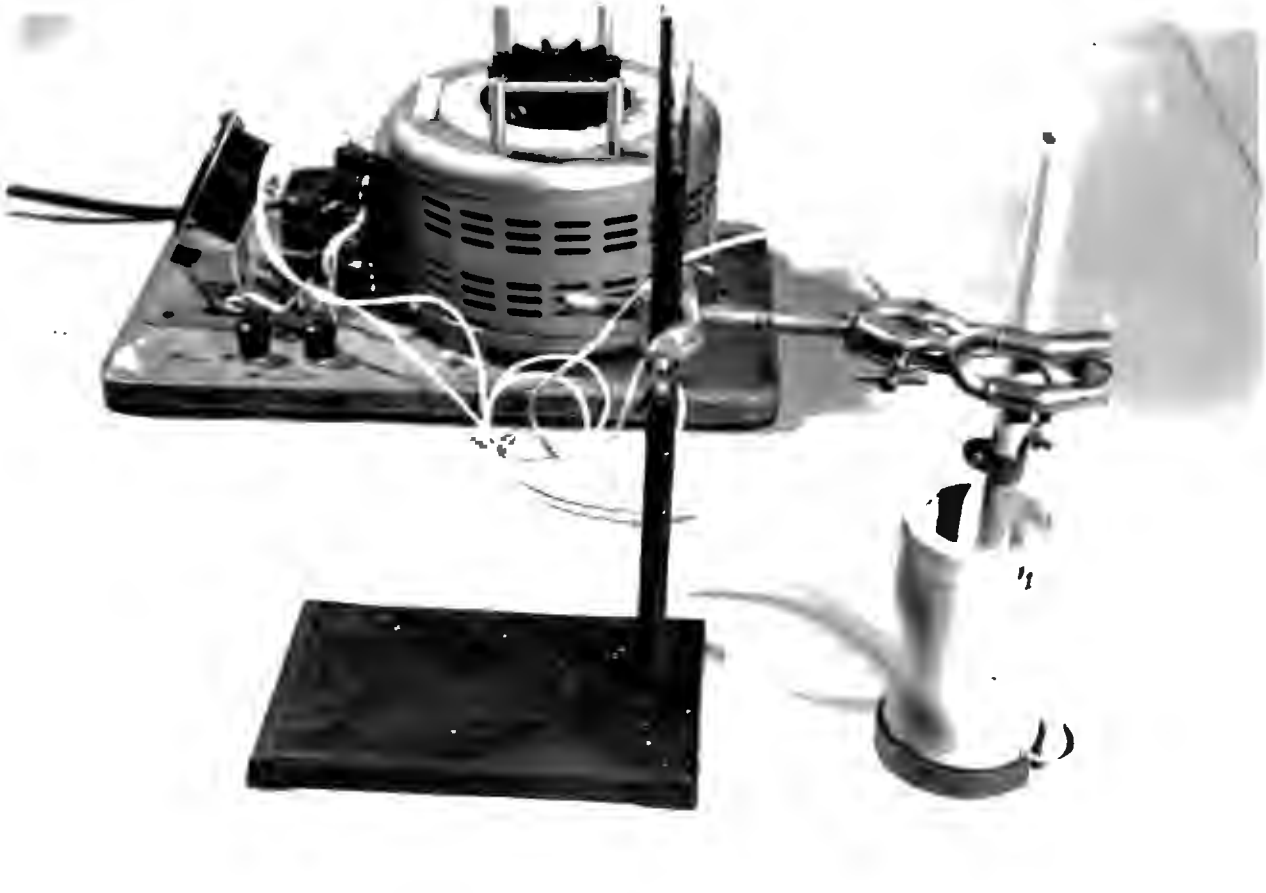

FIGURE 3.6 Stressing set-up for the ceramic tube

Therefor, it was decided to change from the pressure to the thermal stressing technique by placing a heater, controlled by a variable auto transformer, into the centre of the tube as shown in Figure 3.6 above.

The shape of the ceramic cast wax mould - depicted in Figure 3.4 - required the manufacture of a base which was bolted to the bottom of the mould. Care was taken when tightening the clamping bolts so as not to crack the mould. This assembly was then placed on a magnet and secured to the table. The shape of the mould necessitated segmented holography and the individual vertical mould elements were marked for the purposes of clear re-identification.

In order to establish the correct exposure time, test the stability of the set-up, note the object's reaction to stress application etcetera, preliminary double-exposure holograms were taken. Once we were satisfied with the results, the real-time holographic interferometric technique was applied.

A camera equipped with a zoom lens was placed in front of the plate holder and used to record the fringe patterns obtained from the real-time interferometric procedure.

3.2.5. RESULTS

From the double-exposure holograms, it was determined that the best results were obtained using a four to one reference to object beam intensity ratio and approximately three to four seconds total exposure time.

In a way the double-exposure technique is comparable to the 'shot in the dark' principle. That is to say, no measure is available to determine the amount of thermal stressing required to effectively scrutinize the object for defects. On the other hand, real-time holographic interferometry was found to be far superior because an immediate visible result was obtainable when thermal stressing was applied. It was therefore a far more controlled procedure, resulting in the possibility of 'homing in' on defect areas by applying a range of stresses in the suspect area and observing the results.

Real-time holographic interferometry required far more precision in terms of the recording and processing procedures. In order to satisfy stability and location requirements, emulsion backed glass plates had to be used. Correct plate positioning in the frame was essential. A settling period of at least two minutes was necessary prior to recording.

When processing the exposed holographic plate, great care had to be taken not to dislocate it fron its frame as this would almost certainly elliminate the possibility of correctly relocating the processed hologram back into the exact position in which it was recorded .

In addition, the developing process had to be carefully monitored and interrupted when the plate had developed to the correct density. No bleaching of the hologram was allowed, for this would marginally affect the emulsion dimension and thus introduce unwanted fringes in the reconstruction process.

Natural drying of the developed hologram caused the least deformation of the emulsion and usually resulted in only one or two unwanted fringes, visible when the hologram was placed in its original position. Hot air drying was found to affect the emulsion and result in the production of unwanted fringes.

It was found that manipulation of the object/reference beam intensity ratio, achieved by rotating the variable beamsplitter, affected the fringe contrast. In this manner the fainter fringes that characterize real-time holographic interferometry were made brighter and easier to observe.

Thermal stressing was achieved by applying hot air,

by a hair dryer, onto the object. The hot air was either blown directly onto the inspection area or from behind the object and allowed to translate through the material. Heating of the section adjacent to the area of inspection and thereby letting the heat 'flow' to the inspection area was also employed.

3.2.5.1. FIBREGLASS TUBE OBSERVATIONS

Figure 3.7 A B & C depict the interference patterns obtained using real-time holography. The interference patterns in A B & C are arranged in order of increased thermal stressing. It can be seen from the interference patterns that an increase in thermal stressing results in an increase in visible fringes.

Closer observation of the fringe pattern distribution in the preceding figures - A B & C - shows that a fringe concentration is visible situated to the right of the top center of position 1. The location is precisely defined by the fringes. The fringe intensity and irregularity suggest a large displacement with respect to the rest of the tube such as a complete bond break down between the filaments in that region.

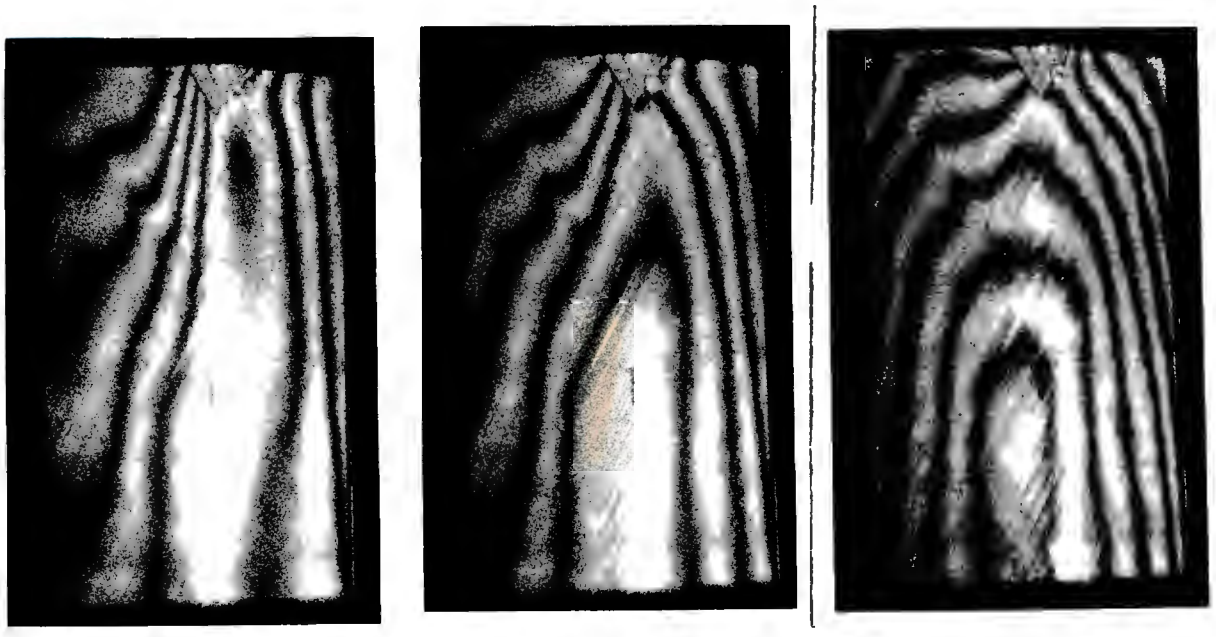

FIGURE 3.7 A B C

Position no. 1

In addition, Figures 3.7 B & C depict a peaking in the fringes located on the upper left half of the tube. This peaking suggests a fibre debond in the tube, thus affecting the thermal expansion characteristic along the fibre debond.

Position 2 of the tube is depicted in Figure 3.8. Here an irregularity of the fringe pattern is visible. However, it is obvious that the fringes visible are produced by a debond located on the edge, just to the right of the "2".

Position 3, when examined produced similar fringes as depicted in Figure 3.7, indicating a break-down in bonding of the filaments.

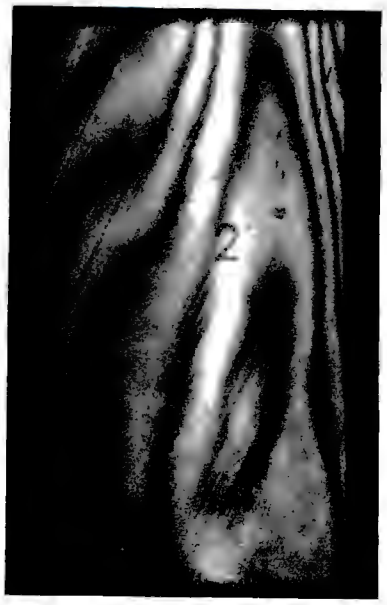

FIGURE 3.8 Position no. 2.

Figure 3.9 presents the fringe pattern obtained from position 4 of the tube. Due to the same elliptic shape of this fringe pattern, one would presume a large flaw in the centre of the semi-elliptical pattern. However, considering the shape of the object and its expected expansion, it can be concluded that there is no flaw present.

When the object is thermally stressed, it is expected to expand radially outward. The area directly in front of the camera will thus expand towards the camera. This constitutes out of plane motion and has been found, as was presented in the literature survey, to produce virtually no fringes with full aperture. Therefore, no fringes are visible directly normal to the angle of viewing.

Because only the top of the tube was exposed to hot air, a temperature gradient exists between the top and the bottom of the tube, i.e. an expansion gradient will also exist. This explains the fringe present at the bottom of Figure 3.9 normal to the angle of viewing.

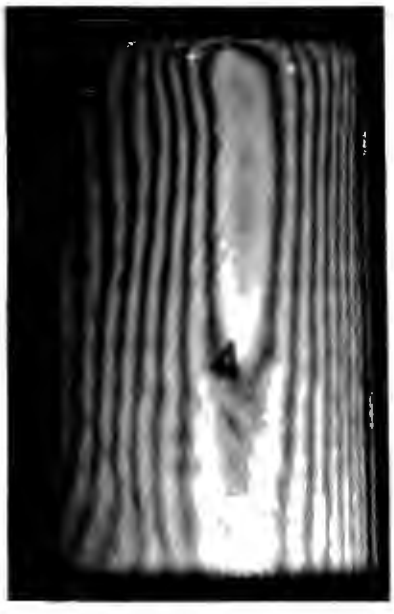

FIGURE 3.9 Position no.4.

Figure 3.10 A & B show the fringe patterns obtained from position 5. Figure 3.10 B shows the fringes obtained with the tube exposed to a greater thermal stressing than in Figure 3.10 A. It is apparent that only at the greater thermally stressed state did the debonding at the top of the tube become visible. This is depicted by the fringe irregularity in the upper centre region of the tube.

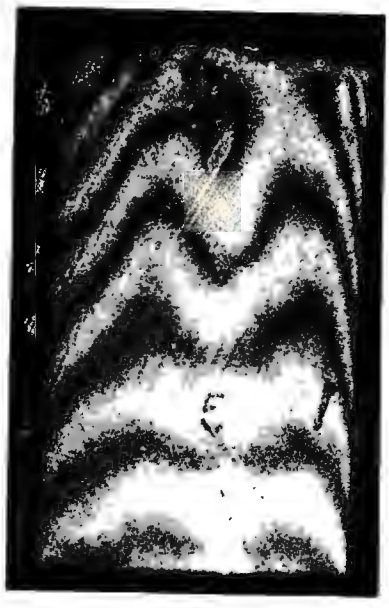

FIGURE 3.10 A

Position no.5

FIGURE 3.10 B

3.2.5.2. AIRCRAFT SPACEFRAME OBSERVATION

Outlined below are the significant results obtained from the tests conducted on the airframe sections. As was to be expected, not all of the sections tested revealed irregularities in the fringe pattern.

Specimen No 2 revealed two flaws of interest - the second of which, had to be fabricated. The first flaw was found on the leading edge of the spaceframe and is depicted in Figure 3.11 A & B.

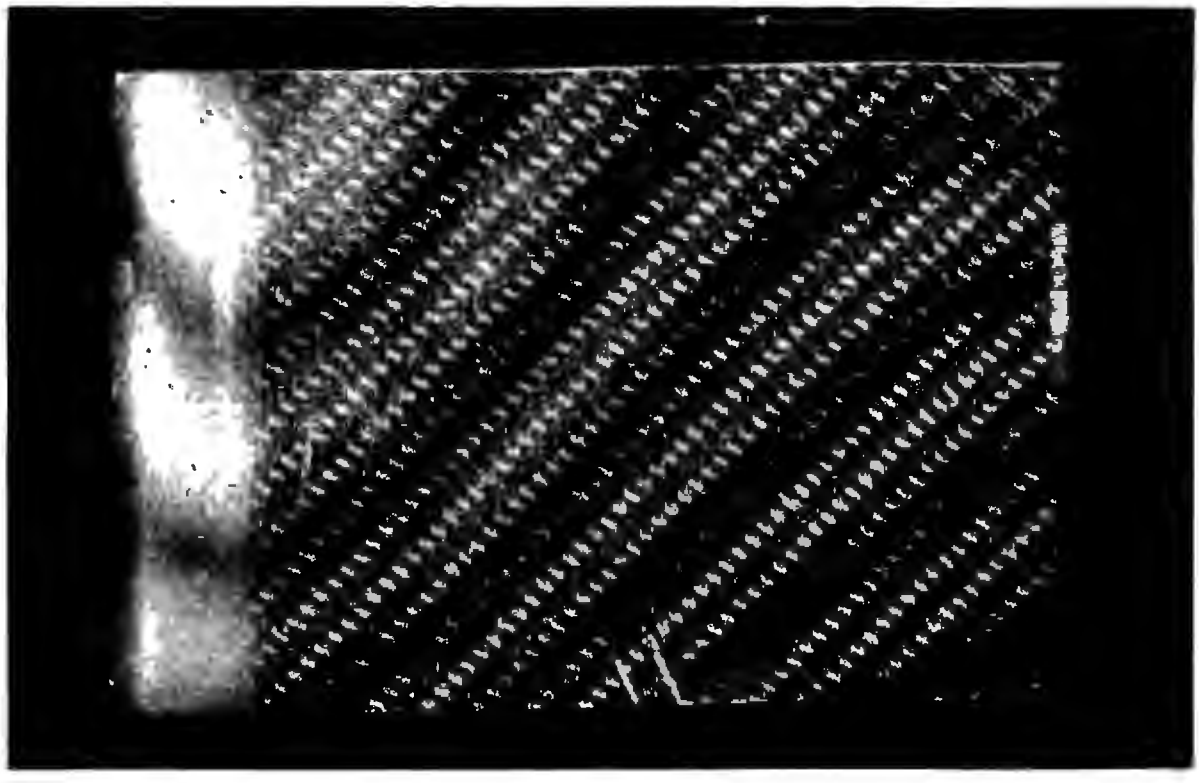

FIGURE 3.11 A Specimen no.2, leading edge.

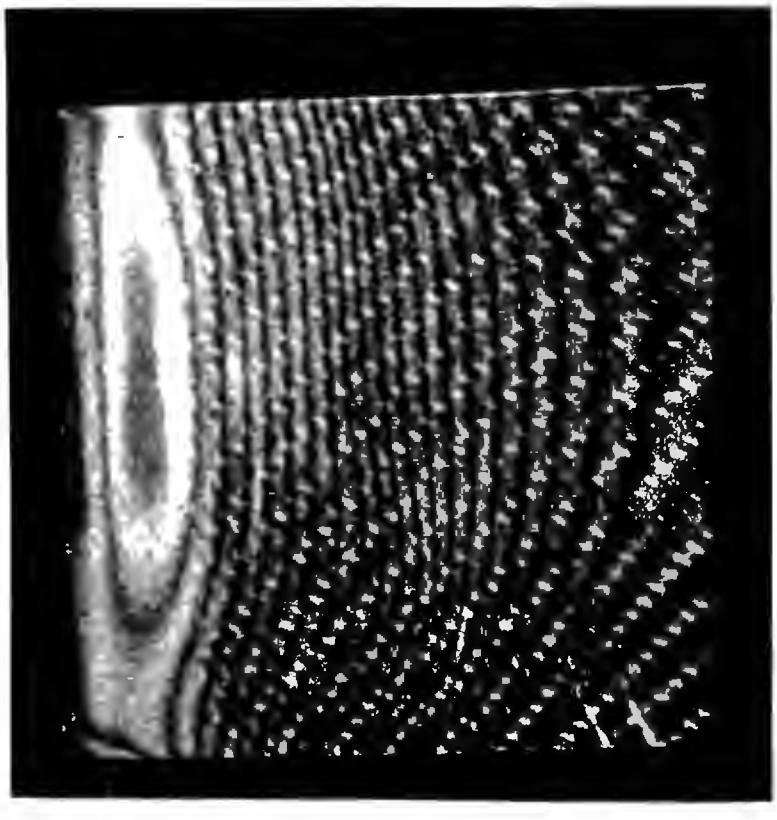

FIGURE 3.11 B Specimen no. 2, leading edge.

The flaw however was only detectable in Figure 3.11 B which represents the fringes obtained at a higher thermally stressed state than Figure 3.11 A, where no obvious flaw could be interpreted from the fringes.

Examination of the specimen following the testing revealed an internal air cavity running along the area of the leading edge, as demarcated via the elliptic fringe.

When the object was received, the trailing edge was found to be completely delaminated at the joint of the upper and lower panel. In order to create an internal delamination, the two panels were epoxied together around the perimeter of the bonding surface.

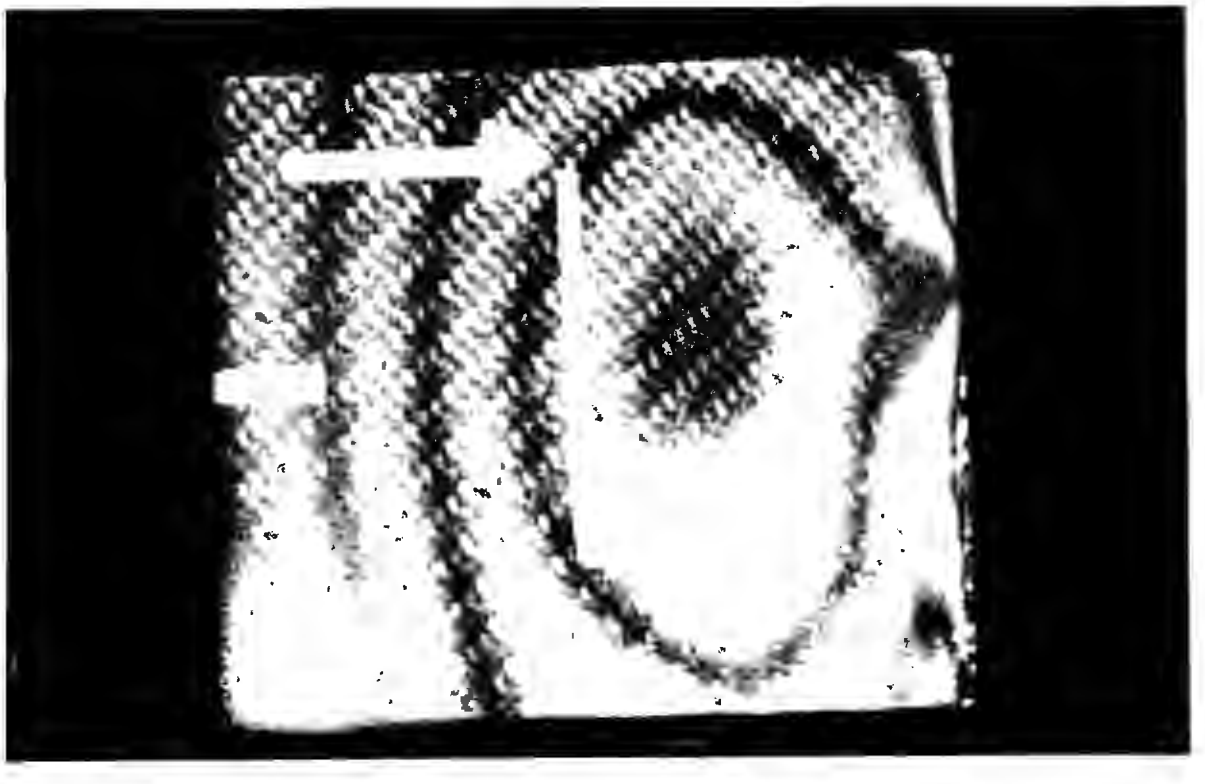

FIGURE 3.12 Specimen no. 2, trailing edge.

When examined. fringe patterns were obtained as is depicted in Figure 3.12, where the large internal debond is clearly visible as a change in the uniform fringe pattern.

The trailing edge of specimen No. 3, when compared to the trailing edge of specimen number two, clearly shows a solidly bonded joint. See Figure 3.13.

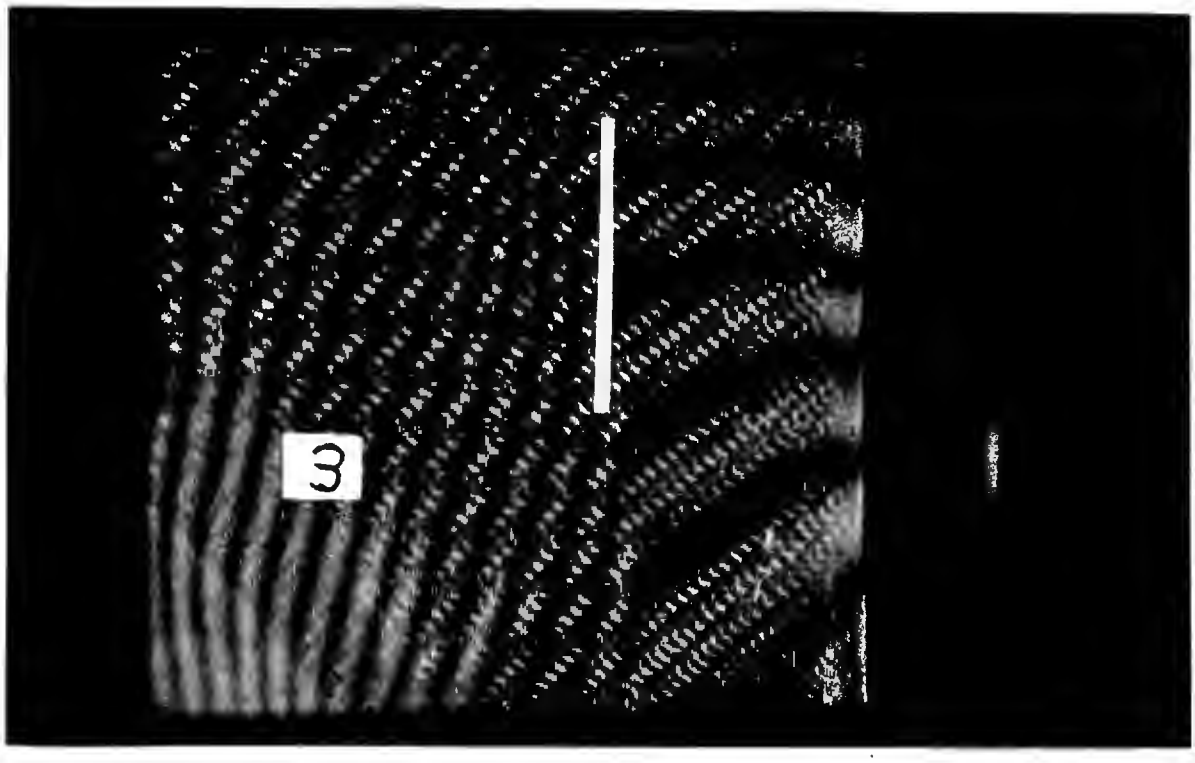

FIGURE 3.13 Specimen no. 3, trailing edge.

The vertical white strip visible in Figure 3.13 demarcates the bonding edge. A change in fringe orientation in the region of the strip was indicative of the internal material structure and therefore, was not to be considered as a material imperfection.

Figure 3.14 shows the fringe pattern resulting from the

central region of specimen No. 3. The circular fringes revealed that an internal flaw was present. Of interest, are the minor distortions of the fringe pattern - depicting the joints of the various carbon fibre mats within the sheet - at two o'clock, five o'clock and seven o'clock.

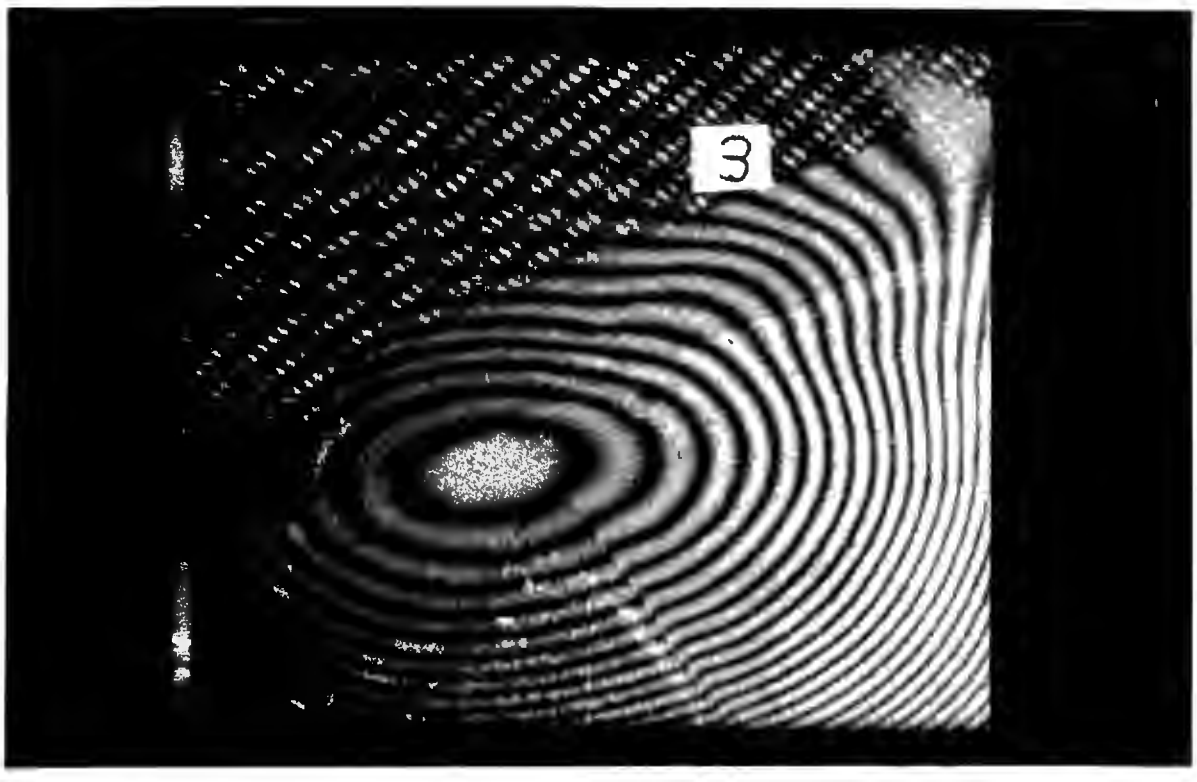

FIGURE 3.14 Specimen no. 3, central section.

The fringe patterns obtained from the tests conducted on specimen No. 4 are presented in Figure 3.15 - the leading edge - and in Figure 3.16 A & B - the trailing edge.

The fringe pattern depicted in Figure 3.15 indicates the presence of an internal defect in the lower half of the leading edge. The broad spaces between the fringes in that region make this self-evident.

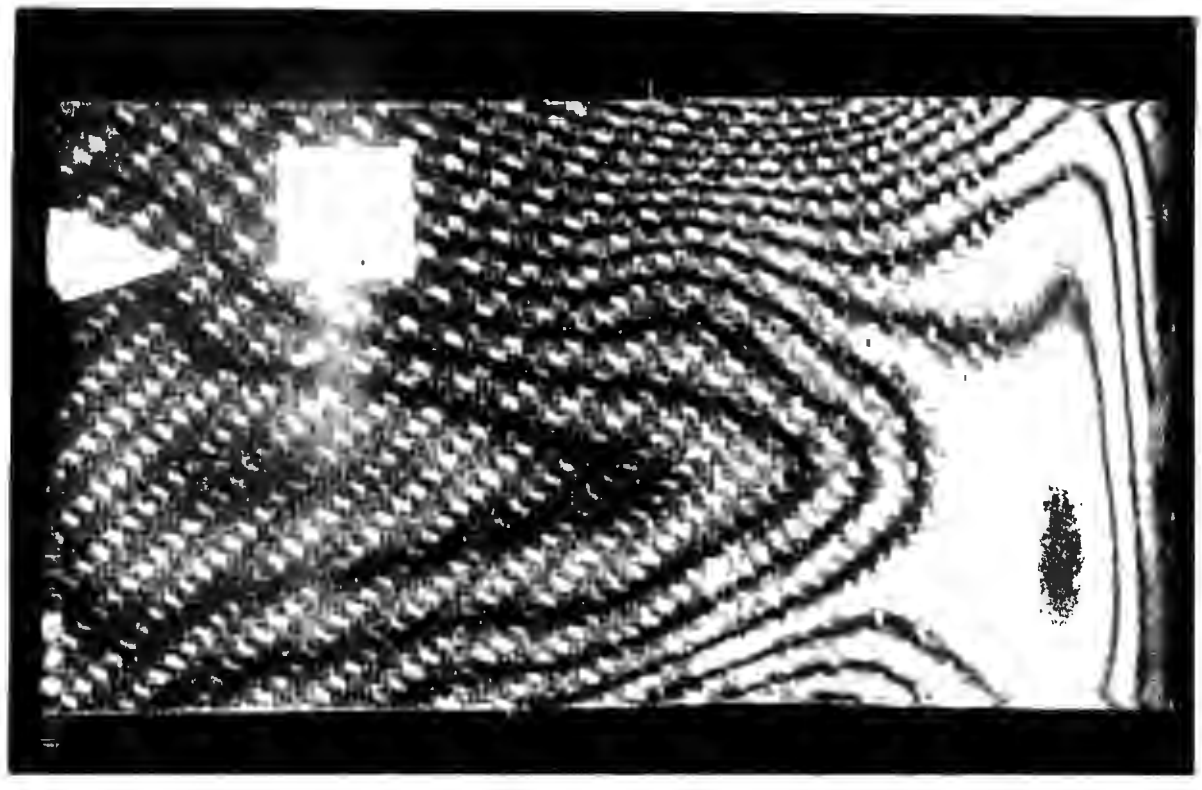

FIGURE 3.15 Specimen no. 4, leading edge.

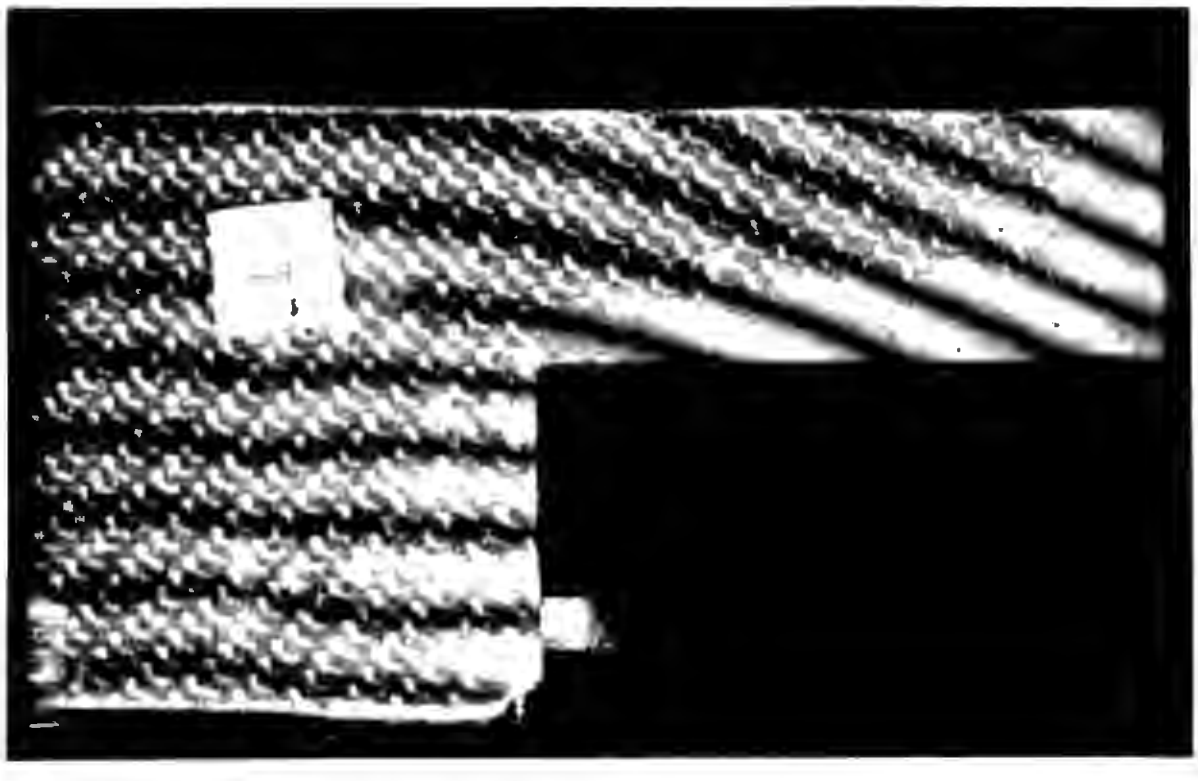

FIGURE 3.16 A Specimen no. 4, trailing edge.

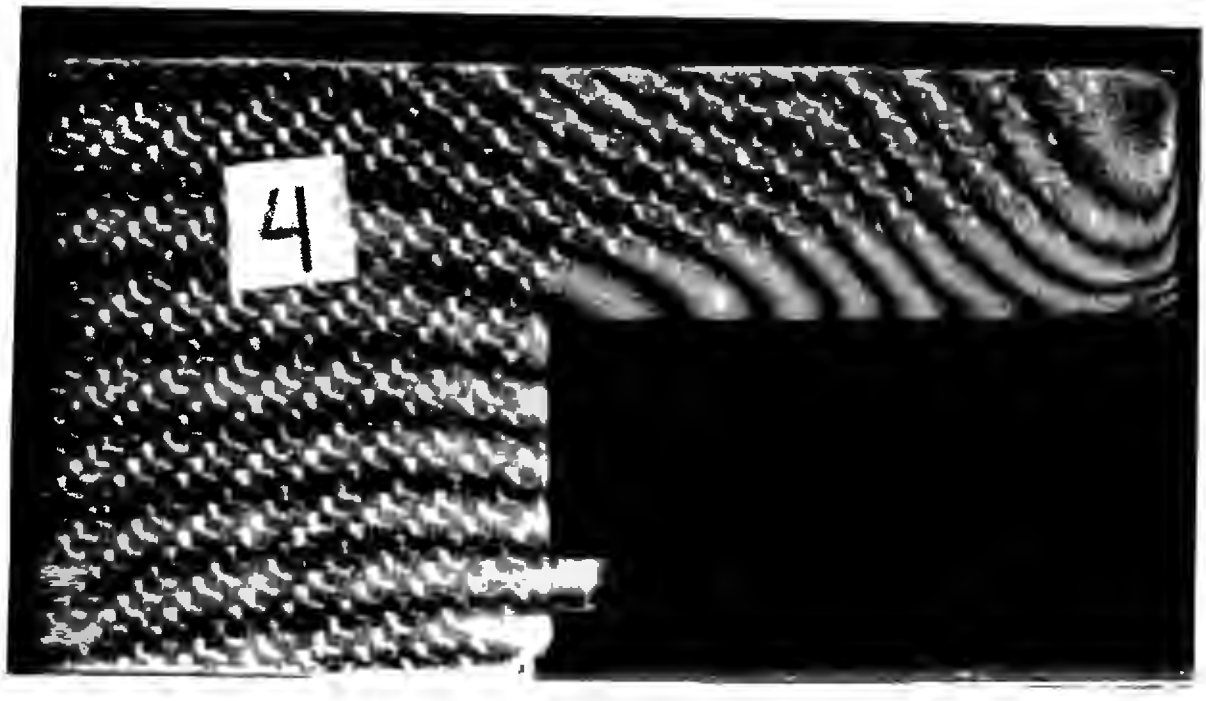

FIGURE 3.16 B Specimen no. 4, trailing edge.

Figure 3.16 again presents two different stress states, 'A' being at a lower thermally stressed state than 'B'. As can be seen in Figure 3.16 A, no flaw is evident from the fringe pattern obtained. However, the circular fringe in Figure 3.16 B indicates the presence of a subsurface defect, thought to be caused by an air inclusion in the top corner of the trailing edge.

The interference patterns obtained from the tests conducted on specimen no. 5 are presented in Figures 3.17 and 3.18. The concentric fringes in Figure 3.17 could be interpreted as indicating a large debonded area, expanding normal to the

surface when stressed. However, the fact that the pattern was repeatable along the specimen, led to the deduction that dissimilar materials within the specimen were responsible for this expansion. The fringe patterns indicate that the internal structure of the specimen was as follows: some form of stringer acting as a stiffener, alternating with a polyurethane foam.

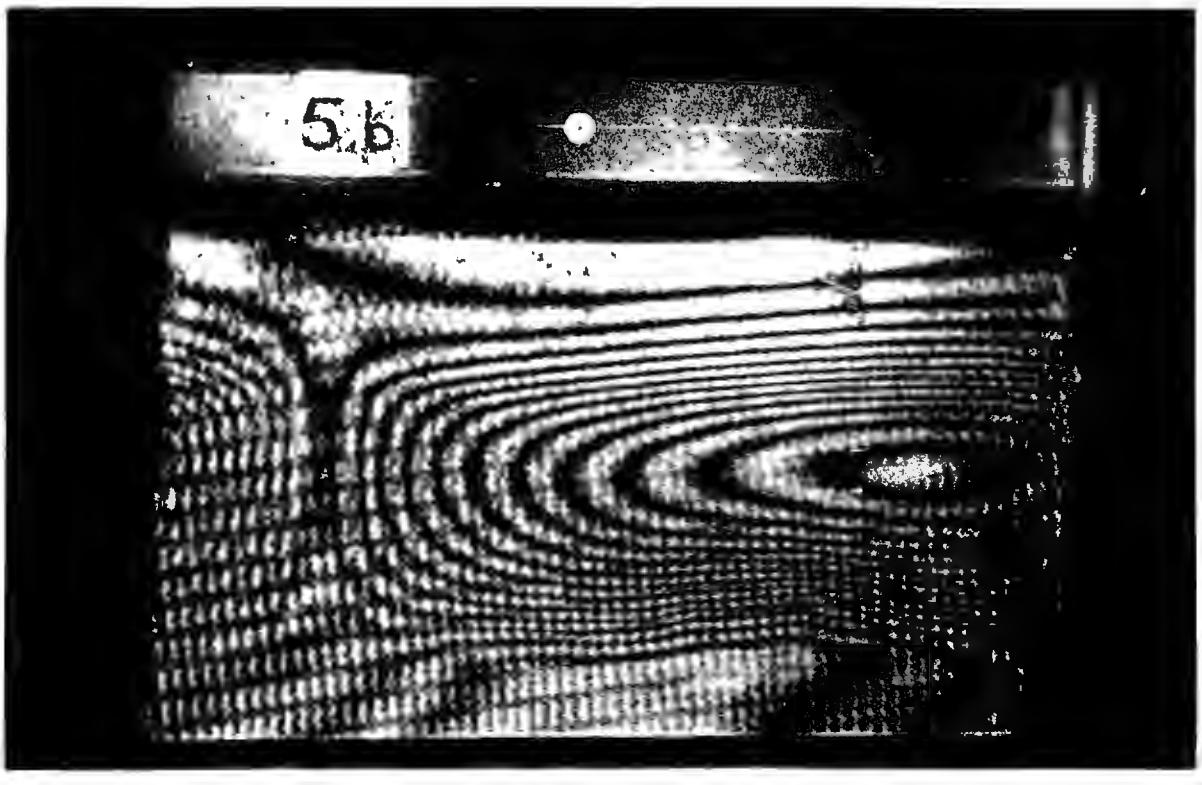

FIGURE 3.17 Specimen no. 5, good section.

On the other hand, Figure 3.18 represents an area of debonding in the lower right-hand side of of the area tested on specimen No. 5, as indicated by the fringe irregularity .

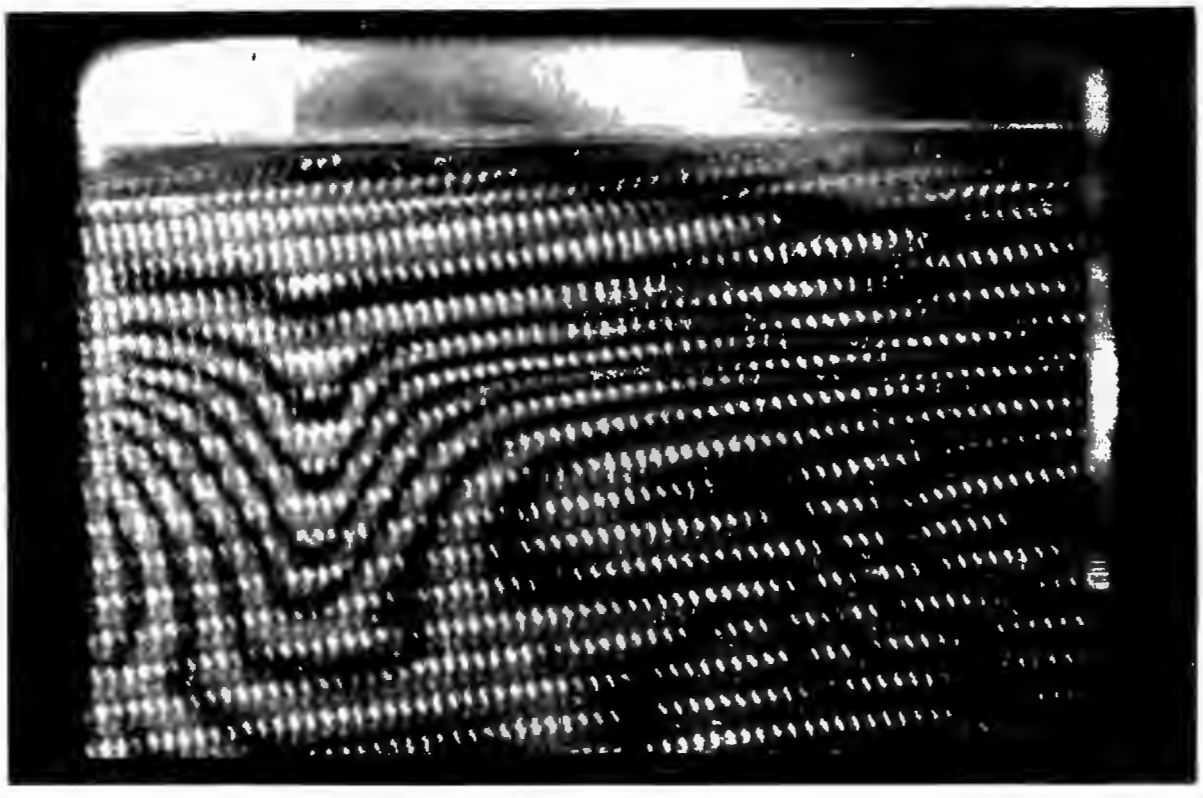

FIGURE 3.18 Specimen no. 5, debonded section.

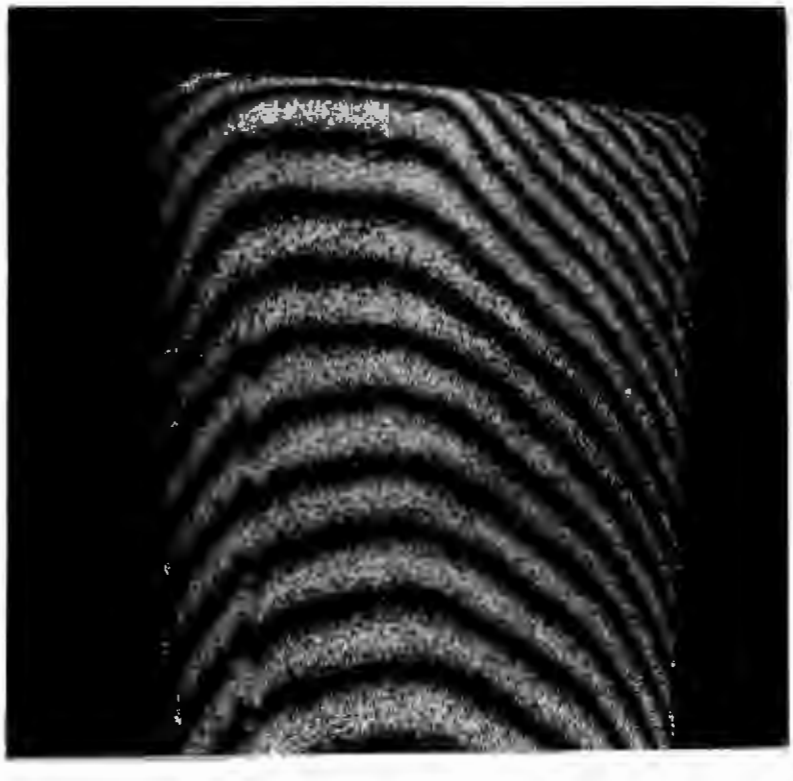

FIGURE 3.19 Specimen no. 6.

Figures 3.19 and 3.20 clearly show that when Specimen no. 6 was tested at both ends, respectively, a series of cracks were revealed. Figure 3.19 indicates the presence and location of a crack running parallel to the edge of the specimen. This is evidenced by means of the zig-zag contour which repeatedly slants vertically, as opposed to the horizontal direction of the fringes.

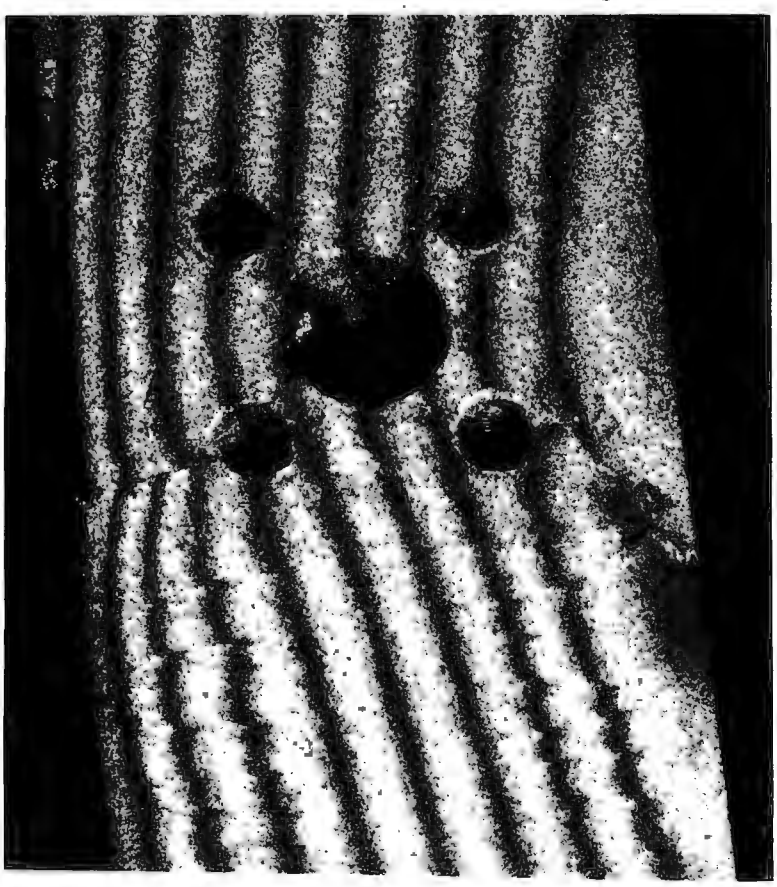

FIGURE 3.20 Specimen no. 6.

The fringe discontinuity in the region of the bottom left hole, as is visible in Figure 3.20, clearly locates the crack running radially outward from the bottom left hole. The 'ragged edge' appearance of the fringes below the crack indicate the location of micro-cracks present in the surface of the specimen in this region.

3.2.5.3. CAST WAX MOULD OBSERVATIONS

The results obtained from the tests conducted on the ceramic cast wax mould are presented in Figure 3.21 and 3.22. As mentioned previously, the base constructed for this mould provided the required stability necessary to conduct the experiments.

Fringe discontinuity was visible with both double-exposure and real-time holography. Real-time holography made it apparent that any type of thermal stressing would reveal the cracks present in the mould, even though the surface of the specimen was extremely rough.

FIGURE 3.21 Ceramic mould, position 2 & 3.

Note the abrupt fringe contour changes below positions '2' and '3' in Figure 3.21, which mark the position of the cracks. In Figure 3.22, the fringe patterns visible at positions '5' and '6' are far more, especially below position '5', which indicates a more severe wall-cracking than shown in Figure 3.21.

FIGURE 3.22 Ceramic mould, position 5 & 6.

3.2.5.4. CERAMIC TUBE OBSERVATIONS

The tests performed on the ceramic tube proved fruitless until the correct stress application technique had been obtained. Using the heater element, a significant amount of

thermal stressing was required before the flaw became identifiable in the fringe pattern obtained. As is shown in Figure 3.23 below, the flaw is visible as a small 'peak' in the fringe pattern, initiating just to the right of the '2' and traversing down the centre.

FIGURE 3.23 Ceramic tube.

When the specimen was sectioned, the flaw - which was created by the inclusion of a 100 micron nylon filament in the extrusion process - was found to be situated in the area as marked by the fringe irregularity. Three other nylon filaments which had been included in the specimen during the extrusion process and which were not revealed by holographic interferometry, were also found.

Closer examination of the specimen revealed that during baking, the three other inclusions - mentioned above - had melted and the "hollow" had fused together, thus removing all but the one flaw detected.

3.2.6. COMMENTS AND CONCLUSIONS

The tests conducted provide strong evidence that holographic interferometry, as applicable to double-exposure and real-time holography is a viable and powerful technique.

Table 3.1 summarises the advantages and disadvantages of real-time and double-exposure holographic interferometry.

TABLE 3.1

STANDARDS	DOUBLE-EXPOSURE	REAL-TIME
emulsion	film or plate	plate
chemicals	standard	standard
bleaching	yes (allowed)	no (not advisable)
processing	no special care	extreme care when developing, washing and drying of plate.
set-up	standard off-axis, stability required only whilst taking the hologram.	standard off-axis, stability required throughout the testing procedure.

STANDARDS	DOUBLE-EXPOSURE	REAL-TIME
stress applied	as applicable to object. No means of knowing effect of stress whilst applying.	as applicable to to object. Direct visual information on effect of stress application.
stress variation	only one stress situation possible per hologram.	numerous stress situations possible during experiment, using only one hologram.
fringe pattern quality	generally high.	variable, can be optimised using a beam splitter.
spurious fringe influence	no influence unless emulsion moves between exposures.	influence related to set-up stability and developing process.
storing of fringe patterns	direct storing of fringe pattern in hologram.	no storing capability. Requires video or photo-graphic storing of fringe patterns.

The experiments conducted clearly illustrate the capabilities of holography as a nondestructive testing technique and a quality inspection tool.

Cracks present in an object are detectable in the fringe patterns obtained irrespective of surface roughness. The identification of the positions of said cracks is facilitated by the discontinuity of the fringe pattern contours in specific areas.

Figure 3.20 clearly shows the detection of micro-cracks which, as yet, have not been conclusively reported in available literature.

The above-mentioned conclusions are valid in situations where fringe localisation on the object surface is achieved during stressing - i.e. occurring either during the rotation of the object about an axis, or during bending due to expansion.

Flaws such as debonds, delaminations and internal flaws are all readily detectable.

Debonding is easily detected due to the fact that the debonded area expands in a haphazard manner which is totally different from the characteristic expansion in that area. From the fringes obtained, the extent of the defect can be interpreted - as is evidenced in the tests conducted on the fibreglass tube. This facilitates the separation of possible repairable sections such as the filament debonding in Figure 3.7 B, from non-repairable areas such as the section of complete bond break-down in Figure 3.7 A.

Delaminations, when detected, cannot readily be interpreted in terms of position and size from the fringe patterns obtained. Their positions can be identified by the concentric fringes formed in the pattern and it is justifiable to assume that the centre of these fringes

indicates the position of the centre of the delamination. The determination of the delamination perimeter is far more difficult to identify and basically amounts to 'educated guess work'.

Clearly the results obtained from the ceramic tube were unexpected as the hardness and density of the material as well as the size of the internal defect were not expected to produce the noticeable fringe irregularity, as is seen in Figure 3.23. The unexpected outcome of these tests warrant further investigation along similar lines.

Care must also be taken when interpreting the fringe patterns obtained from the tests. An understanding of the objects inner structure and the materials employed, is essential. This is emphasised in Figure 3.14 and Figure 3.17. where the abrupt small changes in the fringe contours in Figure 3.14 could easily be interpreted as subsurface cracks and the concentric fringes in Figure 3.17 as the displacement of a delamination.

Holography affords real possibility of inspecting the structural integrity of engineering components in structures. Here however, the fringe patterns expected from a structurally sound object need to be on hand in order to act as a reference.

3.3. QUANTITATIVE HOLOGRAPHIC INTERFEROMETRY

Briers's paper [19] elaborates on four of the most widely accepted techniques, aimed at quantifying holographic interferometry in interpreting surface displacements.

According to Briers [19], two of the techniques examined proved to yield good results. These were the zero-fringe and the fringe-counting techniques which are described in chapter 2.3.8.

3.3.1. AIM

The aim of the project was to apply the two displacement measuring techniques to the well known cantilever experiment. The results obtained would then be compared with the theoretically predicted ones - obtained from the simple beam theory.

3.3.2. THEORETICAL BACKGROUND

Ennos [20] derived the fundamental equation used in the zero-order technique from first principles. The out of plane optical path difference was derived to be as follows:

$$opd = m\lambda \qquad (2.7)\ \text{(repeated)}$$

where opd = optical path difference

m = number of fringes counted

λ = wavelength of laserlight

To relate the optical path difference to the displacement of the object, the equation is modified to produce

$$d = m\lambda/2 \qquad (3.1)$$

where d equals the resolved displacement component along the direction of observation.

If the direction of total displacement is not coincident with either the line of sight or the line of illumination, the resultant object displacement vector can be obtained by considering the angles of offset of the component vector and the line of illumination as depicted in Figure 3.24 below.

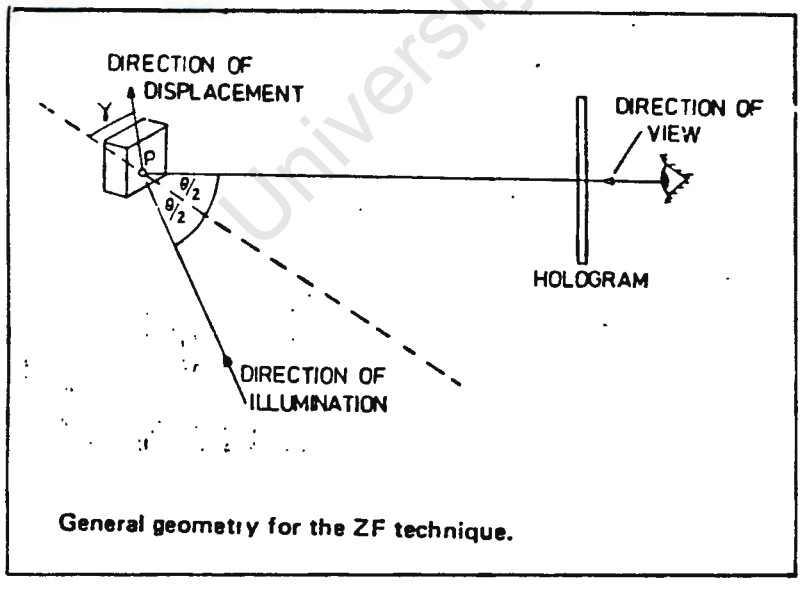

General geometry for the ZF technique.

FIGURE 3.24

Using Figure 3.24 the displacement, as seen in equation 3.2, can be obtained.

$$\text{displacement} = \frac{m\lambda}{2 * \cos(\emptyset/2) * \cos\gamma} \qquad (3.2)$$

If the displacement direction can be arranged to coincide with the bisector of the line of sight and the angle of illumination, then the final equation applicable is presented below.

$$\text{displacement} = \frac{m\lambda}{2 * \cos(\emptyset/2)} \qquad (3.3)$$

The fringe-counting technique makes use of the fact that the fringes produced during the stressing of an object are generally localized some distance from the object. The displacement obtained is normal to the angle of vision, that is, in plane. The equation presented in the literature survey in chapter 2.3.8 which makes use of the parallax effect is listed below.

$dx = N\lambda L/X$ (2.8) (repeated)

where dx = component of translation

N = number of fringes counted

λ = wavelength of laserlight

L = distance between object and hologram

X = distance scanned across the hologram

If dx does not represent the resultant displacement vector, equation 3.4, as expressed below is used to determine the total displacement.

$$dr = \frac{N\lambda L}{X * \sin\delta} \qquad (3.4)$$

where dr = resultant object displacement vector

δ = angle between viewing direction and displacement vector

However the cantilever can be situated in such a manner that the resultant displacement direction is normal to the angle of viewing. Therefore δ is 90 degrees and equation 3.4 reduces to equation 2.6.

The equation of deflection for a cantilever beam is given by the well known expression [27]

$$y = \frac{Fx^2}{6EI} * (x - 3a) \qquad (3.5)$$

Figure 3.25 defines the dimensions.

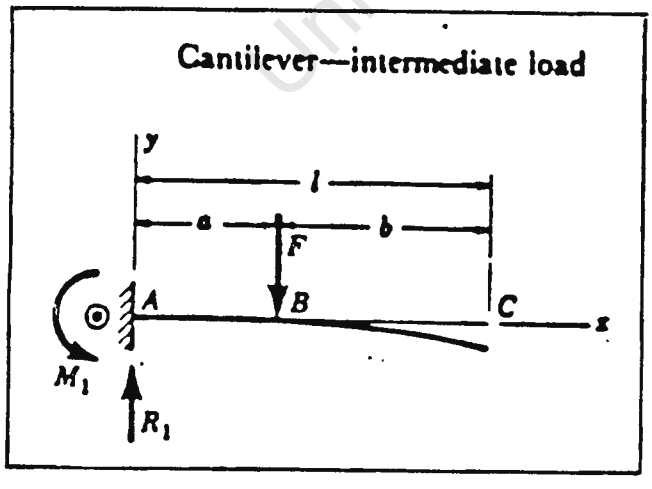

FIGURE 3.25

3.3.3. EXPERIMENTAL PROCEDURE

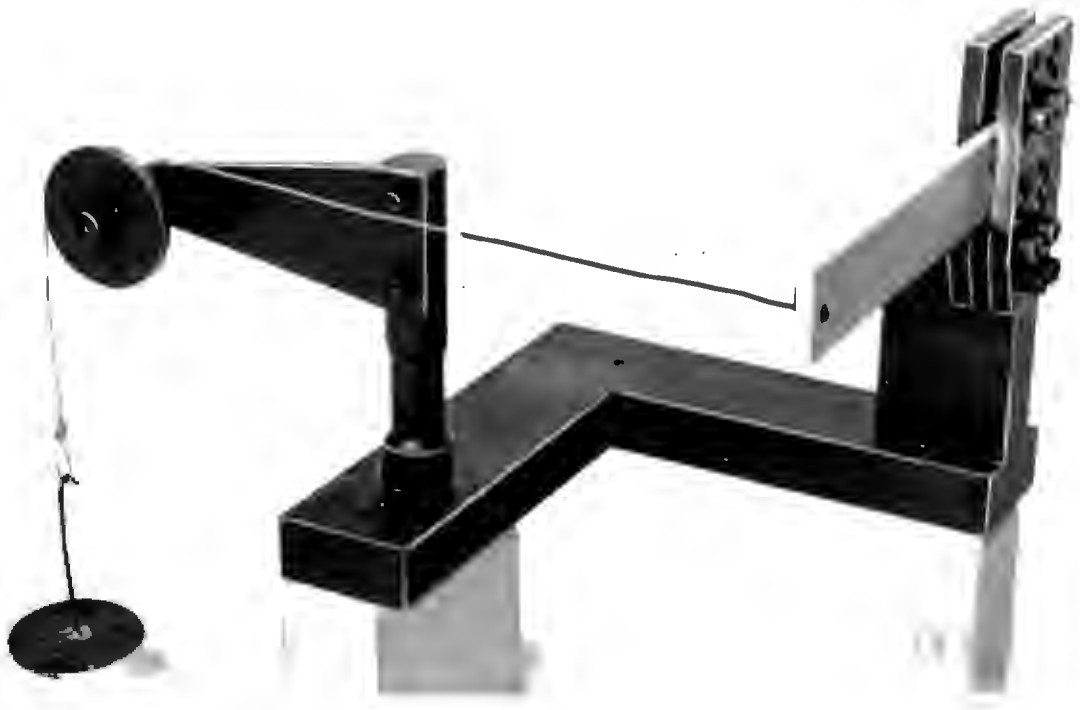

FIGURE 3.26

Cantilever support base & loading mechanism

The configuration was arranged so as to apply the force at the end of the cantilever, normal to the surface, by means of a nylon string. The string was passed over a pulley so that the mass used to apply the force could be loaded onto a small pan. The cantilever was made from tool steel with dimensions of 147 mm (length) x 30 mm (width) x 6 mm (depth). The load was applied at a point 135 mm from the point of fixture.

FIGURE 3.27 Cantilever experimental set-up

1 - laser 2 - mirror 3 - beamsplitter 4 - adjusting mirror

5 - beam expander 6 - cantilever 7 - plateholder 8 - collimating lens

The laser beam is split up into two by the beamsplitter. The reference beam, reflected by the beamsplitter is directed through the beam expander and a lens to produce a collimated reference beam. This beam is directed onto the holographic plate at approximately 35 degrees to the normal. The object beam, passing through the beamsplitter, is directed through the beam expander onto the object and is reflected onto the holographic plate.

Double-exposure holography was employed for the zero-order technique. The holograms were developed, illuminated and the zero-order fringe was established. Finally, the number of fringes visible between the zero-order fringe and the point of load application were counted and noted.

The same set-up that is depicted in Figure 3.27 was used in the fringe-counting technique. Real-time holography was employed so that observation of the fringes produced when the force was applied to the cantilever would be facilitated. The loading of the cantilever was progressively increased and the number of fringes seen passing through the point of load application during scanning, were counted.

3.3.4. RESULTS

The holograms obtained from the zero-order technique depicted static fringes localized on the surface of the cantilever. In all the results obtained the fringes were positioned vertically, the number of fringes obtained being related to the force applied.

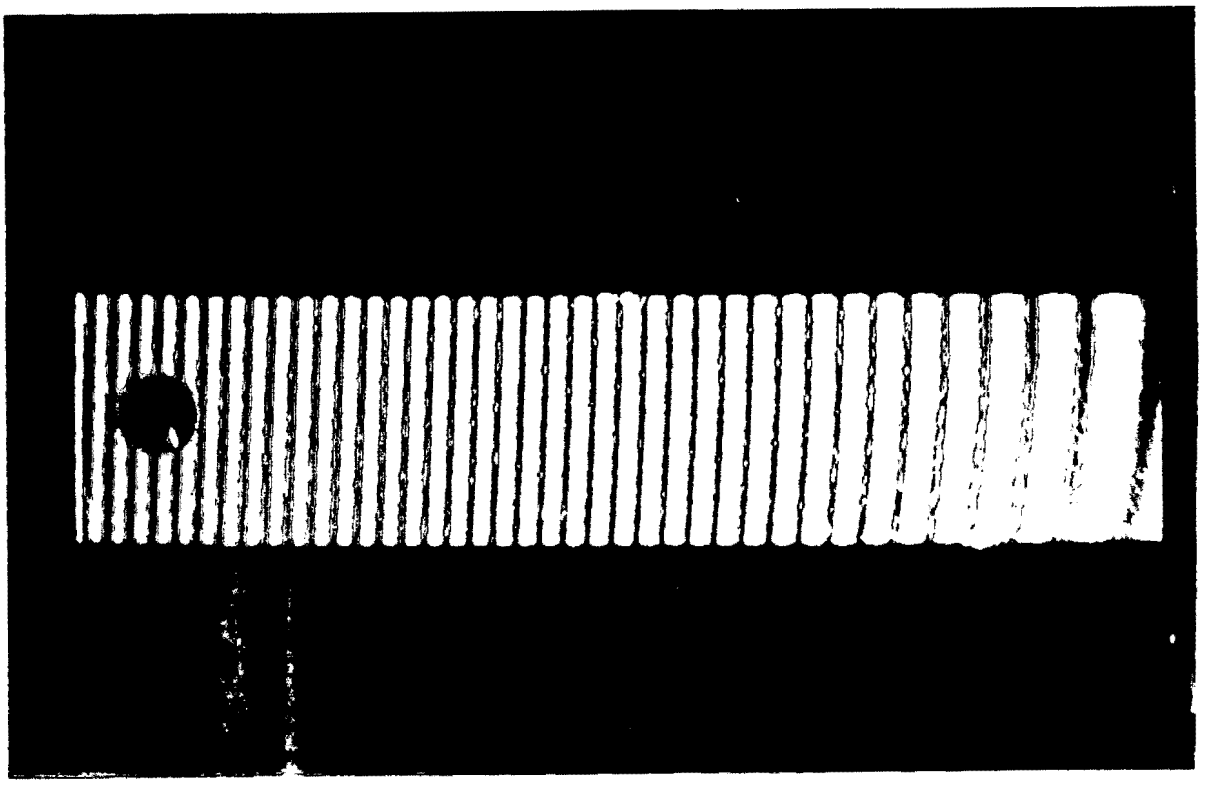

FIGURE 3.28 Typical zero-order fringe pattern.

The angle between the illuminating beam and the line of observation was 23.9 degrees. The set-up was such that the cantilever displacement vector lined up with the bisector as indicated in Figure 2.24, that is, $\emptyset$ = 23.9 degrees and γ = 0 degrees. Equation 3.3 was used to obtain the displacements from the number of fringes obtained, as

tabulated below.

TABLE 3.2 ZERO-ORDER EXPERIMENTAL RESULTS

Loading mass (grams)	No. of fringes	Displacements (mm)
9.98	6	0.001941
32.54	10.5	0.003397
49.89	15.5	0.005014
72.49	21.75	0.007036
95.12	27	0.008735
117.72	34	0.0110
127.72	37	0.01197
140.5	40.5	0.0131
163.1	47	0.01521
190.3	53	0.01715
212.9	59	0.01909

When the fringe-counting technique was investigated, the loading of the cantilever did not result in any static fringes in the interference pattern. However, whilst scanning the hologram, fringes were seen to pass across the cantilever, localised on a plane in front of the cantilever, thus indicating that fringe parallax was present.

Equation 2.8 was employed to determine the resultant

cantilever displacement using the experimentally determined fringes together with L = 0.485 m, X = 0.105 m and λ= 633 nm

The tip displacement results obtained are presented in table 3.3 below.

TABLE 3.3 FRINGE COUNTING EXPERIMENTAL RESULTS

Mass (grams)	No of fringes	Displacements (mm)
100	3.25	0.0095
200	5.5	0.01608
300	8	0.02339
400	10	0.02924
500	12	0.03509

The theoretical deflection using simple beam theory was found to be = $7.482 * 10^{-5}$ mm/gram.

The results obtained from the experiments mentioned above are presented graphically in Figure 3.29 and are compared with the theoretically predicted curve.

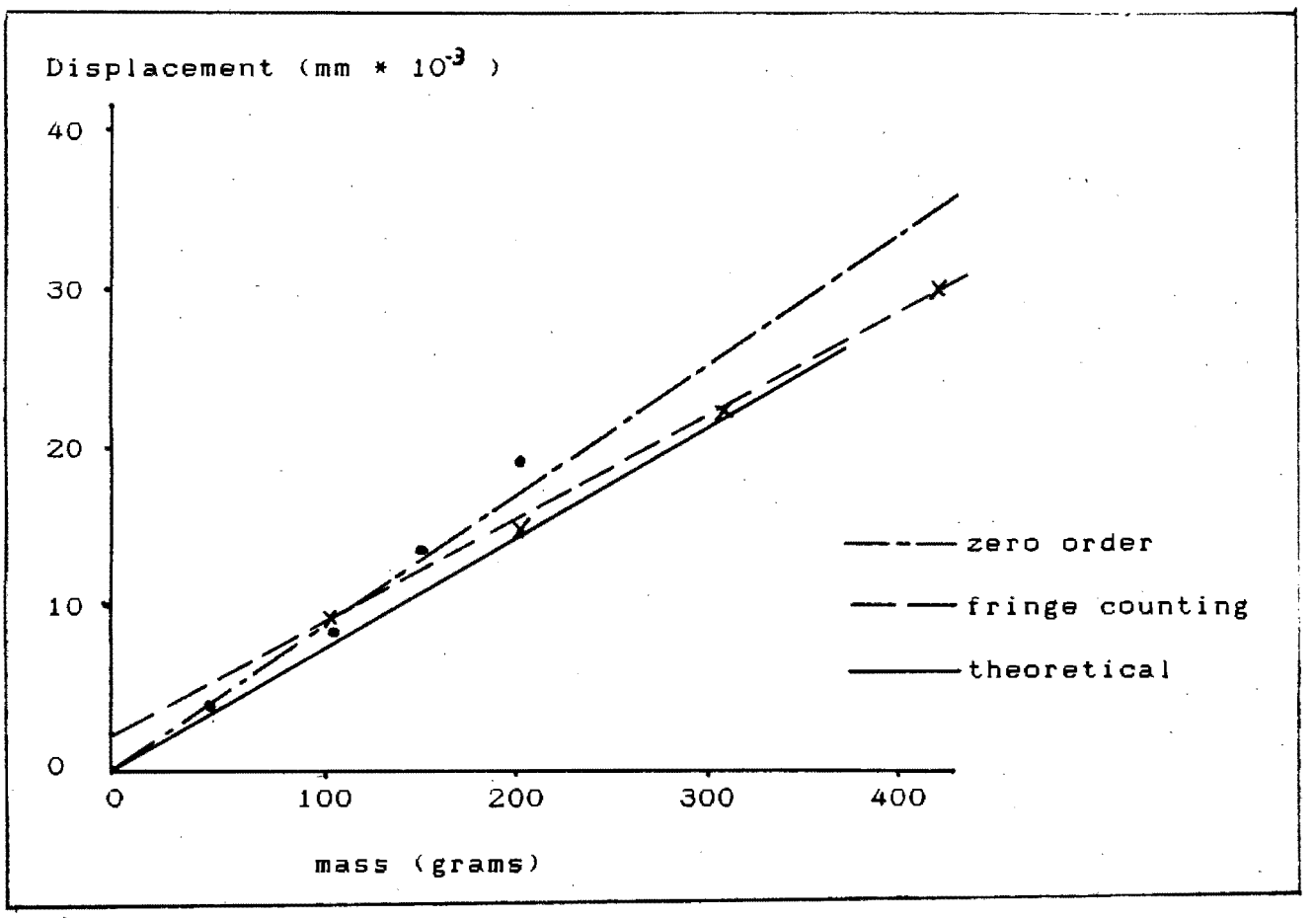

FIGURE 3.29 Graph of the cantilever deflection rates

The slopes of the displacements versus the loads for the various curves are as follows:

zero-order technique - $8.654 * 10^{-5}$ mm/grm

fringe-counting technique - $6.434 * 10^{-5}$ mm/grm

cantilever beam theory - $7.482 * 10^{-5}$ mm/grm

3.3.5. CONCLUSIONS AND DISCUSSION

Both zero-order (out-of-plane) and fringe-counting (in-plane) techniques yield accurate results in relation to the theoretically determined results - circa 85 %.

The graphs presented show that a high degree of linearity of response exists in both tested techniques.

The use of the zero-order technique can provide a permanent visual record of the fringes obtained, whereas the fringe-counting technique is unable to so.

The accuracy of the fringe-counting technique, due to its nature, is dependant on the experimenters interpretational skills.

In both techniques, care has to be taken when obtaining the data required to calculate the object displacements. Any erroneous distance measurement or angle determination will contribute to the error in the displacements obtained.

In addition stability requirements are more critical when using the fringe-counting technique than when using the zero-order technique. This is because real-time holography is employed in the fringe-counting technique and the production of spurious fringes affects the results obtained.

3.4. MULTIPLEXING HOLOGRAPHY

Due to the contemporary progress in the field of transfer holography, especially in the area of multiplexing, it was felt that familiarity with this technique would prove to be

a valuable asset, especially as scant reports of it exist in the literature.

3.4.1. AIMS

As the transfer technique is used in the display or artistic side of holography it is of the utmost importance that more information becomes available in the literature.

Therefore, the main aim of this study was to gain greater insight in the transfer and multiplexing technique. Specific aspects such as available angle of object visibility and separation of the images in a multiplex hologram were to be examined.

3.4.2. PRELIMINARY CONSIDERATIONS

As was stated in the previous chapters, a high quality master transmission hologram of the appropriate object is required in order to make a reflection hologram. A high quality hologram is generally one in which the noise is kept at a minimum level, and the brightness at a maximum level. The noise level within a hologram is controlled by the object versus the reference beam ratio, which also affects the image brightness. Bleaching of the processed hologram generally increases the noise level slightly, but the image

brightness is usually considerably increased. Therefore, the master holograms are normally bleached.

Saxby [28] states that reflection holograms can also be used as master holograms. However, no information regarding the set-up required to make transfer holograms from off-axis reflection holograms was obtainable. Nevertheless, it was decided to attempt to produce a transfer hologram using a reflection hologram as the master.

The multiplexing principle, which utilizes the transfer principle, simultaneously transfers two or more images onto the transfer hologram. To achieve this, the master must consist of two or more sections, each section representing one image. There are three ways of producing such a master, namely:

i Recording the required images as strips onto one holographic plate. To do this a mask is required which masks all but the required strip of the hologram from the object and reference beam when recording one of the objects. Each strip then represents a different object.

ii Recording various objects onto individual masters which are then cut into strips and assembled side by side, each strip representing a different object.

iii Recording various objects as individual holograms and placing the individual holograms side by side to individually project a transfer image onto the transfer plane .

It must be remembered that whichever master assembly is chosen in the transfer principle, the real image is projected onto the transfer plate, that is, the image is focused in a region near the transfer plate. Therefore, the images that are projected by the masters should all be focused at roughly the same point in space. When viewing the resulting transfer hologram, a smooth transition from image to image is observed.

The final images in the transfer hologram can be arranged to change in either the horizontal or vertical viewing direction. In addition, the angle of illumination of the transfer hologram can be selected. The most favoured positions found in presently obtainable transfers is either vertical or horizontal. The images can therefore be arranged to change either in the plane or perpendicular to the plane of illumination. It must be remembered that it is the recording set-up which determines the final orientation and therefore, once it is recorded, it cannot be changed.

3.4.3. EXPERIMENTAL PROCEDURE

It was decided to investigate all three master assemblies mentioned above. The images projected by the masters were to be focused in front of the hologram, normal to the surface centre of the hologram. In addition, the final transfers were to be viewed with the image shift occurring vertically, in the same plane as the plane of illumination. The reasons for these decision were as follows:

- Saxby [26] has reported that up to nine images could be stored in the vertical viewing direction resulting from the elimination of eye parallax in that direction.

- The use of a vertical illumination direction would simplify the viewing of the transfer hologram in ordinary daylight, which is incident from above.

- The recording procedure was simplified as all recording planes were confined to only one plane.

In order to facilitate the above conditions, an assumption particular to holography was employed. Namely, the horizontal plane of the holographic table is taken to represent what is normally considered to be the vertical plane. The resulting transfer hologram has to be rotated by ninety degrees when it is viewed. The horizontal angle between the reference beam and the transfer hologram thus

represents a vertical angle in the reconstruction process.

The abovementioned principle also means that the objects have to be recorded on their side, so that, when the final hologram is rotated, the image is correctly orientated.

All the set-ups used to record the masters employed a collimated reference beam incident at approximately 40 degrees to the normal of the holographic plate. The methods used to produce the required transmission masters are as follows:

i The objects are placed a small distance in front of the emulsion, horizontal and centred with respect to the holograghic plate. A mask is constructed, which vertically masks two thirds of the emulsion at a time. The unmasked third is used to record one of the three objects. Another mask is then used to mask the recorded third as well as an unrecorded third - thereby rendering an unexposed third available for the recording of the second object, which is placed in the same position as the first object. This procedure is then repeated to record the third and final object.

ii Individual, full sized masters are recorded of two seperate objects which are positioned in the same manner as described above. The processed holograms are then vertically cut in half. The right-hand side half

from one hologram and the left-hand side half from the other hologram are then placed side by side and thereby create the master.

iii Two full-sized masters of two different objects are placed side by side to produce the final master. To ensure that the two images produced coincide and produce the same range of visibility in the final transfer hologram, the images are focused along the bisector of the two masters.

To achieve this, the objects, when recording the masters, are positioned close to the holographic plate and are lined up with one of the edges of the plate. Two transmission holograms of two different objects are then recorded, but with one object positioned on its left side and the other on its right side.

To create the final master one of the two transmission holograms and its reference beam is vertically rotated by 180 degrees. This results in the correct orientating of the two objects with respect to each other when illuminated. In addition, the rotation allows the two holograms to be placed side by side and project their images onto the same spot. See Figure 3.30.

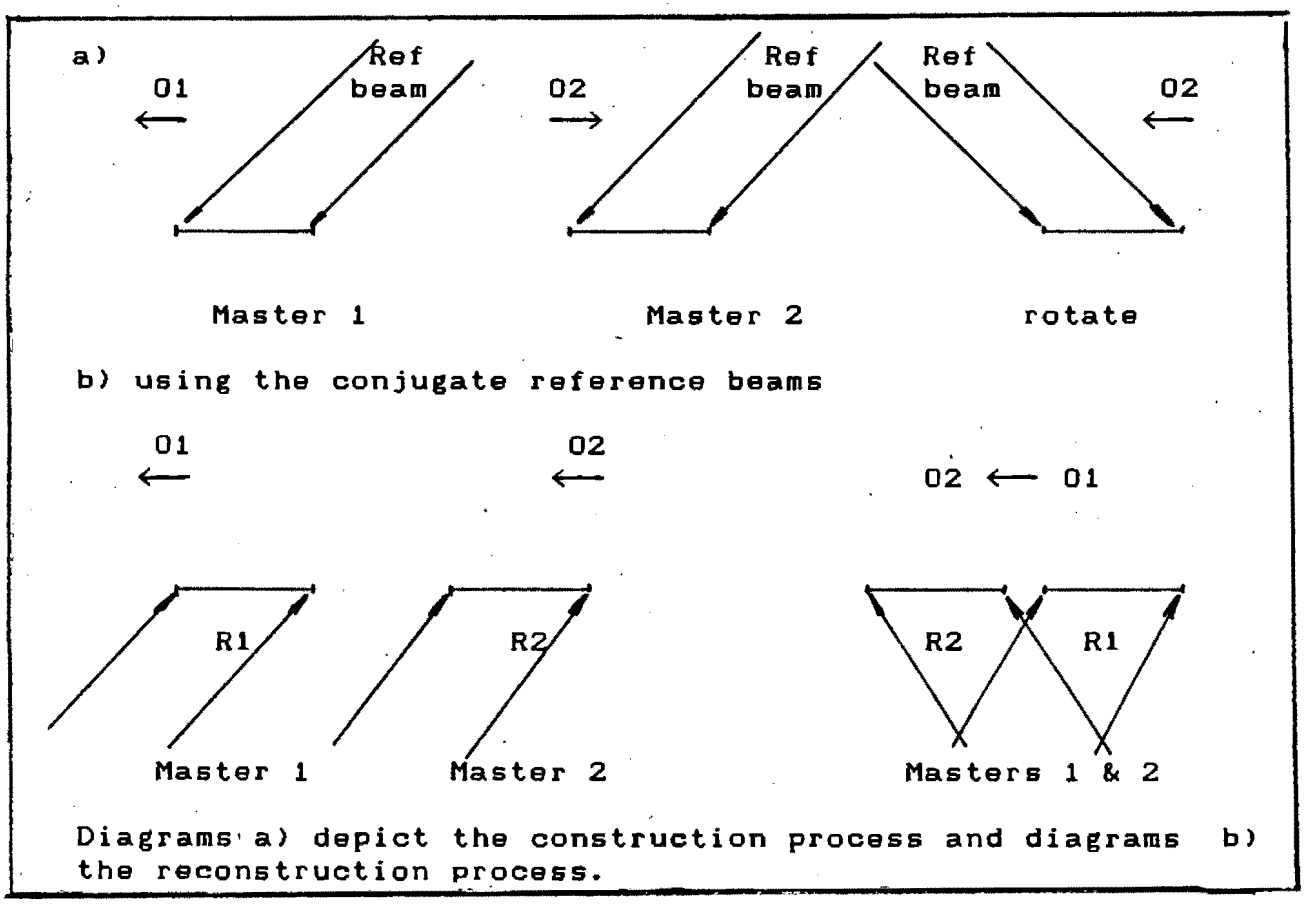

FIGURE 3.30 Master assembly no. iii

For the reflection transfer technique it was decided to first investigate the transfer properties of reflection masters. Any reflection hologram can be used for this purpose, provided that in the transfer process, the reference beam used for the transfer hologram does not illuminate the master hologram. This can be achieved if the image encoded in the master is projected to a sufficient distance from the master.

For the transmission transfer process the most involved set-up was used, namely the one required to produce the transfer using the master, that was proposed in possibility (iii). See Figure 3.31.

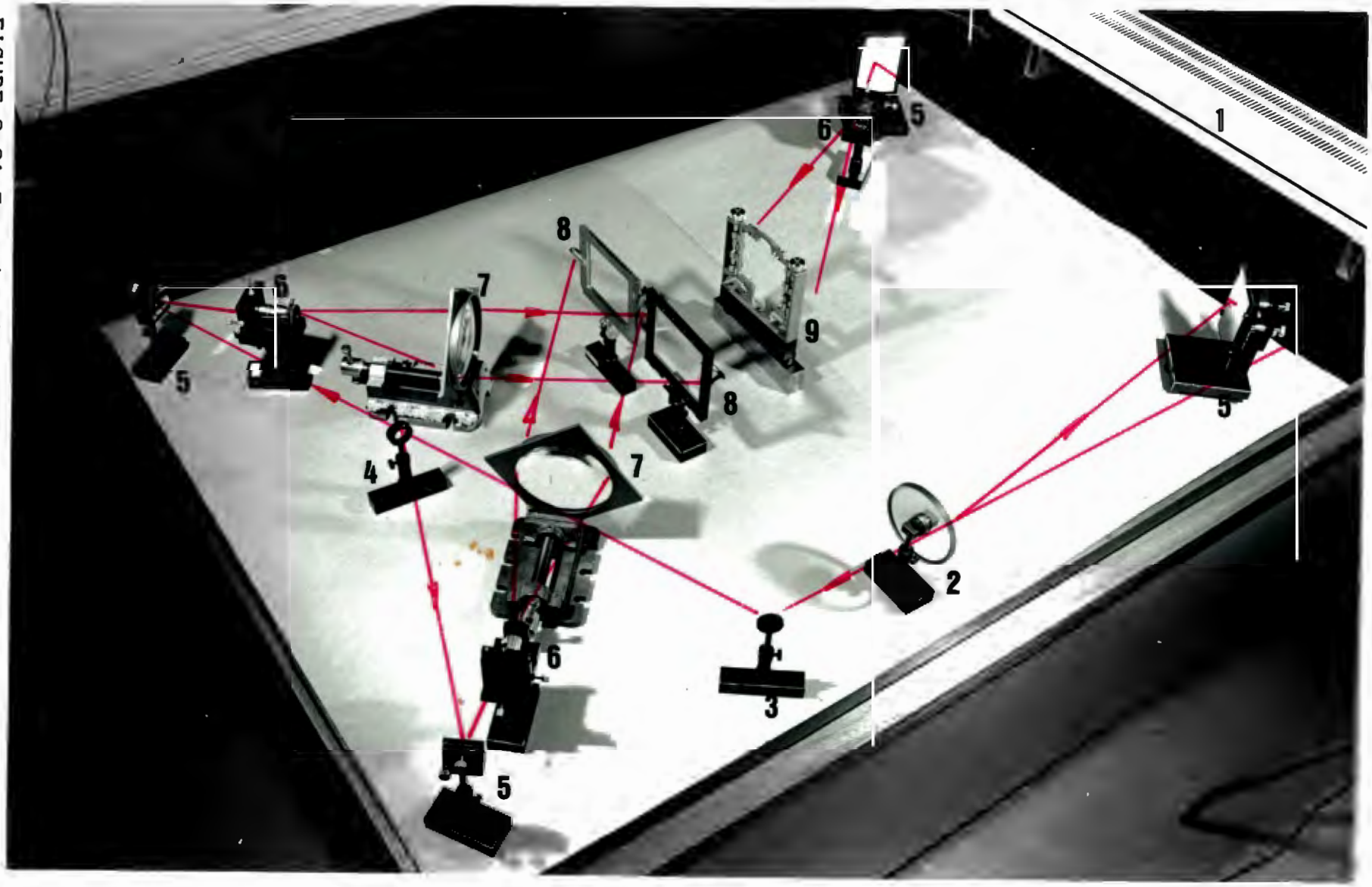

FIGURE 3.31 Experimental transfer and multiplexing set-up.

1 - laser 2 - beamsplitter 3 - mirror 4 - 50% beamsplitter

5 - adjusting mirror 6 - beamexpander 7 - collimating lens 8 - master

9 - transfer holder

Essentially the beam emanating from the laser is split into two beams by the beamsplitter. The reflected beam acts as the reference beam for the transfer hologram. The transmitted beam is split by a fifty percent beamsplitter and each resulting beam is directed through a beam expander and collimating lens onto the individual master. This object beam, which acts as the conjugate of the reference beam used to record the transmission hologram, projects the real image onto the transfer plate.

For the two other master proposals the set-up can be modified by eliminating one of the two beams produced by the fifty percent beamsplitter and by allowing the remaining beam to illuminate the entire master.

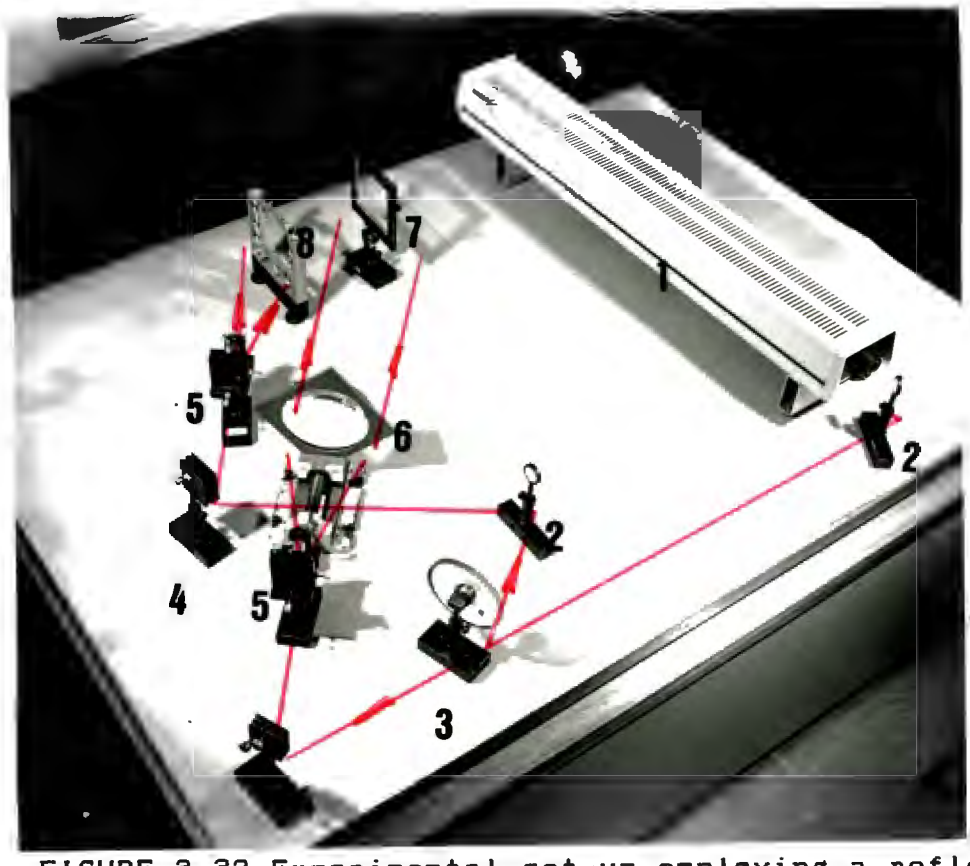

1 - laser
2 - mirror
3 - beamsplitter
4 - adjusting mirror
5 - beam expander
6 - collimating lens
7 - reflection master
8 - transfer holder

FIGURE 3.32 Experimental set-up employing a reflection master

The transfer set-up used for the reflection master is depicted in Figure 3.32.

The beam transmitted through the beamsplitter acts as the conjugate reference beam and is used to illuminate the master, projecting the real image onto the transfer plate. The beam reflected by the beamsplitter is directed onto the transfer plate, constituting the reference beam.

3.4.4. RESULTS

The results obtained from the reflection master transfer technique proved to be unsatisfactory. The transfer technique was successful in that the technique was proven. It was found that by reducing the distance of image projection by the master, a large angle of visibility of the image was obtainable when illuminating the transfer in the reconstruction process. The image produced by the transfer had a very high level of resolution and large parallax was obtainable if the image was recorded as a hologram-plane transfer (see Figure 2.12).

However, it was impossible to produce a bright transfer hologram when using a reflection master. It was not possible to view the transfer using ordinary roomlight. A special stage lamp, of high intensity, was required to yield a satisfactory image when the transfer hologram was

illuminated.

All attempts to optimise the exposure time of the transfer hologram did not yield any marked improvement in the resulting image brightness. The reflection masters used were of a high quality and could therefore not be improved.

As a result, it was decided not to investigate the multiplexing technique, as applicable to reflection masters.

The transfer technique using transmission masters proved to be successful in the experiments conducted. There are however one or two aspects which still require further investigation. The results obtained were as follows:

i With the use of the master - as detailed in (i) of the master configuration investigated - bright transfer images were obtainable. When using overhead illumination, the angle of visibility was in the order of ten degrees which resulted in limited image parallax.

The separation of the individual images, which occurred when changing the position of viewing in the vertical direction, was very defined and sudden. Viewing the images individually was found to be more difficult, and required a steady hand to hold the transfer hologram. However, if the distance between the transfer hologram

and viewer was greater than one meter, it became easier to see the individual images produced.

ii The master configuration (ii) resulted in essentially the same findings as those recorded in (i) above. However, the use of only two transmission hologram halves facilitated easier viewing of the individual images.

By allowing the two master halves to overlap slightly, a blending of the visibility of one image into the other was obtained when the viewing direction was changed vertically.

iii The master configuration, as outlined in (iii), proved to be successful and yielded the best results. The findings were essentially the same as those listed in (ii), but with the advantage that the angle of image visibility was increased to about fifteen degrees, thereby increasing the image parallax. This configuration allowed the easiest viewing of the individual images.

In all the transfers produced it was found that the image resolution was not of the same quality as those obtained when using reflection masters. In ordinary roomlight the images were visible and separable, but appeared to be slightly blurred. This was thought to have been caused by

the various light sources which illuminated the object simultaneously, resulting in various angles of the image being superimposed onto one another.

In ordinary sunlight however, the images were easily and clearly visible, thus proving that the overhead illumination angle facilitates easy hologram viewing.

It was established that some form of dimensional emulsion change ocured when the masters were processed. As a result, the conjugate reference beam used to illuminate the masters in the transfer process, had to be slightly converging. This fact led to the discovery of another factor of the transfer process, namely, that the type of object beam used to illuminate the transfer masters affected the final size of the images projected onto the transfer hologram. Converging the master illumination beam resulted in a reduction in size of the final image, whilst allowing the master illumination beam to diverge, resulted in an enlargement of the produced image. The transfer plate holder had to be repositioned when the projected image was either enlarged or reduced.

Enlarging the produced image resulted in a reduction of the viewing angle, whereas decreasing the produced image size resulted in a reduction of the image resolution. A transfer hologram that was produced by using the master configuration, outlined in (iii), is presented in Figure 3.33.

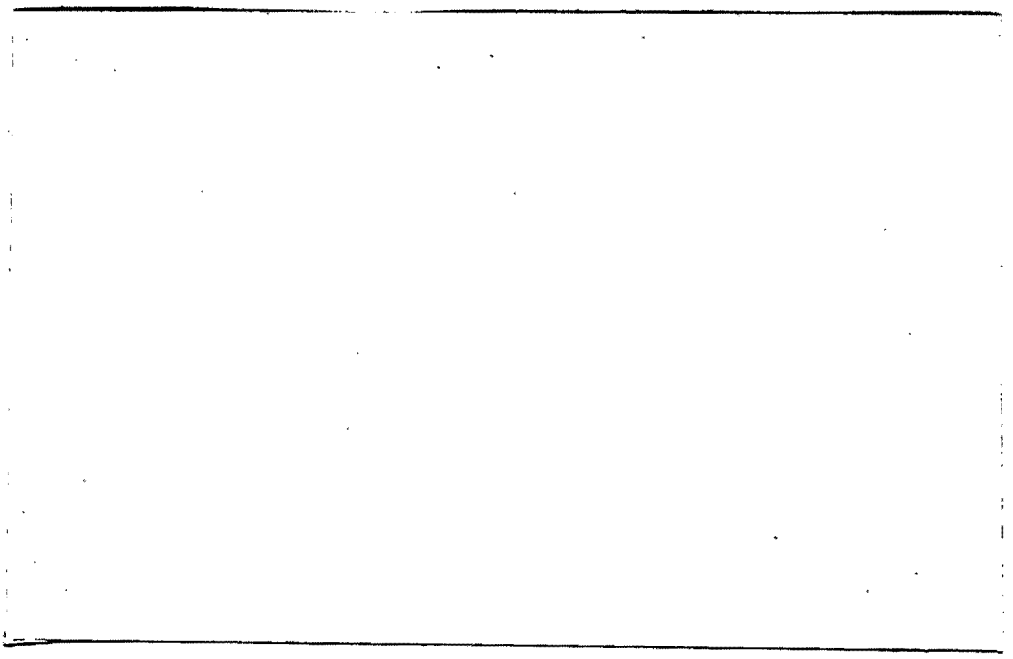

FIGURE 3.33 Transfer hologram produced using master assembly no iii.

3.4.5. COMMENTS AND CONCLUSIONS

From the results obtained, it can be concluded that the transfer technique using reflection masters, has as yet, not been mastered. This has led to the opinion that the chemical developing process should be closely examined, as all the other recording variables have been experimented with, and have not yielded the desired results.

The transfer and the multiplexing technique, using transmission masters, although examined and proven, has as yet not

yielded results which are comparable with the commercially available holograms. The main discrepancies between the holograms produced for this thesis and the commercial holograms are the angle of image viewing and the resultant parallax, as well as the image resolution of the transfer images.

It is felt, that the inferior image resolution is related to the emulsion shrinkage experienced in the master holograms. Therefore, in order to obviate this problem, further work should be conducted on the chemical processing of the exposed holograms.

In addition, it is recommended that the focused image technique should be investigated, as its capabilities of also producing hologram-plane reflection holograms and of precisely localising the image on the produced hologram, might yield results that are superior to those that were obtained by the transfer technique.

REFERENCES

1. Gabor, "A new microscopic principle", Proc. Roy. Soc. London (1948) A 197.

2. Leith & Upatnieks, "Reconstructed wavefronts and communication theory", J. of the Opt. Soc. of Amer., 52, (1962) 1123 - 30.

3. Hecht, Optics (Second edition), (1987) 577 - 90

4. Leith & Upatnieks, "Wavefront reconstruction with continuous-tone objects", J. of the Opt. Soc. of Amer., 53, (1963) 1377 - 81.

5. Leith & Upatnieks, "Wavefront reconstruction with diffused illumination and three-dimensional objects", J. of the Opt. Soc. of Amer., 54, (1964) 1295 - 301.

6. Denisyuk, "On the reproduction of the optical properties of an object by the wavefield of its scattered radiation", Optics & Spectroscopy, 15, (1963) 297 - 84

7. Powell & Stetson, "Interferometric vibration analysis by wavefront reconstruction", J. of the Opt. Soc of Amer., 55, (1965) 1593 - 8.

8. Burch, "The application of lasers in production", The Production Engineer, 44, (1965) 431 - 42.

9. Brooks, "Interferometry with a holographically reconstructed comparison beam", Appl. Phys. Letters, 7, (1965) 248 - 9.

10. Erf, Holographic Non Destructive Testing (1974) 221 - 27.

11. Kersch, "Advanced concepts of holographic NDT", Mater. Evaluat., XXIX, (1971) 125.

12. Vest, "Holographic detection of microcracks", J. Basic Eng. Trans. ASME, Ser, D93, (1971) 273.

13. Erf, Holographic Non Destructive Testing (1974) 323 - 32.

14. Allen, "Experimental and analytical investigation of the behaviour of cylindrical tubes subject to axial compressive force", J. Mech. Eng. Sci., 10, (1968) 182 - 97.

15. Viénot, "Hologram interferometry: Surface displacement fringe analysis as an approach to the study of mechanical strains and other applications to the determination of anisotropy in transparant objects",in Robertson & Harvey ed., The Engineering uses of Holography, (1970) 133 - 50

16. Ennos & Archibold, "Displacement measurement from double-exposure laser photographs", Optica Acta, Vol 19 No 4, (1972) 253 - 71.

17. Sollid, "Holographic interferometry applied to measurement of small static displacement of diffusely reflecting surfaces", Applied Optics, Vol 8 no 8, (1969) 1587 - 95.

18. Erf, Holographic Non Destructive Testing (1974) 343 - 54.

19. Briers, "The interpretation of holographic interferograms", Optical & Quantum Electronics, 8, (1976) 469 - 501.

20. Ennos, "Measurement of in-plane surface strains by hologram interferometry", J. Phy. E. (J. Sci. Instrum.), (1968) 731 - 4.

21. Aleksandrov & Bonch-Bruerich, "Investigation of surface strains by the hologram technique", Soviet Physics : Technical Physics, 12, (1967) 258 - 65.

22. Haines & Hildebrandt, "Surface deformation measurement using the wavefront reconstruction technique", Applied Optics, Vol 5 No 4,(1966) 595 - 602.

23. Ennos et al, "The application of holography to the comparison of cylindrical bores", J. Sci. Instrum., 44, (1967) 489.

24. Brown, "Holography uses in Nondestructive testing with particular emphasis on tires", SPIE Proc. (1973)

25. Unterseher et al, "Holographic handbook, Making holograms the easy way", (1982) 212 - 39.

26. Saxby, Practical holography (1988) 180 - 99.

27. Shigley, Mechanical engineering design, (1983) 804.

28. Saxby, Practical holography, (1988) 95 - 127.

APPENDIX A

Chemical composition of the developers used in the laboratory are as follows:

Initial formula

Solution A

Distilled water	500 ml
Pyrogallol	5 g

Solution B

Distilled water	500 ml
Sodium carbonate	60 g

Mix equal parts of solution A and B directly before use.

Bleach

Distilled water	1000 ml
Para-benzoquinone	1.5 g
Boric acid	1.5 g
Potassium bromide	30 g

Revised formula

Solution A

Destilled water	700 ml
Pyrogallol	15 g
Metol	5 g
Destilled water to make	1000 ml

Solution B

Destilled water	700 ml
Sodium carbonate	60 g
Pottasium hydroxide	20 g
Destilled water to make	1000 ml

Solution C

Destilled water	700 ml
Sodium sulfite	100 g
Destilled water to make	1000 ml

Mix equal parts of solution A and B directly before use. Solution C can be added by up to 25% of total volume of solution A and B to affect final color replay of reflection holograms.

Bleach

Destilled water	700 ml
Potassium dichromate	5 g
Sodium hydrogen sulfate	80 g
Destilled water to make	1000 ml